THE ROLE OF CHOLESTEROL SEQUESTRATION AND ACCUMULATION IN THE ENDOCYTIC PATHWAY IN DEVELOPMENT OF NEURODEGENERATIVE DISEASE

HUANG ZHILI
(M.Sc., NUS, SINGAPORE)

A THESIS SUBMITTED

FOR THE DEGREE OF DOCTOR OF PHILOSOPY

DEPARTMENT OF BIOCHEMISTRY

NATIONAL UNIVERSITY OF SINGAPORE

2009

ACKNOWLEDGEMENTS

I would like to express my heartfelt thanks and appreciation to my supervisor, Associate Professor, Li Qiutian, Department of Biochemistry, National University of Singapore, for his valuable suggestions and guidance, as well as his consistent encouragement throughout the course of this study.

I would like to give my special thanks to Ms. Tan Boon Kheng for her wonderful assistance and unfailing help. I would like to express my appreciation to my friends, Shao Ke, Miao Lv, Wen Chi, Qing Song, Wei Shi, Li Yang, Hao Sheng and Wang Ya for their friendship and support. The wonderful time we have studied together is unforgettable.

I would like to express my thanks to Associate Professors Tang Bor Luen, Steve Cheung and Tan Tin Wee for their encouragement and support.

I am also grateful to National University of Singapore for awarding me a Research Scholarship.

Last but not least, I would like to express my deepest appreciation to my beloved parents, my husband, my son and all my family members for their support and understanding. This thesis is dedicated to them with love.

Table of contents

List of publications (published paper, manuscript prepared for submission, abstract presented in conference)

Published papers

Huang Z, Hou Q, Cheung NS, and Li QT.

Neuronal cell death caused by inhibition of intracellular cholesterol trafficking is caspase dependent and associated with activation of the mitochondrial apoptosis pathway

Journal of Neurochemistry, 2006, 97, 280-291.

Shao K, Hou Q, Go ML, Duan W, Cheung NS, Feng SS, Wong KP, Yoram A, Zhang W, Huang Z, and Li QT.

Sulfatide-tenascin interaction mediates binding to the extracellular matrix and endocytic uptake of liposomes in glioma cells.

Cellular and Molecular Life Sciences, 2007, 64(4):506-515.

Zhang W, Duan W, Cheung NS, Huang Z, Shao K, and Li QT.

Pituitary adenylate cyclase-activating polypeptide induces translocation of its G-protein-coupled receptor into caveolin-enriched membrane microdomains, leading to enhanced cyclic AMP generation and neurite outgrowth in PC12 cells.

Journal of Neurochemistry, 2007, 103(3):1157-1167.

Abstracts submited for conference:

1st Asia pacific conference and exhibition on anti-aging medicine

"From molecular mechanisms to therapies"

23-26 June 2002, Raffles City Convention Centre, Singapore.

P05, Neuroprotective effect of human bcl-2 and PTEN expression in AMPA receptor-mediated apoptosis in cultured murine cortical neurons.

Huang ZL, Li QT, Qi RZ, Cheng HC, Qi DX, Choy MS, Lee MK, Teo TS, Bernard O, Beart PM, and Cheung NS.

Pp 75.

The future of neurobiology at NUS

03-04 Feb 2004, Clinical Research Centre Auditorium, MD11, Faculty of Medicine, National University of Singapore.

P19, Cholesterol accumulation in the endocytic pathway induces apoptotic neuronal cell death.

Huang ZL, Li QT.

Pp 35.

Summary

Niemann-Pick type C (NPC) disease is characterized by accumulation and sequestration of unesterified cholesterol in the endocytic pathway and progressive neurodegeneration. The cellular mechanism for loss of neurons of the central nervous system (CNS) under NPC phenotype is still under investigation. Rab proteins constitute the largest branch of the Ras GTPase superfamily and regulate each of the four major steps in membrane traffic: vesicle budding, vesicle delivery, vesicle tethering, and are involved in modulation of cellular cholesterol transport and homeostasis.

In this study, I demonstrate inhibition of intracellular cholesterol trafficking in primary neurons by class 2 amphiphiles, which mimics the major biochemical and cellular feature of NPC1, led to not only impaired mitochondrial function but also activation of the mitochondrial apoptosis pathway.

In activation of this pathway, both cytochrome-c and Smac/Diablo are released but apoptosis-inducing factor (AIF) is not involved. Treatment of the neurons with taurine, a caspase-9 specific inhibitor, could prevent the amphiphile-induced apoptotic cell death, suggesting that formation of apoptosome, followed by caspase-9 and caspase-3 activation, might play a critical role in the neuronal death pathway.

cAMP has been shown to improve the survival *in vitro* of several neuronal types when added to the medium. In this study, I demonstrate that significant upregulation of Rab7

expression and mild increase of rab9 expression with treatment of cAMP and forskolin to primary neurons and NPC1 fibroblasts, through activation of ERK, leading to survival of cells. In this process, cholesterol trafficking is modulated, and cholesteryl ester is increased in both types of cells.

In summary, this study show that cAMP and forskolin have effects on the endocytic trafficking via regulation of the expression of Rab GTPase, and may provide insight into the mechanism of the molecular basis of neurodegeneration in NPC1 disease and therapeutic strategies for treatment of this disorder.

List of Figures

List of abbreviations

AIF	apoptosis-inducing factor
APS	ammonium persulfate
cAMP	N6,2'-O-dibutyryladenosine 3',5'-cyclic monophosphate sodium salt
DEVD	Asp-Glu-Val-Asp
DMSO	dimethyl sulfoxide
DMEM	dulbecco's modified eagle medium
EMEM	minimum essential medium eagles
ERK	mitogen-activated protein kinase
FC	free cholesterol
FCS	fetal calf serum
FMK	fluoromethylketone
Fors	forskolin
HBSS	Hank's balanced salt solution
LDL	low density lipoprotein
LPDS	lipoprotein deficient serum
MTT	3-(4, 5-dimethylthiazol-2-yl)-2, 5-diphenyl tetrazolium bromide
NB	neurobasal medium
NPC1	Niemann-Pick disease type C1
PBS	phosphate-buffered saline
PD	PD98059, 2'-amino-3'-methoxyflavone
PI	propidium iodide
PVDF	polyvinylidene fluoride

SBT	soybean trypsin inhibitor
SDS	sodium dodecyl sulfate
siRNA	small interfering RNA
TLC	thin layer chromatography
TUNEL	terminal deoxynucleotidyl transferase-mediated dUTP end-labeling
U18666A	3β-[2-(diethylamino) ethoxy] androst-5-en-17-one

Chapter 1. Introduction

1.1 Cholesterol trafficking and homeostasis

Cholesterol is an essential component of animal cellular membranes and precursor for biosynthesis of steroid hormones and bile acids. The intracellular cholesterol homeostasis is essential for many biological functions of mammalian cells. At cellular level, cholesterol homeostasis is maintained by regulated cholesterol uptake, *de novo* synthesis, intracellular transport and efflux.

Eukaryotic cells form the 27 carbon atom-bearing cholesterol molecule from scratch starting with acetate as substrate. Cholesterol synthesis is a complex biosynthetic process which takes place in the endoplasmic reticulum, and involves acetyl-CoA and other enzymes, many of which are located in the endoplasmic reticulum (ER) (Urbani and Simoni, 1990). The enzyme 3-hydroxy-3-methylglutaryl-coenzyme A (HMG-CoA) reductase catalyzes the rate-limiting reaction in cholesterol biosynthesis pathway (Brown and Goldsein, 1980). In the biosynthetic secretory pathway, cholesterol concentration is lowest in the ER. The ER is the primary site of cholesterol synthesis and esterification, and it is the crucial regulatory compartment in cholesterol homeostasis, although ER is a cholesterol-poor organelle, comprising only 0.5-1% of total cellular cholesterol (Lange et

al., 1999). Recent data indicate that excess free cholesterol may exert its cytotoxic effects via the ER (Feng et al., 2003). It increases through the Golgi apparatus, with the highest concentration in the plasma membrane (Liscum and Munn, 1999). Transport between ER and PM is dynamic, because it has been estimated that the entire PM cholesterol-pool cycles to the ER and back with a half-time of 40 minutes (Lange et al., 1993).

The cholesterol content and the expression level of cholesterol-specific enzymes show strong region-specific variation (Bae et al, 1999; Runquist et al., 1995; Turley et al., 1998; Zhang et al., 1996;). The brain contains five to ten times more cholesterol than any other organ and this sterol represents 2–3% of the total weight and 20–30% of all lipids in the brain. There is solid evidence that most if not all of this cholesterol is produced in situ rather than imported from the blood (Edmond et al., 1991; Jurevics et al., 1995; Turley et al., 1998), probably because lipoprotein particles, which mediate the intercellular transport of sterols and other lipids, cannot pass the blood-brain barrier. Nervous tissue is capable of cholesterol synthesis and the synthesis rate and cholesterol content increase drastically during brain development (Dietschy et al., 2001; Sastry, 1985).

Apart from de novo synthesis, cells can acquire cholesterol by uptake of lipoprotein (Simons and Ikonen, 2000) through specific receptors in the plasma membrane (Brown and Goldstein, 1986). LDL binds to LDL-receptors that cluster in clathrin-coated vesicles, which subsequently become uncoated. Four general compartments in the endocytic pathway, defined by different protein and lipid compositions: (1) early or sorting

endosomes; (2) the endocytic recycling compartment (ERC) or recycling endosomes; (3) late endosomes; and (4) lysosomes. Late endosomes are normally dynamic structures, but they become static, enlarged, and cholesterol-rich in NPC cells (Ko et al., 2001)

Although the itinerary of the LDL receptor in this pathway is well-described, the fate of LDL-derived cholesterol is the subject of much investigation (Alberts et al., 2002; Brown and Goldstein, 1986). At the final stage of endocytosis, both proteins and lipids enter the lysosomes for subsequent metabolism, releasing unesterified cholesterol to other intracellular sites and plasma membrane (Fielding and Fielding, 1997). Lysosomes are thus generally regarded as the end-point of the endocytic pathway. Low-density lipoprotein particles contain apolipoprotein (Apo) B as major protein component and draw their load from newly synthesized material in the endoplasmic reticulum. The reverse cholesterol transport, whereby cells from different organs eliminate excess cholesterol through the liver, is mediated by high-density lipoprotein (HDL) particles. HDL particles contain ApoA1 and acquire cholesterol directly from the plasma membrane. This transfer is probably mediated by members of the ATP-binding cassette (ABC) transporter family (Dietschy and Turley, 2001; Schmitz and Orso, 2001),

Regardless of whether cells acquire cholesterol by synthesis or uptake, the molecule must be distributed to the different cellular membrane compartments. Cholesterol moves against a steep concentration gradient to reach the PM, where cholesterol has important functions, by vesicular transport through the Golgi. ATP depletion or low temperature inhibited rapid ER to PM cholesterol transport (DeGrella et al., 1982; Urbani et al., 1990).

Excess cellular cholesterol from other compartments returns to the ER for esterification, through a negative feedback mechanism. The ER may also accommodate some excess free cholesterol via its large surface area and ability to synthesize phospholipids, thus maintaining an acceptable cholesterol-to-phospholipid ratio (Blanchette-Mackie, 2000; Tabas 2002).

Cholesterol is also transported from endocytic recycling compartment (ERC) to PM via vesicular transportation and it also traffics in the opposite direction from PM to ERC, which is a rapid and ATP-independent non-vesicular transport (Hao et al., 2002).

In humans, the central nervous system, being only 2% or less of the mass of a normal individual, is particularly enriched in unesterified cholesterol and contains approximately a quarter of all the unesterified cholesterol present in the body (Dietschy and Turley, 2001). The neuronal cells acquire cholesterol mainly by de novo biosynthesis and, to a much less extent, by turnover among the glial cells and neurons probably involving receptor-mediated endocytosis, as the former secrets large amount of apolipoprotein E (ApoE) and ApoE receptors are abundantly found on the latter (Herz and Bock, 2002). Cholesterol in the brain may play an important role in synaptic development and plasticity, brain growth, neuron repair and remodeling, and even maintaining the normal function of this important organ (Dietschy and Turley, 2001; Herz and Bock 2002; Koudinov and Koudinova, 2001; Mauch et al., 2001).

The cholesterol content of cellular membranes is tightly controlled by elaborate mechanisms that balance the level of cholesterol synthesis, uptake and release. A prominent feedback pathway involves sterol-sensing elements in the membrane and proteolytic activation of transcription factors that enhance the expression of cholesterol synthesizing enzymes and lipoprotein receptors (Brown and Goldstein, 1999; Hampton 2002; Sakai and Rawson 2001).

The disruption of cholesterol homeostasis is related to many biological and pathological abnormalities. Excess cholesterol kills macrophages by caspase-dependent apoptosis (Tabas 2007). The enrichment of mitochondria in free cholesterol, resulting in decreased mitochondrial membrane fluidity. The homeostasis of cholesterol and its trafficking to mitochondria may be of relevance in the pathophysiology of encompasses alcoholic and non-alcoholic steatohepatitis (Garcia-Ruiz et al., 2006). By promoting cholesterol accumulation and plaque vulnerability and by locally regulating hemostasis, arterial mast cells in atherosclerotic lesions have the potential to contribute to the clinical outcomes of atherosclerosis, such as myocardial infarction and stroke. Recent research showed CLN6p deficiency caused cholesterol accumulation in lysosomes. Alterations in protein/lipid intracellular trafficking would affect the composition and function of endocytic compartments, including lysosomes. Dysfunctional endosomal/lysosomal vesicles may act as one of the triggers for apoptosis and cell death, and for a secondary protective inflammatory response (Teixeira et al., 2006).

1.2 Apoptosis and neurodegenerative diseases

Cell death has been divided into two general groups: apoptosis, a programmed cell death in which the cell plays an active role; and passive necrotic cell death. Morphologically, cells typically round up, form blebs, undergo zeiosis (an appearance reminiscent of boiling), chromatin condensation, nuclear fragmentation, and the breaking off of cellular fragments called apoptotic bodies. Phosphatidylserine, normally placed asymmetrically such that it faces internally on the plasma membrane (due to a flipase that flips the phosphatidylserine so that it faces internally), appears externally during apoptosis (Fadok et al., 1992). Apoptosis plays a role in tissue remodeling during normal development of the mammalian nervous system (Nijhawan 2000). Caspases are cysteine proteases that mediate apoptosis in a wide range of cell systems, including neuronal injury. It is largely accepted that caspases play a key role in both the initiation and execution pathways of apoptosis. In particular, caspase-3 has been implicated as a key cell-death protease involved in the execution phase of apoptosis (Earnshaw 1999; Thornberry and Lazebnik 1998; Yuan et al., 1993).

Upon activation, caspases cleave a variety of intracellular polypeptides, including major structural elements of the cytoplasm and nucleus, components of the DNA repair machinery, and a number of protein kinases, which then lead to the stereotypic morphological and biochemical changes that characterize apoptotic cell death.

Necrosis is generally characterized by early swelling of the cytoplasm and disintegration of cellular structures, which ultimately culminate in cell lysis and subsequent release of cellular debris into the extracellular space. Necrosis occurs following severe cellular injury and is usually associated with an inflammatory response (Dive et al., 1992; Searle et al., 1982).

The biochemical mediation of apoptosis occurs through two general pathways: an intrinsic pathway, mediated by the mitochondrial release of cytochrome-C and resultant activation of caspase-9; and an extrinsic pathway, originating from the activation of cell surface death receptors such as Fas, and resulting in the activation of caspase-8 or caspase-10 (Salvesen and Dixit 1997).

Following release from the mitochondria, cytochrome-C interacts with a cytosolic protein, Apaf-1, *via* the WD-40 repeats of Apaf-1, leading to the exposure of a (d) ATP-binding site on Apaf-1. Occupation of this (d) ATP-binding site induces a conformational change that results in heptamerization. The resultant exposure of the Apaf-1 caspase activation and recruitment domain (CARD) recruits caspase-9 into this apoptosomal complex, and the resulting induced proximity of caspase-9 molecules leads to their activation (Boatright et al., 2003)

Neurodegenerative diseases are characterized by the progressive death of neurons and result in memory loss, movement problems, cognitive deficits, emotional alterations and behavioral problems. Neurodegenerative disorders affect neural activities at many levels. Neurodegenerative disorders can disrupt molecular pathways, synapses, neuronal

subpopulations and local circuits in specific brain regions, as well as higher-order neural networks. Abnormal network activities may result in a vicious cycle, further impairing the integrity and functions of neurons and synapses, for example, through aberrant excitation or inhibition. Neurodegenerative conditions are the result of multiple specific processes, many of which are related to the cellular signaling events specific to the brain. Neuronal cell death via apoptosis is believed to be one of the chief events involved in Alzheimer's disease (AD), other neurodegenerative diseases (Cotman et al., 1995; Eckert et al., 2003; Friedlander et al., 2003; Nijhawan et al., 2000; Yuan et al., 2000).

Cholesterol homeostasis breakdown is the unifying primary cause and the major target for therapy of sporadic and familial AD, neuromuscular diseases, Niemann-Pick type C disease and Down syndrome. Recent work has shown neuronal cholesterol accumulation in early postnatal NPC1- deficient mice, suggesting a primary role for cholesterol in brain (Reid et al., 2004).

Niemann-Pick disease type C (NPC) is a hereditary autosomal recessive lipid storage disorder characterized by cholesterol accumulation in the liver, spleen, and central nervous system and progressive neurodegeneration and premature neuronal cell loss (Patterso et al. 2001).Mutations in two independent genes result in the clinical and biochemical NPC phenotype (Vanier MT, et al., 1996). NPC disease is biochemically distinct from Niemann-Pick disease type A and type B, which are caused by genetic defects in sphinogomyelinase activity (Brady et al., 1966). This disorder is caused by mutation in the NPC1 gene in about 95% of the cases, or in the NPC2 gene in the rest of

5% cases. The human NPC1 gene was identified and cloned three decades ago (Carstea et al. 1997).

The NPC1 disease gene encodes a 1278 amino acid, polytopic protein with 13 transmembrane domains. The region between amino acids 615 and 797 shares approximately 30% identity with the sterol-sensing domains (SSD) of 3-hydroxy-3-methylglutaryl CoA (HMGCoA) reductase, SREBP cleavage-activating activating protein (SCAP), and Patched (Davies and Ioannou , 2000).

The amino terminus contains a region with a leucine zipper motif (amino acids 55–165) that is highly conserved among NPC1 orthologs and is referred to as the NPC1 domain. Within NPC1 there is a large, cysteine-rich luminal loop (amino acids 855–1098), which contains a ring-finger motif that may mediate protein– protein interactions (Watari et al., 2000).

NPC1 also possesses a carboxyl-terminal dileucine motif that is required for proper targeting of the protein to the endocytic pathway (Watari et al. 1999).). Studies of the subcellular distribution of NPC1 localize the protein to a late endosomal compartment that is lysosome-associated membrane protein-2 positive, Rab7 positive, and cation-independent mannose-6-P receptor negative (Frolov et al. 2001; Higgins et al., 1999; Neufeld et al. 1999; Zhang et al. 2001a). Messenger RNA encoding NPC1 is present in neurons in vivo, with remarkable regional differences in the expression level (Falk T, 1999; Prasad A, 2000). The subcellular localization of the NPC protein has showed

depending on the adaptor complex AP-3 (Berger et al, 2007). NPC1 could function as a cholesterol pump, or it could affect localization of another lipid with cholesterol following passively. Recent reports showed that NPC1 protein influences the delivery of cholesterol to the sterol regulatory element binding protein (SREBP):SREBP cleavage activation protein (SCAP) complex (Guo et al., 2008), purified NPC1 protein bound cholesterol and oxysterols to a 1278-amino acid membrane protein (Infante et al., 2007).

The NPC2 disease gene encodes a 132 amino acid-soluble lysosomal protein that was identified through a proteomic survey of the lysosome (Naureckiene et al. 2000).

NPC2 is a soluble cholesterol-binding protein in the lumen of late endosomes and lysosomes (Naureckiene et al., 2000; Ko et al., 2003). Because late endosomes have internal membranes, NPC2 could transfer cholesterol from these to the limiting membrane, where cholesterol efflux occur (Prinz 2002). The NPC2 protein has been shown to specifically bind cholesterol with a 1:1 stoichiometry and submicromolar affinity (Friedland 2003; Ko et al., 2003), although it has no apparent homology with other cholesterol binding proteins, such as sterol carrier protein 2, caveolin, StAR protein, or MLN64. The structure of the apo form of bovine NPC2 has been solved, revealing an immunoglobulin-like fold that is stabilized by three disulfide bonds, as well as a pocket that has been proposed to bind cholesterol (Friedland et al. 2003). Mutational analysis of residues surrounding this hydrophobic pocket has identified single amino acid substitutions that prevent both cholesterol binding and restoration of cholesterol trafficking in NPC2 mutant cells (Ko et al. 2003).

The NPC phenotype can also be reproduced by treatment of normal cells with steroids like progesterone or with hydrophobic amines (class II amphiphiles) like U18666A. The mechanism of U18666A action is unknown, a putative membrane protein-binding site has been described but not identified (Underwood et al., 1996).

1.3 Endocytotic pathway and Rab proteins

Members of the Rab family of small GTPases are involved in multiple trafficking events in both endocytotic and biosynthetic pathways, and are located in specific intracellular compartments. During dynamic trafficking processes, Rab domains get into contact via their effectors, generating directional Rab cascades which can result in Rab conversion accompanying cargo transport and organelle maturation.

Rab proteins and Rab-associated proteins play their important role in hypopigmentation (Griscelli syndrome), eye defects (Choroideremia, Warburg Micro syndrome and Martsolf syndrome), disturbed immune function (Griscelli syndrome and Charcot-Marie-Tooth disease) and neurological dysfunction (X-linked non-specific mental retardation, Charcot-Marie-Tooth disease, Warburg Micro syndrome and Martsolf syndrome). Alterations in Rab function play an important role in the progression of multifactorial human diseases, such as infectious diseases and type 2 diabetes (Corbeel and Freson, 2008).

The rabs, which are related to ras GTPase, are involved in regulating vesicular traffic. They are a large family in eukaryotes, with approximate 60 rabs in the human genome (Sabra et al., 2002). Rab proteins are regulators of membrane traffic. They act by cycling between GTP-bound active states to GDP-bound inactive states. When Rabs are bound to GTP, they recruit other proteins to membranes that regulate vesicle budding, the selection of cargo, vesicle docking, and fusion (Edinger et al., 2003), and inactivation by GAPs (Grosshans et al., 2006; Pfeffer and Aivazian, 2004; Zerial and McBride, 2001).

Individual rab proteins are found on distinct organelles of the secretory and endocytic apparatus, suggesting that each protein controls a different step of membrane traffic. The endocytic pathway can be dissected into three distinct Rab-specific stages; the (early) endosome (Rab5), the sorting/recycling endosome (Rab4, Rab11), and the lysosome/vacuole as the target organelle for degradation (Rab7). Clathrin coated vesicle (CCV) mediated transport in the early endocytic pathway is regulated by Rab5, whereas recycling processes, during which internalized material is transported back to the plasma membrane, are regulated by Rab4 at the level of the early endosome and Rab11 on recycling endosomes. Rab domains on organelles are not static, but merge in a dynamic manner during protein transport (Pfeffer et al., 2003; Zerial et al., 2001; Zhao et al., 2002). However, many of the details of rab function are not fully understood.

Rab7 functions in the endocytic pathway of mammalian cells by regulating traffic from early to late endosomes and lysosomes. It has previously been shown that interfering with rab7 function inhibits this transport step, thereby blocking traffic from the cell surface to

lysosomes and preventing lyosomal degradation (Feng et al., 1995; Vitelli et al., 1997). A key role of rab7 may be the regulation of the level of functional proteins at the cell surface. Even if this activity is not necessary for cell survival, it may well be required for the other function of cells in tissues and organs (Edinger et al., 2003). Evidence from a study of osteoclast polarization and bone resorption also showed Rab7, a small GTPase that is associated with late endosomes, is highly expressed and is predominantly localized at the ruffled border in bone-resorbing osteoclasts. The late endocytotic pathway is involved in the osteoclast polarization and bone resorption, in which Rab7 is important in osteoclast function (Zhao et al., 2001).

Overexpression of wild-type Rab7 or Rab9 (but not Rab11) in Niemann-Pick type C lipid storage disease fibroblasts resulted in correction of lipid trafficking defects, including restoration of Golgi targeting of fluorescent lactosylceramide and endogenous GM(1) ganglioside, and a dramatic reduction in intracellular cholesterol stores (Choudhury et al., 2002). Similar result was shown by Narita et al. that correction of membrane traffic in NPC cells by Rab9 overexpression that may lead to new therapeutic approaches for treatment of this disease (Narita et al., 2005).

Cholesterol contributes to regulate the Rab7 cycle, and that Rab7 in turn controls the net movement of late endocytic elements. Motor functions can be regulated by the membrane lipid composition via the Rab7 cycle (Lebrand et al., 2002; Gurenberg et al., 2002)

Along the endocytic pathway, Rab5a is a rate-limiting catalyst of internalization, and Rab7 controls trafficking through late endosomes to lysosomes. Rab5a and Rab7 in autonomous thyroid adenomas (where the cAMP cascade is constitutively activated). Particulate Rab7 and iodine shifted toward lysosomal fractions, indicating that progression along the degradation pathway also was promoted. Thyroid-stimulating hormone or forskolin increased Rab5a and Rab7 but not Rab8 expression. This result suggested that thyroid-stimulating hormone, via cAMP, enhances the expression of Rab5a and Rab7, which promote Tg endocytosis and transfer to lysosomes, respectively, resulting in accelerated thyroid hormone production (Croizet-Berger et al., 2002).

Rab11-mediated ERC cholesterol accumulation decreases ACAT activity about 40%, both in the presence and absence of LDL, but does not affect esterification of cholesterol delivered directly to the PM (Holtta-Vuori et al., 2002).

In yeast, the Ypt1 protein (a homolog of human Rab1) functions at the ER-to-cis Golgi and cis-to-medial Golgi trafficking step, Ypt31 and its homolog Ypt32 (both homologs of human Rab11) are important for the exit from the Golgi apparatus, and the Sec4 protein controls the traffic of vesicles from the trans-Golgi network (TGN) to the plasma membrane (Cao et al., 1998; Guo et al., 1999; Ortiz et al., 2002; Suvorova et al., 2002).

Evidence for a Rab–tether cascade from the Golgi to the plasma membrane has been presented. On the secretory vesicles, Ypt32 recruits Sec2, to exocytic vesicles, which in turn can recruit the Rab Sec4 to drive exocytosis Sec4-GTP then binds to the exocyst, a

large eight-subunit complex that tethers vesicles to the plasma membrane (Guo 1999; Ortiz 2002).

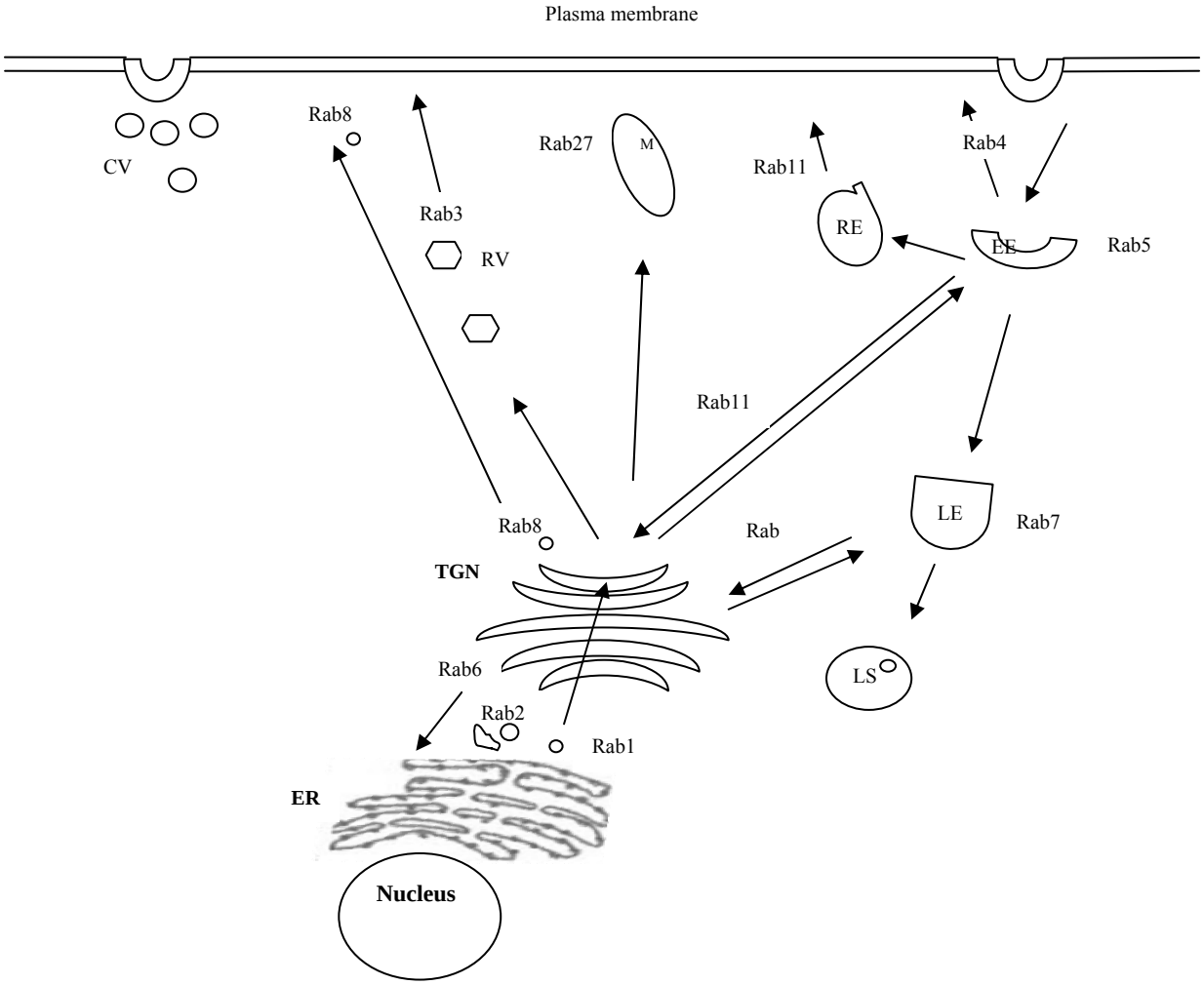

Figure 1.1 Rab proteins involved in different vesicles transportation.
ER: endoplasmic reticulum; TGN: *trans*-Golgi network; CV: constitutive secretory vesicles; RV: regulated secretory vesicles; M: melanosomes; EE: early endosomes; LE: late endosomes; RE: recycling endosome; LS: lysosomes.

1.4. Cellular signaling and cAMP

Cyclic AMP is generated by adenylyl cyclases from ATP and is degraded by phosphodiesterases (Tasken and Aandahl, 2004). Mammals express one soluble and nine transmembrane isoforms of adenylyl cyclase (Chen et al., 2000; Cooper, 2003).Cell permeable analogues of cAMP have been shown to improve the survival of cells (Michel et al., 1996; Nakao 1998; Schildberg et al., 2005; Vaudry et al., 1998).

Promotion of cell survival by cAMP or forskolin could be via ERK1/2 signaling. ERKs are members of the mitogen-activated protein kinase superfamily, have been well characterized and are known to be involved in cell survival (Jiang et al., 2005; Jin et al., 2002; Park and Cho 2006; Passeron et al., 2008; Zhang and Abdel-Rahman 2008).

Especially, ERKs are involved in a wide range of neuronal functions including differentiation, synaptic plasticity, survival, migration (Thelen et al, 2002), and long-term changes in gene expression (Hevroni et al., 1998) that may underlie aspects of learning and memory (Impey et al., 1999. Gobert D, 2008). For example, cAMP signaling can regulate the sensitivity of the axon to netrin-1 or cause it to switch from being an attractant to a repellent cue (Ming et al., 1997; Hopker et al., 1999; Moore and Kennedy, 2006). Axons of developing mammalian neurons contain mRNA encoding the cAMP-responsive element (CRE)-binding protein (CREB). CREB is translated within axons in response to nerve growth factor (NGF) and is retrogradely trafficked to the cell body. Axonal derived CREB enables specific transcriptional responses to signaling events at

distal axons which promotes neuronal survival (Llewellyn JC, et al., 2008). It has also suggested that the elevation of intracellular cAMP level promotes the trophic responsiveness of axotomized RGCs. Thus, different neurotrophic factors, such as a brain derived neurotrophic factors and ciliary neurotrophic factor, have been used in combination with cAMP to promote the survival of axotomized RGCs (Cui 2003; Mansour-Robaey 1994; Watanabe 2003). Cilostazol was reported to promote survival of axotomized retinal ganglion cells in adult rats. The main pharmacological effect of CLZ is to increase the intracellular cAMP level by blocking the hydrolysis of cAMP by phosphodiesterase-3 (Kashimoto et al., 2008). Elevation of cAMP in mesenchymal stem cells transiently upregulates neural markers and improve cellular adaptation to changes in culture conditions (Rooney et al., 2008).

On the contrary, increased cAMP levels enhanced Bax translocation to the mitochondria, resulting in the release of cytochrome c, caspase-3 activation, and apoptosis induction (Hsiung et al., 2008). cAMP increased the spontaneous release and decreased the KCl-induced release of [3H]-1-methyl-4-phenylpyridinium and dopamine and suggested that cAMP impairs the vesicular monoamine transporter (Ribeiro et al., 2002).

1.5. Current therapeutic strategies on NPC1 disease

Attempts at therapy on Niemann–Pick Type C disease to date have focused on reduction of the accumulating molecules that are presumed to have direct or indirect toxic effects

and such therapeutic approaches to bypass the cholesterol trafficking defect in NPC1 disease might delay disease progression.

Inhibition of glycosphingolipids (GSLs) synthesis in NPC cells with N-butyldeoxygalactonojirimycin led to marked decreases in GSL but only small decreases in cholesterol levels. Both annexin 2 and 6, membrane-associated proteins that are important in endocytic trafficking, show distorted distributions in NPC cells. Altered BODIPY lactosylceramide targeting, decreased endocytic uptake of a fluid phase marker, and mistargeting of annexin 2 (phenotypes associated with NPC) are reversed by inhibition of GSL synthesis. It is suggested that accumulating GSL is part of a mislocalized membrane microdomain and is responsible for the deficit in endocytic trafficking found in NPC disease (te Vruchte et al., 2004). Study showed partial blockage of sterol biosynthesis with a squalene synthase inhibitor CP-340868 in early postnatal NPC null mice brains reduces neuronal cholesterol accumulation, reduces GM3 ganglioside accumulation, and diminishes astrogliosis in the brain but may inhibit myelin maturation (Reid et al., 2007). Recently, the oral medication miglustat has been offered as a possible therapy aimed at reducing pathological substrate accumulation on a 3-years-old NPC1 patient, but the outcome of such trial has far from conclusive (Paciorkowski et al., 2008).

Neurosteroids are necessary for neuronal and glial function, alterations in sequestration of intracellular cholesterol may result in altered neurosteroidogenesis, and subsequently alter neuronal and glial function. A few studies has used neurosteroid to treat NPC1

mouse. Neurosteroid allopregnanolone (ALLO) treated NP-C mice had substantially increased survival and delays in neurologic impairments, coinciding with marked improvements in neuronal survival, and reduction of gangliosides. These data suggest that neurosteroids play an important role in brain development and maturation and may be an effective therapy for NP-C and perhaps other lysosomal storage diseases (Mellon et al., 2004).

Langmade SJ used neurosteroid allopregnanolone (ALLO) and T0901317, a synthetic oxysterol ligand to treat on npc1 (-/-) mice. They showed ALLO and T0901317 therapy preserved Purkinje cells, suppressed cerebellar expression of microglial-associated genes and inflammatory mediators, and reduced infiltration of activated microglia in the cerebellar tissue, and this compound has the ability to activate pregnane X receptor-dependent pathways in vivo, therefore suggestion was raised that treatment with pregnane X receptor ligands may be useful clinically in delaying the progressive neurodegeneration in human NPC disease (Langmade 2006). Griffin et al. used concentration of pregnenolone, DHEA and allopregnanolone were all significantly less in brains of NP-C mice than they were in brains of age-matched wild type mice. Adult NP-C brains had significantly diminished expression of P450scc, 3βHSD, 5α reductase and 3α HSD. This reduction in expression of these neurosteroidogenic enzymes was seen in the cortex and in the cerebellum.Treatment with allopregnanolone – providing the neurosteroid in drinking water, as a timed-release pellet, and as an injection, and each treatment had some efficacy (Griffin et al., 2004). Allopregnanolone functions is by augmentation of $GABA_A$ receptor channel opening, through alteration of the kinetics of entry to and exit

from desensitized states of the receptor (Zhu et al., 1996 and 1997), and it has effect on treatment of NP-C mice, but more effective in combination with a synthetic LXR ligand (Langmade et al., 2006), however, another GABA-ergic neurosteroid, ganaxolone, treatment was not as effective.

Genetic therapy may be a potential approach to rescue neurodegeneration. Recent study showed that a prion-promoter-driven Npc1 cDNA transgene could rescue neurodegeneration in Niemann-Pick C mice and overexpression of NPC1 is not harmful to the mice (Loftus et al., 2002).

1.6. The aim and significance of this study

Cholesterol plays many well-described roles within the cell, but how cholesterol moves to and from key organelles to perform these roles is not as well-known. The cellular mechanism for loss of neurons of the central nervous system (CNS) under NPC phenotype is still under investigation. Most current models of NPC involve defective or slowed cholesterol efflux from late endosomes, but the precise defect is unknown. It is not known whether cholesterol accumulation and neuronal apoptosis caused by progesterone or U18666A treatment affects adversely the mitochondrial functions, and if so whether mitochondrial dysfunction triggers the cascade of neuronal apoptosis. Attempts at therapy on Niemann–Pick Type C disease to date have focused on reduction of the accumulating molecules that are presumed to have direct or indirect toxic effects and such therapeutic approaches to bypass the cholesterol trafficking defect in NPC1 disease might delay disease progression. Few reports that genetic intervention on NPC1 could be a potential approach to rescue neurodegeneration. Our study aims to contribute to the understanding of cholesterol in the process of neurodegeneration and the development of effective prevention and therapeutic intervention for neurodegenerative diseases.

In this project, the following studies will be carried out:

(1) The effect of progesterone and U18666A on cholesterol homeostasis of primary cultured embryonic cortical neurons and the consequence of such cholesterol accumulation and sequestration.

(2) The mechanism of intracellular cholesterol accumulation induced neuronal apotosis.

(3) The effect of cAMP and forskolin on rescue of neuronal injury induced by U18666A.

(4) The mechanism of restoration of cholesterol homeostasis.

Chapter 2. Materials and Methods

2.1. Chemicals

Progesterone, taurine, poly-D-lysine, butyl-cyclic AMP, forskolin and mouse monoclonal anti-ß-actin antibody, and minimum essential medium eagles purchased from Sigma (St. Louis, MO).

3β-[2-(diethylamino) ethoxy] androst-5-en-17-one (U18886A) was from BioMol (Plymouth Meeting, PA).

Neurobasal™ (NB) growth medium, B27 supplement, glutamax-I, Alex Fluor® secondanary antibodies, EnzChek® caspase-3 assay kit, MitoTracker® Green, propidium iodide, Hoechst 33342 and mouse monoclonal anti-COX-IV antibody were from Invitrogen (Grand Island, NY).

Protein assay kit was obtained from Bio-Rad (Hercules, CA). Polyvinylidene difluoride (PVDF) membranes and SuperSignal enhanced chemiluminescence's reagent were bought from Pierce (Rockford, IL).

Mouse monoclonal anti-cytochrome c and anti-MAP2 antibodies, rabbit polyclonal anti-Rab5, anti-Rab7, anti-Rab9 and anti-Rab11 antibodies were obtained from Santa Cruz Biotechnology (Santa Cruz, CA).

Mouse monoclonal anti-caspase-3 and anti-nucleoporin P62 antibodies were from BD PharMingen (San Diego, CA).

Rabbit polyclonal anti-AIF, mouse monoclonal anti-Smac/Diablo and anti-caspase-9 antibodies, Rabbit polyclonal anti-phosphoERK and non-phosphoERK were purchased from Cell Signaling Technology (Beverly, MA).

The *in situ* cell death detection kit (TUNEL), protease inhibitor and phosphotase inhibitor were from Roche (Basel, Switzerland).

Caspase-3 specific inhibitor Z-DEVD-FMK was obtained from Merck (Darmstadt, Germany)

2′-Amino-3′-methoxyflavone (PD98059) and fluor^{TM} save reagent was from Calbiochem (San Diego, CA).

3-(4, 5-dimethylthiazol-2-yl)-2, 5-diphenyl tetrazolium bromide (MTT) was from Duchefa (Harlem, The Netherlands).

The ApoGlow Rapid Apoptosis Screening Kit was from Cambrex (East Rutherford, NJ).

BCS scintillation cocktail was purchased from Amersham (Little Chalfone, Buckinghamshire, England).

Rabbit anti-goat IgG HRP conjugated, goat anti-mouse IgG HRP conjugated, Goat anti-rabbit IgG HRP conjugated, prestained broad range precision protein standards, ammonium persulfate, acrylamide/Bis solution, Bromophenol blue and RC DC protein assay kit were purchased from Bio-Rad (Hercules, California).

2.2. Instruments and other general comsumables

The instruments and general consumables used in this work include

BECKMAN LS6000 Scintillation Counter (Beckman Coulter, Inc., 4300N. Harbor Boulevard, Fullerton, CA),

Biological Safety Cabinet Class II (Gelman Science Inc., Washtenaw County Circuit Court),

CO_2 Incubator (Heraeus Kulzer Australia Pty Ltd., Unit 3, 4 Gibbes Street, Chatswood, Australia),

Dry-Bath (Medical Research Council, 20 Park Crescent, London, W1B 1Al, UK), Eppendorf Centrifuge 5810R (B.BRAUN, postfach 1120, 34209 Melsungen, Germany), pH meter (Beckman Coulter),

OLYMPUS IX71 Fluorescence Microscope, OLYMPUS FV300 and FV500 laser scanning confocal microscope (Olympus Technologies Singapore Pte Ltd, 41 Science Park Road, #04-17/18, The Gemini, Singaproe Science Park II, Singapore), Orbital Shaker 100 (ARMALAB, LLC, Bethesda, MD),

Oven, Water Bath (MEMMERT, GmbH Co. KG, Schwabach, Germany),

PowerPac Basic Power Supply 100 (Bio-Rad Laborateories, 2000 Alfred Nobel Drive, Hercules, California),

Vortexer (VWR Scientific, 1310 Goshen Parkway, West Chester, PA),

Ultrasonic Water Bath (ITS Science and Medical, 219 Henderson Road, Henderson Industrial Park, Singapore),

Blue MAXIM Polypropylene conical tube, Serological Pipette (Becton Dickinson Labware, Becton Dickinson and Company, Franklin Lakes, NJ, USA),

Fast Turn Cap Mini PolyQ Vial (Beckman Coulter, Inc., 4300 N. Harbor Boulevard, Fullerton, CA),

NUNC culture paltes and flask (NUNC, Apogent Company, NUNC A/S Kamstrupvj, Roskilde, Denmark).

2.3. Primary cell culture

2.3.1. Animal

Swiss Albino mouse, pregnant with estimated 15 days gestation, were housed in NUS animal holding unit.

2.3.2. Isolation and digestion media

The isolation and digestion media for neuronal cells were prepared as followings:
Hank's balanced salt solution (HBSS) was purchased from Invitrogen. Solution I was HBSS medium with 0.3% BSA (w/v) and 1.2 mM $MgSO_4$. Solution II was HBSS medium with 0.02% trypsin (w/v), 0.3% BSA (w/v), 0.0008% (w/v) DNaseI and 2.7 mM $MgSO_4$. Solution III was HBSS medium with 0.05% soybean trypsin inhibitor (w/v), 0.3% BSA, 0.0008% DNaseI (w/v) and 2.7 mM $MgSO_4$. Solution IV was HBSS medium with 0.008% soybean trypsin inhibitor (w/v), 0.3% BSA, 0.0008% DNaseI (w/v) and 1.44 mM $MgSO_4$. All solutions were filtered through 0.2 μm filter unit.

2.3.3. Culture medium

Neuronal plating medium

Dulbecco's Modified Eagle Medium supplemented with heat inactivated fetal bovine

serum (10%, v/v), glutamine (2mM), penicillin (100 unit/ml) and streptomycin (100 µg/ml).

Neurobasal with B27 medium

Neurobasal™ medium supplemented with B27 (2%, v/v), glutamax-I (0.025%, v/v), penicillin (100 unit/ml) and streptomycin (100 µg/ml).

2.3.4. Isolation procedure

The Brains were obtained from E15 embryos and meninges were removed The neocortices were then dissected from the brains (Figure 2.1).

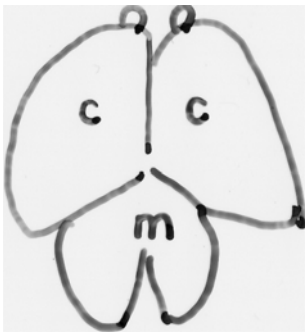

Dorsal view of isolated brain.
c: cerebral hemisphere; m:midbrain

↓

The meninges were striped away by forceps. Left and right hemispheres were separated by a blade.

↓

Medial view of left part of brain.
c: cerebral hemisphere; m: midbrain;
t: thalamus.

The midbrain and thalamus were removed by forceps.

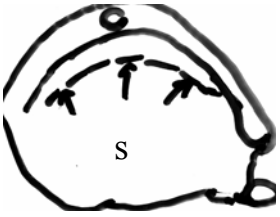

Medial view of cerebral hemisphere.
s: basal ganglia.

Cut through the dotted line to remove hippocampus.

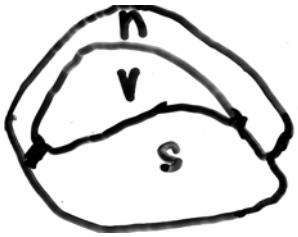

Mdical view of cerebral hemisphere after hippocampus were removed. n: neocortex; v: ventricle; s: basal ganglia.

Neocortex was separated from the basal ganglia by forceps.

Medial view of neocortex separated from the basal ganglia, except for its most posterior part.

The neocortex was completely separated from the basal ganglia and was now ready for trypsin digestion.

Figure 2.1 Flowchart showing the procedures of neocortex isolation from murine embryonic brain.

The neocortices were collected into 50 ml of solution I and centrifuged at 1000 rpm for 1 min at 15°C. The supernatant was discarded, and 20 ml of solution II were added to the pellet. The neocortices were incubated in 37°C water bath for 5 min.

Twenty ml of solution IV were then immediately added into the tube to prevent over digestion. The neocortices were centrifuged at 1000 rpm for 5 min at 15°C. Supernatant was discarded and 20 ml of solution III were added to the tube. A syringe (20 ml in size) fitted with a 14 G needle was used to dissociate neurons by gently aspirating for 10

strokes. The neuronal cell suspension was transferred to a new tube by Gilson 1ml pipette and the last 0.3ml of cell suspension at the bottom of tube was discarded.

The neurons were then centrifuged at 1000 rpm for 5min at 15°C. The collected neurons were resuspended with plating medium and the cells were ready for counting and seeding. The neurons were cultured in neurobasal and B27 medium from day one *in vitro* (DIV1) onward.

2.3.5. Culture vessels

Poly-D-lysine (PDL) was used to coat the surface of culture vessels. 0.1mg/ml PDL in double distilled H_2O was filtered through 0.2 nm filter unit and 2 ml, 1ml, and 0.5ml of PDL was applied to each well of 6-well, 12-well, and 24-well culture plate, respectively. The plates was left in CO_2 incubator overnight, and washed with double distilled H_2O three time. After air-dried, the PDL coated plate was ready to use. Similar procedure was applied to coating coverslips, except that the PDL concentration is 1.0 mg/ml for coating coverslips.

2.3.6. Cell counting and seeding

Trypan blue stain (Sigma) and a hemocytometer was used to determine total cell counts and viable cell numbers. Trypan blue is one of several stains recommended for use in

exclusion procedures for viable cell counting. This method is based on the principle that live cells do not take up the dye, whereas dead cells do.

A cell suspension in neuronal plating medium, was mixed with same volume of 0.4% (w/v) trypan blue solution (dilution factor = 2), which was then stood for 5-15 min.

With the coverslip in place, a small amount of trypan blue stained cell suspension mixture was transferred to both chambers of the hemocytometer (Bright line counting chamber, Hausser Scientific, Horsham, PA). While transferring the cell suspension, the edge of the coverslip was carefully touched with the pipette tip and allowed each chamber to fill by capillary action.

The cells were counted in the two 1 mm center square and eight 1 mm corner squares. Each square of the hemocytometer, with coverslip in place, represents a total volume of 0.1 mm^3 that is equivalent to approximately 10^{-4} ml. Therefore, cells per ml = the average count per square x dilution factor x 10^4.

2.3.7. Cell viability assay

Cell viability was measured by the MTT method (Hansen *et al*., 1989). In brief, MTT (500 μg/ml) was added to cells and incubation was continued for 30 min at 37ºC. The culture medium and MTT in excess were removed and dimethyl sulphoxide (DMSO) was added to extract the MTT formazan formed by mitochondrial dehydrogenases which are

active only in live cells (Denizot and Lang, 1986; Hansen *et al*., 1989). Absorbance of the homogeneous extracts was read at 550 nm with a microplate reader (SpectraMax190, Molecular Devices). Cell viability was normalized relative to the control cells, whose viability was taken as 100%, treated for the same period with the corresponding vehicle (0.03% ethanol + 0.02% DMSO).

2.3.8. Cell treatment

The neurons were cultured in neurobasal and B27 medium from DIV1 onward.

Neurons were treated with progesterone (50 μM) or U18666A (2 μg/ml) in the presence or absence of Taurine (20 μM), cAMP (0.3 mM), forskolin (20 μM) and/or PD98666A (20 μM). The detail time-course study described in each result.

2.4. Cell line culture

2.4.1. Cell source

NPC1 fibroblasts ($npc^{-/-}$, GM3123) were purchased from Coriell Institute for Medical Research. .

2.4.2. Culture media

Complete EMEM medium

Minimum Essential Medium Eagles supplemented with heat inactivated fetal bovine serum (15%, v/v), Glutamine (2mM), penicillin (100unit/ml) and streptomycin (100μg/ml)

Delipidated EMEM medium

Minimum Essential Medium Eagles supplemented with 15% (v/v) heat-inactivated lipoprotein deficient serum (LPDS), Glutamine (2mM), penicillin (100unit/ml) and streptomycin (100μg/ml)

Serum free medium

Minimum Essential Medium Eagles supplemented with Glutamine (2mM), penicillin (100unit/ml) and streptomycin (100μg/ml)

Frozen medium

Minimum Essential Medium Eagles supplemented with 40% (v/v) heat inactivated fetal bovine serum with 10% DMSO and 2 mM-L glutamine.

2.4.3. Buffer

Cell lysis buffer

10 mM Tris/HCl (pH 7.4), 1 mM EDTA, 150 mM NaCl, 1% NP-40, 0.5% dexocycholate, 1% SDS and 2% protease inhibitor cocktails

1x PBS buffer

1.76 mM KH_2PO_4, 10 mM Na_2HPO_4, 137 mM NaCl, 9 mM KCl, pH7.4

Trypsin-EDTA

0.05% trypsin and 0.02% EDTA

2.4.4. Initiating a cell line

EMEM growth medium (10ml) in NUNC T75 flask was pre-equilibrated in 37^{o}C CO_2 incubator. The class II culture hood was irradiated with ultraviolet rays for 15 min. All pipettes, centrifuge tubes and culture flasks were sterilized.

The cells were removed from the liquid nitrogen tank and placed in 37^{o}C water bath immediately. After being thawed, the cells were rapidly transferred into centrifuge tube containing 10ml EMEM growth medium and were centrifuged at 300g for 5 min at room temperature.

The supernatant was discarded and the cells were resuspended in 5 ml EMEM growth medium and transferred into the pre-equilibrated EMEM growth medium in T75 flask. The cells were then placed into CO_2 incubator with a setting of 37^{o}C in a humidified atmosphere containing 5% CO_2.

The cells were passaged when the cells were about 80-90% confluence.

2.4.5. Passaging cells

The cells in a T75 flask were washed once with warm PBS buffer before trypsinization. The cells were then added with 2 ml trypsin-EDTA and were incubated at 37^{o}C for 5min. The action of trypsin-EDTA was stopped with 10 ml complete EMEM medium and the cells were gently dislodged and resuspended. Twenty percents of the resuspended cells were transferred to a new T75 flask with 15ml fresh complete MEME medium and the cells were incubated in the cell culture incubator.

2.4.6. Frozen cells

The subconfluent cells were trypsinised and spun at 300g for 5 min at 4^{o}C. The cell pellet was resuspended in the freezing medium and store in NUNC cryovial, followed by placing in ice for 30 min, -20^{o}C 2 hr, and -80^{o}C overnight. The cells were then transferred to liquid nitrogen tank.

2.4.7. Treatment

Cells were subcultured when they grew to 80% confluence. Subcultured cells were seeded into 6-well NUNC plate, at a density of $1x10^5$ viable cells per well. After 24h hour, cells were treated with LDL (50 μg/ml) in the presence or absence of other reagents such as cyclic AMP and forskolin for up to 48h as indicated in the results. Control cells were incubated with LPDS EMEM medium. Cells were also treated with cAMP (0.3 mM) or forskolin (20 μM), details indicated in the results.

2.5. Apoptosis Assay

2.5.1. Terminal transferase dUTP nick end labeling (TUNEL)

The primary cortical neurons were stained for apoptotic DNA fragmentation with the *in situ* cell death detection kit (TUNEL) according to the manufacturer's instructions (Roche, Basel, Switzerland). The neurons were treated with progesterone (50 μM), U18666A (2 μg/ml) or the corresponding vehicle (0.03% ethanol + 0.02% DMSO) for 72 h and fixed with 4% paraformaldehyde in PBS (pH 7.4) for 1 h at 25°C and then incubated in the permeabilization solution (0.1% Triton X-100 in 0.1% sodium citrate) for 2 min on ice after the neurons were rinsed with PBS. Subsequently, the cells were rinsed again with PBS and 50 μl TUNEL reaction mixture containing fluorescein dUTP

and terminal deoxynucleotidyl transferase (TdT) were added to each sample including the controls. The neurons were incubated for 60 min at 37^{o}C in a humidified atmosphere in the dark before viewed with fluorescence microscopy (Olympus 1X71).

2.5.2. Propidium iodide and Hoechst dye double staining

Propidium iodide (ex/em, 535 nm/617 nm) and Hoechst dye 33342 (ex/em, 350 nm/460 nm) were dissolved in PBS to 1mg/ml as stock.

Cells were treated as desired. Remove half volume of the medium, add half volume of fresh medium pre-mixed with PI and Hoechst33342 with a final concentration of 1 μg/ml of each dye. Cells were then incubated in CO_2 incubator for 5 min.

After wash with PBS, cells in PBS were immediately view under confocal microscope.

2.5.3. Caspase activity assay

The activity of caspase-3-like proteases was assayed by using the EnzChek® Caspase-3 Assay kit obtained from Molecular Probes (Eugene, OR), which measures DEVDase activity. In brief, the control and treated neurons were washed twice with PBS at 37^{o}C and harvested by centrifugation (350xg, 4^{o}C, 10 min). The pellet was resuspended in 50

μl of cell lysis buffer and incubated on ice for 30 min. The lysed cells were then centrifuged (1,000xg; 4^{o}C, 5 min) to pellet the cellular debris. The supernatant (50 μl) from each sample was transferred to individual microplate well. The specificity of the assay was verified by including Ac-DEVD-CHO inhibitor (20 μM, final concentration) in selected samples. A working solution containing the substrate Z-DEVD-AMC (100 μM) was then added to each sample and control. The fluorescence intensity was measured with the Gemini XPS microplate spectrofluorometer and normalized to the caspase activity of the control neurons.

2.6. Assessment of mitochondrial function with ATP to ADP ratio assay

The ATP/ADP ratio was measured using the ApoGlow Rapid Apoptosis Screening Kit from Cambrex (East Rutherford, NJ) based on the luciferase assay and in accordance with the manufacturer's instructions. In brief, the neurons in 96-well plate were treated for 6 – 72 h with either progesterone (50 μM) or U18666A (2 μg/ml) before 100 μl of nucleotide releasing reagent per well were added and the incubation continued for 5 min. The bioluminescence was measured ("reading A") with a LMaxII luminometer (Molecular Devices, CA) immediately after the addition of 20 μl nucleotide monitoring reagent per well. After 10 min, 20 μl of ADP converting reagent was added per well and luminescence was recorded ("reading B"). "Reading C" was obtained 5 min later and ATP/ADP ratios were calculated as A/(C-B).

2.7. Subcellular fractionation

Subcellular fractionation was performed according to the method of Wang *et al*. (2004) with slight modifications. In brief, the neurons were harvested and washed with ice-cold PBS, resuspended in hypotonic homogenation buffer containing 10mM KCl, 1.5mM $MgCl_2$, 1mM Na-EDTA, 1mM Na-EGTA, 1mM dithiothreitol, 10mM Tris-HCl, pH 7.4 with protease inhibitor mixture (Roche, Basal, Switzerland) and kept on ice for 20 min before homogenized with 20 strokes with a Dounce homogenizer. The extent of cell lysis (~80%) was confirmed in preliminary experiments with a light microscope. The homogenate was centrifuged at 150xg for 5 min at 4°C to remove unbroken cells, and followed by 720x*g* to obtain the pellet of nuclei. The "nuclear" fraction was washed twice with 250 mM sucrose in hypotonic buffer. The post-nuclear fraction was further centrifuged at 10,000x*g* for 30 min at 4°C, and the supernatant was collected as the "cytosolic" fraction, while the pellet was collected as the "mitochondrial" fraction. The subcellular fractions were then analyzed by SDS-PAGE and Western blot for cytochrome c, AIF and Smac/Diablo (see "Western blot analysis").

2.8. Sodium dodecyl sulfate polyacrylamide gel electrophoresis and Western blotting

For mitochondrial release or nuclear translocation of pro-apoptotic proteins, the samples were prepared as above. For caspase activation analysis, upregulation of Rab proteins and

phosphorylation of ERK, control cells and cells were treated with various reagent (details described in the results) and were lysed in RIPA buffer containing 10 mM Tris/HCl (pH 7.4), 1 mM EDTA, 150 mM NaCl, 1% NP-40, 0.5% dexocycholate, 1% SDS and protease inhibitors and phosphotase inhibitor (Roche, Basal, Switzerland). The cells were kept on ice for 10 min and then centrifuged at 1,000rpm for 10 min at 4ºC. The supernatant of each sample was kept for SDS-PAGE and Western blot analysis.

Cell lysates were mixed with loading buffer and heated at 100^{o}C for 5min before used

10-12% SDS polyacrylamide gels were prepared.

The precision protein standard from Bio-Rad (Hercules, CA) were used molecular weight marker. Sample (contain about 10-30 μg protein) was loaded to the gel. The gel was run at 40 volt when the dye advanced in the stacking gel. The voltage was adjusted to 100 volt once the dye appeared in the resolving gel. The electrophoresis was terminated where the dye was near the bottom of resolving gel.

The protein in the gel was then transferred to PVDF membrane with a protocol of transferring at 100 volt for one hour in a cold room or 30 volt overnight in a cold room.

The membrane with transferred proteins was blocked for 1 h in 5% skim milk at room temperature or overnight at 4^{o}C. Thereafter, the membrane was incubated with anti-

caspase-3 (dilution ratio, 1:1000), anti-caspase-9 (dilution ratio, 1:1000), anti-cytochrome c (dilution ratio, 1:1000), anti-COX-IV (dilution ratio, 1:1000), anti-AIF (dilution ratio, 1:500), or anti-Smac/Diablo (dilution ratio,1:500) antibody, anti-Rab5 (1:1000), anti-Rab7 (1:1000), anti-Rab9 (1:1000) and anti-Rab11 (1:1000), and anti-phosphoERK (1:1000) for one hour at room temperature or overnight at 4^{o}C. Washed membranes were then treated with horseradish peroxidase-conjugated anti-rabbit IgG (dilution ratio, 1:2500) or anti-mouse IgG (dilution ratio, 1:3000) for 1 h at room temperature and the enzyme was finally reacted with the SuperSignal enhanced chemiluminescence reagent (Pierce, Rockford, IL). Films were exposed to the chemiluminescence signal and developed in the dark room with a Kodak developer.

Quantitaive analysis of band density was performed with software Metamorph.

2.9. Immunocytochemitry

The cells were seeded on 13mm size coverslips in 24 well NUNC plates and were treated as desired. After treatment, the cells were fixed with 4% paraformaldehyde (PFA) for 20 min at room temperature. The PFA was quenched with 0.1M NH_4Cl for 2min and the cells were washed with PBS for three repeats of 1 min in each time.

The cells were permeabilized with 0.1% Triton-x100 (v/v) in PBS for 10min and were blocked with 5% goat serum for one hour at room temperature. After blocking, cells were incubated with anti-MAP2 (1:500) or anti-AIF (1:200) in 1% goat serum at room temperature for one hour. Cells were washed with PBS for three repeats of 5 min in each

time. Secondary antibody (Alexa Fluor ® antibody from Invitrogen) was diluted to 1:2000 in 1% goat serum, and cells were incubated for one hour at room temperature in the dark. The cells were washed with PBS for three repeats of 5 min in each time. Coverslips were mounted to the slide with FluorSave™ reagent (Calbiochem).

Slides were stored in the dark and viewed under Olympus IX71 microscope, Olympus FluoView 300 confocal microscope, or Olympus FluoView 500 confocal microscope.

2.10. Short RNA interference

Rab 7 siRNA (h) is a pool of 3 target-specific 20-25 nt siRNAs designed to knock down expression of human gene rab7. Rab7 saran (mouse) is a pool of 3 target-specific 20-25 not sinus designed to knock down expression of mouse gene rab7. Both were purchased from Santa Cruz Biotechnologies (Ding W, *et al.* 2006). A scrambled sequence of Saran (Santa Cruz Biotechnologies, Santa Cruz, CA) that has been shown not to affect any known cellular genes was used as the negative control.

Transfections of siRNA were carried out with lipofetamin2000 (Invitrogen). Cortical neurons were cultured for 5 day. At 6 day in vitro, before transfection, the appropriate amount of siRNA was diluted in 150 µl of Opti-MEM I reduced serum medium in one tube. In another tube 3 µl of Lipofectamine2000 were also diluted in 150 µl of Opti-MEM I reduced serum medium. Both of these two solutions were mixed gently by

pupating up and down. After incubation at room temperature for 5 min, these two solutions were mixed gently, and incubated for 20 min at room temperature to allow the siRNA:Lipofectamine2000 complexes to form. Cells were then rinsed with Opti-MEM I reduced serum medium once and the neurons were transfected with Rab7 siRNA (mouse) at concentration 40 pmol/ml, 0.3 ml/well of 24-well plate.

After 4 h, the transfection medium was replaced with fresh neurobasal culture medium. The neurons were harvested and analyzed 48 h after transfection.

NPC1 fibroblasts were cultured for 24 h to 60% confluence, and the same transfection procedure as done in neuron was carry out. NPC1 fibroblasts were transected with Rab7 saran (human), 40 pmol/ml, 1 ml/well in 6-well plate After 6 h, the medium was changed to fresh DMEM medium for further incubation till 48 h.

Western blot with anti-Rab7 (Santa Cruz) was used to assess the efficiency of transfection. The effect of Rab7 siRNA on cellular cholesteryl oleate formation was also examined

2.11. Thin-layer chromatography

The cells were treated with various reagents for 36h and co-incubated with [^{3}H]oleic acid (1 μCi/ml) at 37 °C for further 16 h. The labeled cells were then washed with PBS and harvested by trypsinization. Lipids in the medium and cells were extracted with

chloroform/methanol mixture (2:1) and separated by thin-layer chromatography (TLC) on a silica gel G plate with petroleum ether/diethyl ether/formic acid (100:25:2.5, v/v/v) as the developing system. The areas corresponding to cholesteryl oleate were scraped off and the radioactivity was measured by liquid scintillation counting (Kitatani, et al. 2002).

Chamber preparation

Developing solvent was prepared by mixing petroleum ether/diethyl ether/formic acid (100:25:2.5, v/v/v) thoroughly by shaking or vortex. Appropriate volume of developing solvent was added into the chamber so that it was 0.5 cm in height from the bottom of the chamber. The chamber was sealed and left for at least one hour so that the atmosphere in the chamber became saturated with the developing solvent.

TLC plate preparation

The TLC palte was cut into appropriate size. A pencil was used to draw a line across the plate one cm above the bottom of the plate. Under the line, light marks were used to indicate the names of the samples. Enough space between the samples should be left so that they would not run together, about 4 samples on a 5 cm wide plate was advised. The plates should be handled carefully so that the coating of adsorbent would not be disturbed. The plate was activated at 100^{o}C for one hour before use.

Sample preparation and application

Lipids samples were extracted with chloroform/methanol mixture (2:1, v/v) for 3 times and the organic phases were combined together and dried under nitrogen flow at room

temperature or in freezing dryer. The lipid pellet was re-dissolved in appropriate volume of chloroform/methanol (2:1, v/v). The lipid solution was then applied to the TLC plate with a microliter microcap. This was done by using a microcap to dip into the solution of the sample to be spotted, thereafter, the end of the microcap was gently touched to the absorbent on TLC plate, repeat five times on for a same sample. A total of 5 μl sample was then applied to the plate. The spot was air-dried. A non radioisotope labeled Cholesteryl oleate was used as marker. Care was taken not to disturb the coating of the absorbent.

TLC development

The prepared TLC plate was placed in the developing chamber, which was then sealed, and left undisturbed. TLC development was stopped when the solvent was about half a centimeter below the top of the plate.

Visualization of the spots

The TLC plate was taken out of the developing chamber and air-dried. The plate was sprayed with visualizing solvent and heated at $100^{o}C$ for 5 min immediately after spraying.

Cholesteryl oleate analysis

The spot representing cholesteryl oleate was scraped off. The ^{3}H radioactivity of the spot was measured by a scintillation counter.

2.12. Protein assay

Protein content was determined by using the protein assay kit from Bio-Rad (Hercules, CA) based on the Lowry method (Lowry *et al*., 1951) and bovine serum albumin was used as a standard. Protein determination was performed with Bio-Rad RC DC protein assay kit II.

2.13. Filipin staining for unesterified cholesterol

The pre-fixed cells were incubated with 50 μg/ml filipin in PBS for 30 min at 37ºC and washed with PBS then viewed under fluorescence microscope (Norman et al., 1972; Prattes, 2000).

2.14. Microscopy

The Olympus IX71 was fitted with 100W HBO lamp, condenser with long working distance universal, aperture iris diaphragm adjustable. Olympus IX71 fluorescence microscope was used to dectect filipin staining (ex/em, 338nm/480nm) in cortical neuron and NPC1 fibroblast. The images were captured and processed with software DP70.

The Olympus FluoView 300 laser scanning confocal microscope or FluoView 500 laser scanning confocal microscope was mounted with laser systems with large selection of

wavelengths: multi argon laser, krypton laser, helium-neo laser, helium-cadmium laser and ultraviolet laser. They were equipped with efficient scanning modes, i.e. XYZ scanning was used to acquire a series of confocal optical XY images through the thickness of the sample. Up to five channels of detection may be imaged simultaneously. Moreover, brightfield and differential interference contrast (DIC) images can be simultaneously recorded.

The Olympus FluoView 300 laser scanning confocal microscope or FluoView 500 laser scanning confocal microscope was used to detect the fluorescent labeling with propidium iodide (ex/em, 535 nm/617 nm); Hoechst dye 33342 (ex/em, 350 nm/460 nm); MitoTracker (ex/em, 490 nm/ 516 nm); Alexa fluor 488 (494 nm/519 nm), Alexa Fluor 596 (596nm/615nm). The images were captured and process with software of FlowView.

2.15. Statistical analysis

Statistical analyses were performed using the SPSS statistical package (version 11.0, Chicago, IL). Data were presented as mean ± SE. One-way or two-way (when indicated) ANOVA, followed by post hoc Bonferroni test, was used to estimate the significance of cell viability and other parameters in response to various treatments.

Chapter 3. Neuronal cell damage caused by disruption of intracellular cholesterol trafficking

3.1. Introduction

Niemann-Pick disease type C (NPC) is a hereditary autosomal recessive disorder characterized by progressive neurodegeneration and premature neuronal cell loss (Patterson *et al*., 2001). Cholesterol accumulation in late endosome/lysosomes due to dysfunction of intracellular cholesterol trafficking is regarded as the major biochemical and cellular feature of this disorder (Pentchev *et al*., 1986; Liscum *et al*., 1989; Kobayashi *et al*., 1999; Mukherjee and Maxfield, 2004). In NPC1-deficient neurons, impaired cholesterol transport alters cholesterol distribution between cell bodies and axons (Karten *et al*., 2002; 2003). In particular, the amount of cholesterol within the mitochondrial membranes of NPC1-deficient mouse neurons is significantly elevated, leading to mitochondrial dysfunction and ATP deficiency (Yu *et al*., 2005).

A variety of pharmacological agents named class 2 amphiphiles such as U18666A (3-β-[2-(diethylamino)ethoxy]androst-5-en-17-one) and progesterone are widely used to induce impairment of intracellular cholesterol trafficking and cholesterol accumulation similar to NPC phenotype (Butler *et al*., 1992; Lange and Steck, 1994; Lange *et al*., 2000; Cheung *et al*., 2004). In primary neurons, inhibition of intracellular cholesterol trafficking has recently been demonstrated to cause caspase-dependent apoptosis (Cheung *et al*.,

2004). However, it is not known whether cholesterol accumulation caused by U18666A treatment affects adversely the mitochondrial functions, similar to what occurred *in vivo* (Yu *et al*., 2005), and if so, whether mitochondrial dysfunction triggers the cascade of neuronal apoptosis.

Cell death through apoptosis is considered to play an important role in a number of neurodegenerative disorders such as Alzheimer's disease (Su *et al*., 1994; Yaar *et al*., 1997), Huntington's disease (Hickey and Chesselet, 2003) and Parkinson's disease (Tatton *et al.,* 2003). Neuronal apoptosis can be induced by triggering the death receptor pathway or by activation of organelle-mediated death cascades via perturbation of intracellular homeostasis (Putcha *et al*., 2002). For example, damage to mitochondria may cause release of pro-apoptotic proteins such as cytochrome c, Smac/Diablo and AIF (Susin *et al*., 1999; Newmeyer and Ferguson-Miller, 2003; Polster and Fiskum, 2004; Uren *et al*., 2005). Once in the cytosol, cytochrome c, together with Apaf-1 (apoptotic protease-activating factor 1) and dATP/ATP, induces apoptosome-mediated caspase-9 activation, which in turn processes downstream effector caspases such as caspase-3 and causes apoptosis (Li *et al*., 1997). On the other hand, Smac/Diablo binds to and antagonizes inhibitors of apoptosis (IAPs) (Du *et al*., 2000; Verhagen *et al*., 2000). While it is widely believed that formation of apoptosome and subsequent activation of caspase-9 and caspase-3 play a prominent role in apoptotic neuronal cell death (Yuan and Yankner, 2000), apoptosis can occur via caspase-independent pathway mediated by nuclear translocation of AIF (Cregan *et al*., 2002; Wang *et al*., 2004; Cheung *et al*., 2005).

In this study, I demonstrate that exposure of primary cortical neurons to class 2 amphiphiles can induce impairment to mitochondrial function similar to what was

observed in NPC1-deficient neuronal cells. More importantly, I revealed the details of the mitochondrial apoptosis pathway induced by inhibition of intracellular cholesterol transport, which may explain the molecular mechanisms of neurodegeneration in NPC1 disease and provide clues for development of therapeutic strategies to treat this disease.

3.2. Results

3.2.1. Morphology of cultured cortical neuron and expression of MAP2

Upon attachment to the substrate, a continuous lamella extended around the cell body, on day one to day two in vitro, several neurites emerged. Some of neuron polarized and axon in some neurons formed. With longer culture days, neuronal cell body has increase in size and an extensive, intertwined network of axons and dendrites has developed (Figure 3.1).

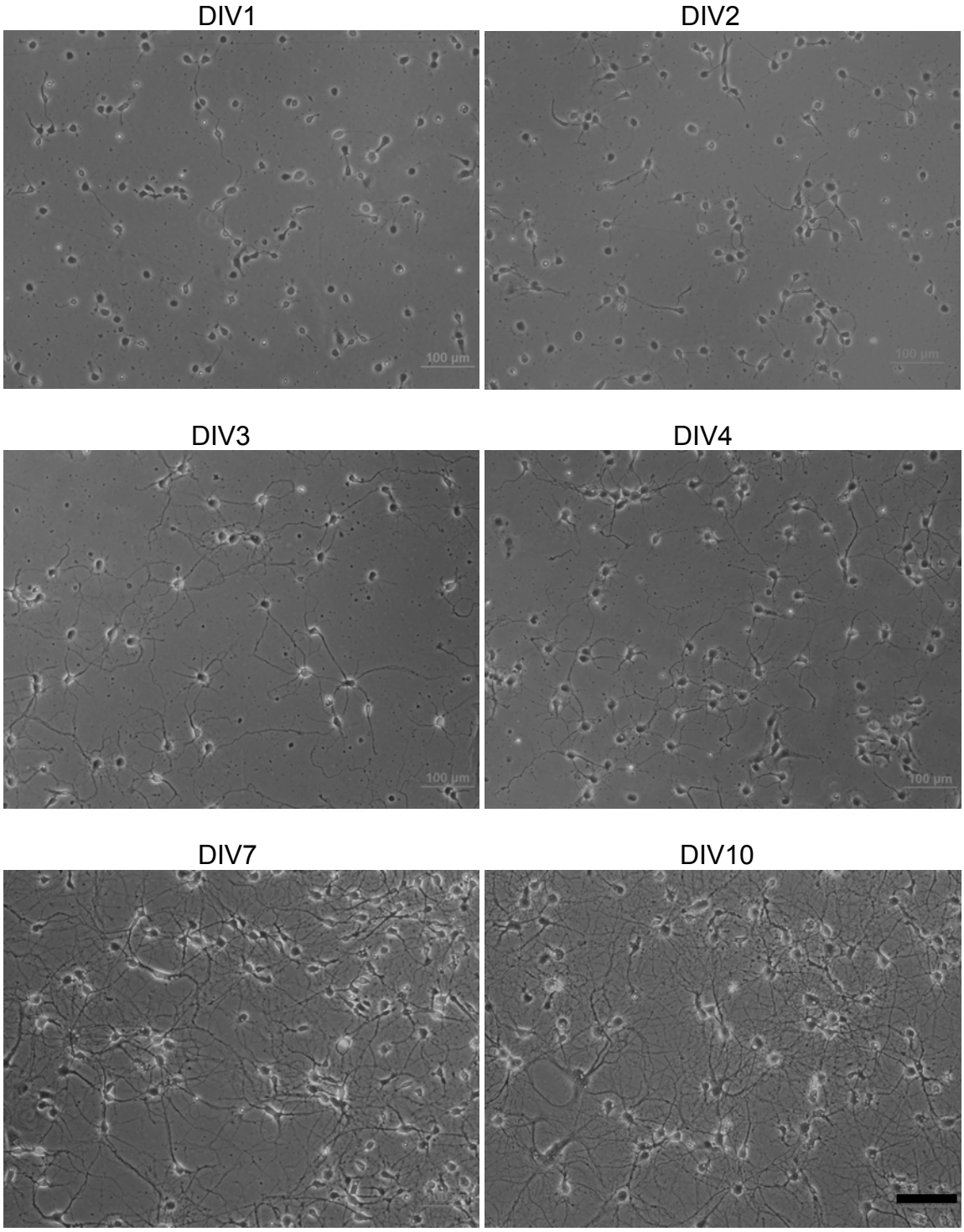

Figure 3.1 Neocortical neuron growth at different development stages by phase contrast microscopy. DIV1: Day 1 in vitro. Bar = 100 µm.

The microtubule-associated protein MAP2 is the marker of neuronal dendrite. Cortical neurons on culture day 7 *in vitro* were fixed with 4% paraformaldehye and immunostained with anti-MAP2 antibody, the secondary antibody was tagged with Fluor 488. Figure 3.2 showed that most of the cells were MAP2 positive, indicating the purity of neuron culture. Cheung et al. in their study has described the purity of culture by this method could reach 97% (Cheung et al., 1998).

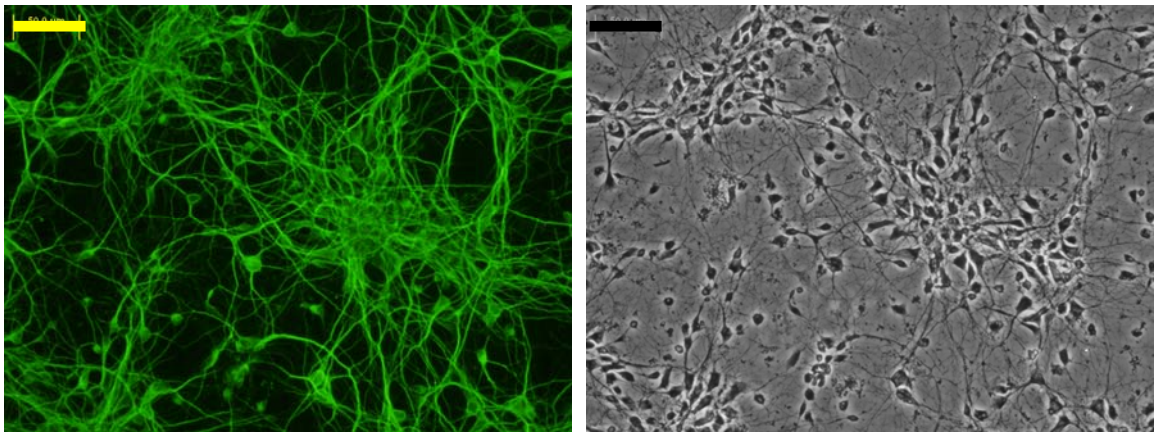

Figure 3.2 MAP2 expression in cortical neuron on DIV7. Bar = 100 μm.

3.2.2. Progesterone- and U18666A-induced apoptotic cell death in primary cortical neurons

The primary cortical neurons were treated with 0.1-50 μM progesterone for 24 h. 48 h and 72 h and the cell viability was measured by the MTT assay (Fig. 3.3 A). When progesterone concentration was relatively low (≤ 10 μM), no neuronal cell death was observed after treatment for 72 h. However, at higher progesterone concentrations (≥ 25 μM), cell viability started to decrease at 24 h after treatment and was significantly

reduced in the following 48 h. Approximately 50% of the neurons treated with 50 μM progesterone had died at 72 h. Similar amount of neurons died when treated with 2 μg/ml U18666A for 72 h. The cell death appeared to be time and dose dependent.

The nature of the progesterone-induced neuronal cell death was determined *in situ* by the TUNEL assay in which fragmented nuclear DNA is labeled by terminal deoxynucleotidyl transferase, which catalyzes polymerization of labeled nucleotides to the free 3'-OH DNA ends. The fluorescein labels incorporated are then visualized by fluorescence microscopy. As illustrated in Fig. 3.3 B, treatment with progesterone (50 μM) or U18666A (2 μg/ml) caused a marked increase in the number of TUNEL-positive neurons, compared to the control cells. Quantitative analysis showed that progesterone (50 μM) or U18666A (2 μg/ml) treatment of the primary cortical neurons for 72 h resulted in a TUNEL-positive staining for approximately 55 % of the cells (Fig. 3.3 C). The rate of cell death obtained from both MTT assay and TUNEL staining was similar, implying that the neuronal cell death was predominately of apoptotic nature. Morphological evaluation using Hoechst 33342 staining revealed that neurons undergoing progesterone- or U18666A-induced cell death displayed typical apoptotic features, including chromatin condensation and DNA fragmentation (Fig. 3.3 B). Although a substantial number of neurons were TUNEL-positive and stained by Hoechst 33342, only a small number of unfixed neurons were stained by the membrane-impermeable propidium iodide (PI) (Fig. 3.3 B). Quantitative analysis revealed that there were < 15% dead neurons detectable by PI staining after 72 h treatment with 50 μM progesterone or 2 μg/ml U18666A (data not shown), which further confirmed the apoptotic mechanism of the neuronal cell death

observed.

A.

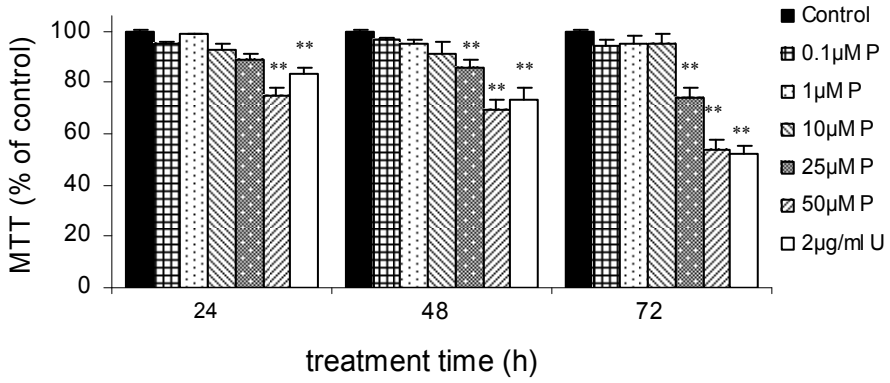
MTT (% of control)
100
80
60
40
20
0
24
48
72
treatment time (h)
Control
0.1μM P
1μM P
10μM P
25μM P
50μM P
2μg/ml U
**

B.

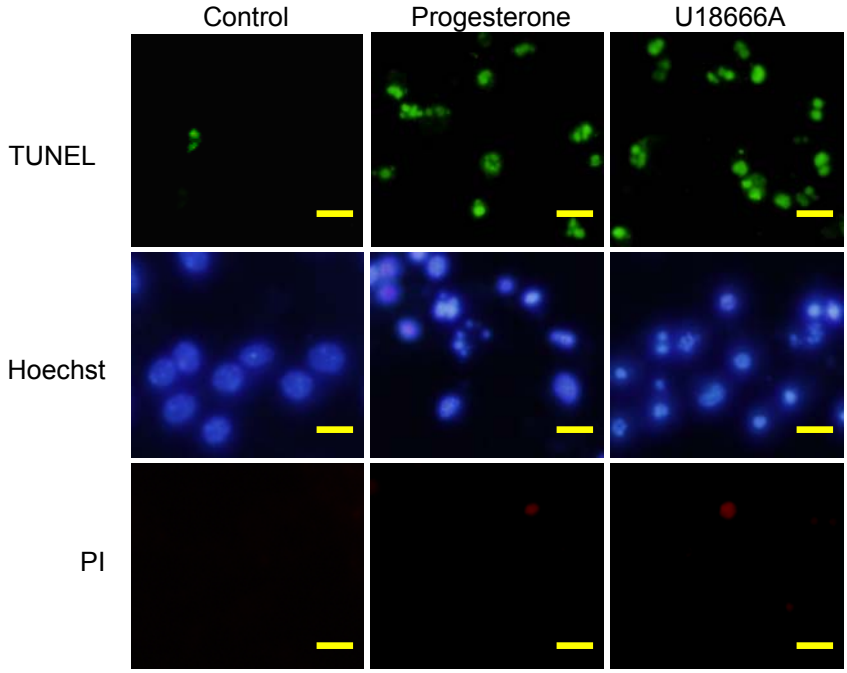
Control
Progesterone
U18666A
TUNEL
Hoechst
PI

C.

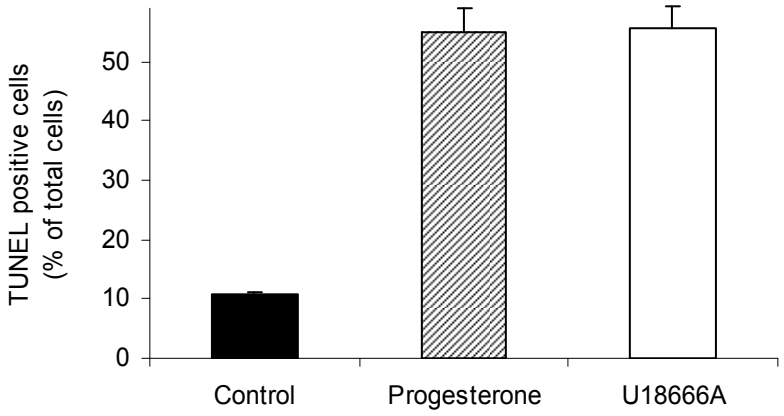

Figure 3.3 Neuronal cell death induced by progesterone and U18666A. (A)MTT assay of Neuronal cell treated with progesterone (P, 0.1-50 μM) and U18666A (U, 2 μg/ml). All Data represent the mean ± SE of three independent experiments. $^{**}p < 0.01$ versus the control for each point. (B) Top row, TUNEL assay of DNA fragmentation (green). Middle and bottom row, double-staining of cells with Hoechst 33342 (blue) and Propidium iodide (red). The cells were treated with 50 μM progesterone or 2 μg/ml U18666A for 72 h. Representative images from three independent experiments. Bar = 10μM. (C) The relative amount of TUNEL-positive cells after 50 μM progesterone or 2 μg/ml U18666A for 72 h.

3.2.3. Intracellular cholesterol accumulation

To examine whether cholesterol accumulation in the cortical neurons occurs at the earlier stage of progesterone or U18666A treatment, the unesterified cholesterol was stained with filipin and cholesterol accumulation was observed as early as 6 h after exposure of the neurons to 50 μM progesterone or 2 μg/ml U18666A (Figure 3.4).

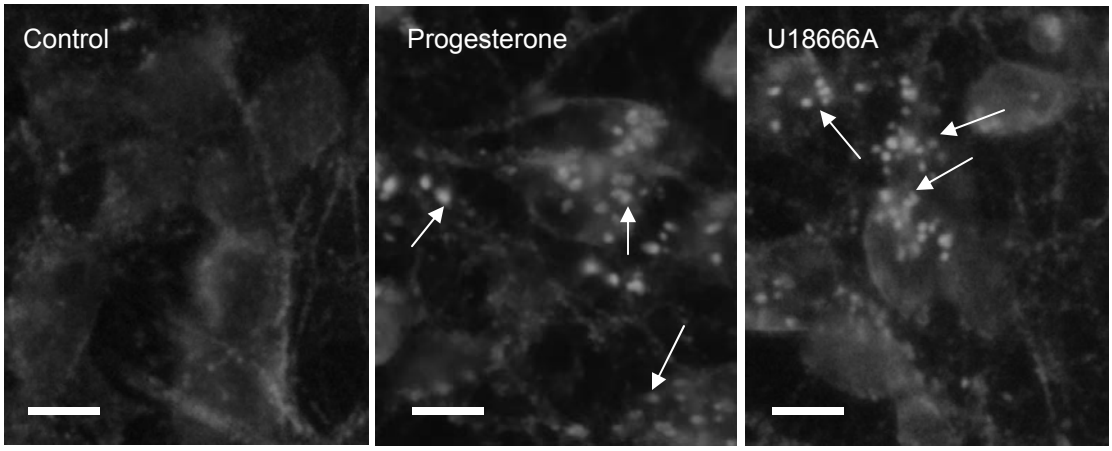

Figure 3.4 Progesterone and U18666A induced intracellular cholesterol accumulation. The neurons were treated with 50 μM progesterone or 2 μg/ml U18666A for 6h. Arrows indicate the accumulated cholesterol as stained by filipin. Bar = 10 μM.

3.2.4. Reversal effect of U18666A and irreversible effect of progesterone on cell viability

The neurons were treated with 50 μM progesterone or 2 μg/ml U18666A. The drug contained media were removed after several of incubation time of 3 h, 6 h, 9 h, 12 h, 24 h, and 48 h respectively, and the neurons were washed with fresh media twice and were replenished with no drug contained media till a total time of 72 h. The neurons viability at 72 h was assessed by MTT assay. Compared to control cells, cells with 3 h, 6 h, 9 h, 12 h, 24 h and 48 h of progesterone incubation showed the survival rates were 96%, 98%, 98%, 74%, 65% and 55% respectively. Whereas cells with 3 h, 6 h, 9 h, 12 h, 24 h and 48 h of U18666A incubation showed the survival rates were 90%, 77%, 65%, 63% and 58% respectively. The results showed that progesterone-induced neuronal cell death could be

prevented if the treatment was terminated at or before 9 h of drug incubation. However, the effect of U18666A on neuronal cell death was not readily reversed even it was removed at 3 h of drug incubation (Figure 3.5).

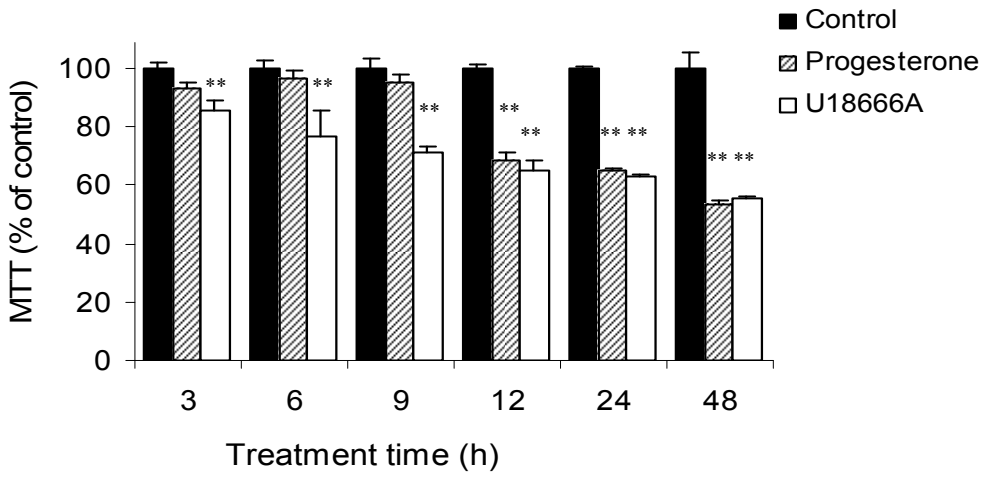

Figure 3.5 Reversible effect of progesterone and irreversible effect of U18666A on cell viability.
** $p < 0.01$.

3.2.5. Progesterone- and U18666A-induced impairment of mitochondrial function

In brain neuronal mitochondria isolated from cerebral cortices of NPC1 mice, severe mitochondrial dysfunctions and subsequent decrease in the activity of ATP synthase have been observed, probably due to the altered cholesterol metabolism in brain neuronal mitochondria of such animals (Yu *et al*., 2005). Since progesterone and U18666A have

been reported to induce NPC-like phenotype such as accumulation of cholesterol in the endocytic pathway (Liscum and Faust, 1989; Roff *et al*., 1991; Butler *et al*., 1992; Lange and Steck, 1994; Kobayashi *et al*., 1999; Lange *et al.,* 2000; Ko *et al*., 2001; Cheung *et al*., 2004), they might as well cause apoptotic cell death by impairing mitochondrial function in neurons. To approach this issue, I examined the effect of 50 μM progesterone and 2 μg/ml U18666A treatments on the intracellular ATP/ADP ratio. The ATP/ADP ratio was determined with ApoGlow Rapid Apoptosis Screening Kit (Cambrex, NJ) at the different time-points. I observed that ATP/ADP ratio was significantly decreased after the neurons were exposed to either 50 μM progesterone or 2 μg/ml U18666A for 12 h or longer (Figure 3.6).

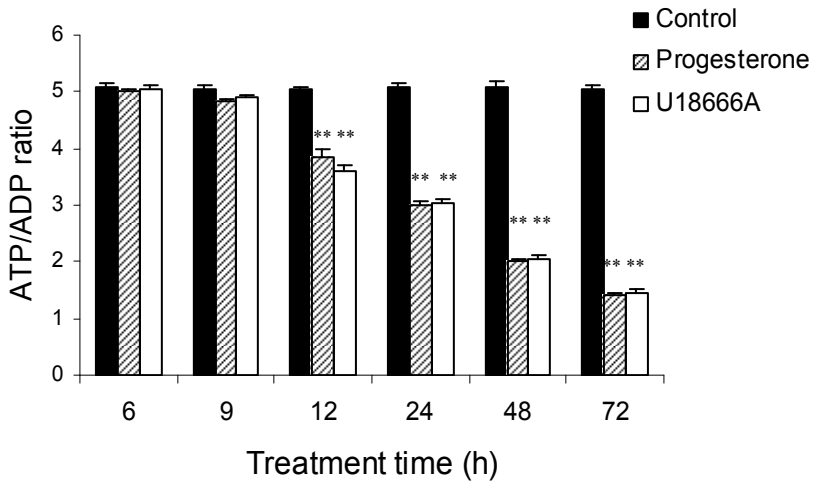

Figure 3.6 Decrease in ATP/ADP ratio following exposure of the neurons to either progesterone or U18666A. All data present the mean ± SE of three independent experiments. ** $p < 0.01$ versus the control for each time point.

3.2.6. Caspase-3 activation in primary cortical neurons treated with progesterone and U18666A

Since the mitochondrial death pathway is known to lead to cleavage and thus activation of the terminal caspases responsible for the proteolysis of many proteins (Earnshaw *et al*., 1999), I proceeded to determine whether caspase-3 activation was involved in the observed apoptotic neuronal cell death following administration of the amphiphiles. The activity of caspase-3 was initially monitored using the EnzChek® Caspase-3 Assay kit (Molecular Probes, OR). Incubation of the neurons with 50 μM progesterone for up to 12 h apparently had no significant effect on caspase-3 activity (Figure 3.7 A), while maximum caspase-3 activity (4-fold increase compared to the control) was observed at 24 h post progesterone treatment, or 12 h later than the time showing the drop of the ratio of ATP/ADP (Figure 3.6). To further confirm the involvement of caspase-3 in progesterone- and U18666A-induced apoptosis, presence of a cleaved 17-kDa subunit of the inactive 32-kDa procaspase-3 was assessed by Western blot analysis (Fig. 3.7 B). This cleavage of procaspase-3 to the active 17-kDa fragment was observed in neurons treated with either 50 μM progesterone or 2 μg/ml U18666A (Fig. 3.7 B).

To further test the role of caspase-3 in apoptosis induced by the amphiphiles, the neurons were treated in the presence of a cell-permeable caspase-3 specific inhibitor, Z-DEVD-FMK. Fig. 3.7 C shows that 25 μM Z-DEVD-FMK suppressed the neuronal injury to a level similar to that observed before with the pan-caspase inhibitor Z-VAD-FMK (Cheung *et al*., 2004), suggesting that the most likely executioner caspase involved in the

progesterone- and U18666A-induced neuronal cell death was caspase-3.

A.

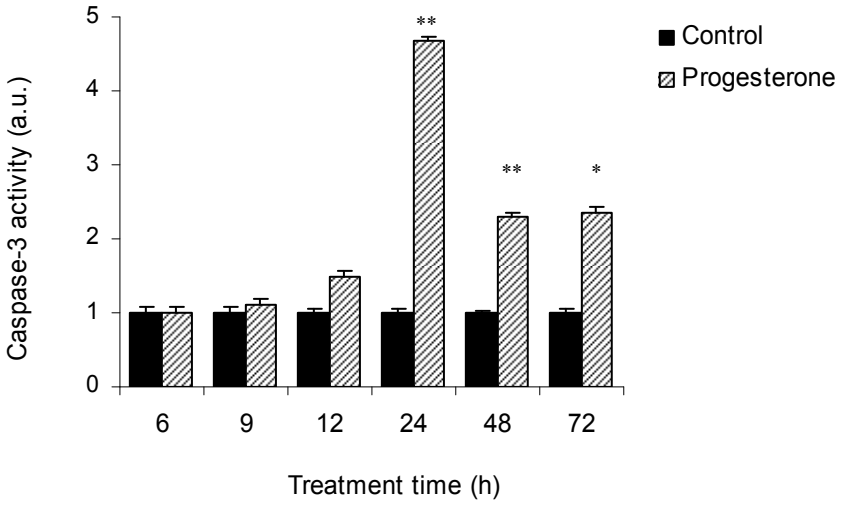

B.

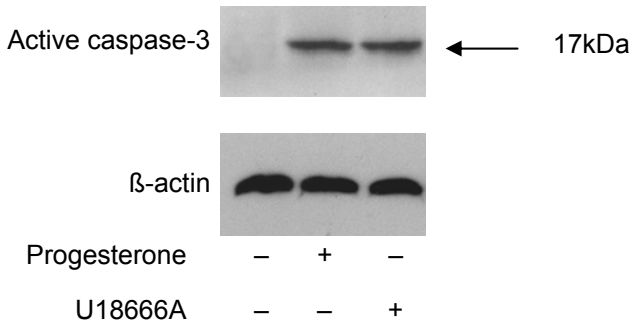

C.

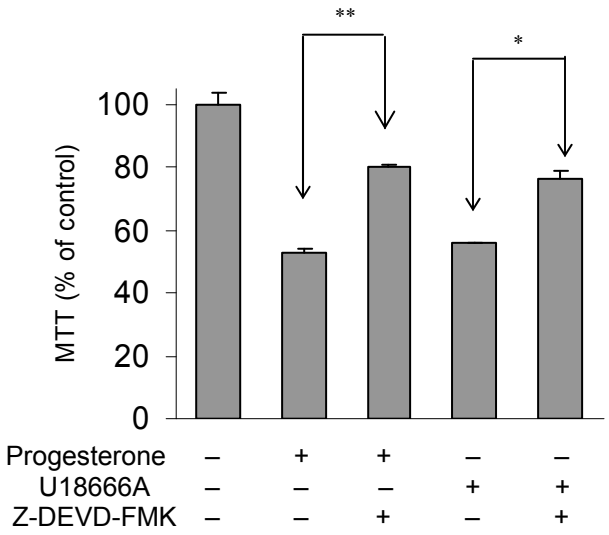

Figure 3.7 Activation of caspase-3 in cultured neurons exposed to progesterone or U18666A. A. The neurons were exposed to 50 μM progesterone for 6 – 72 h. Cells were harvested and caspase-3 activity determined in the cellular extracts as described in Materials and Methods. Data represent the mean ± SE of three independent experiments.* $p < 0.05$; ** $p < 0.01$ versus the control for each time point. B. Western blot analysis of caspase-3 activation in 50 μM progesterone- or 2 μg/ml U18666A-treated neurons (72 h). β-Actin was used as a loading control. The blots are representative of 3 independent experiments. C. Inhibition of progesterone (50 μM)- and U18666A (2 μg/ml)-induced neuronal cell death by caspase-3 specific inhibitor Z-DEVD-FMK (25 μM). The MTT assay was performed after the neurons were treated with the amphiphiles for 72 h in the presence or absence of the caspase-3 inhibitor. Data represent the mean SE of three independent experiments.* $p < 0.05$; ** $p < 0.01$.

3.2.7. Release of cytochrome c and Smac/Diablo from mitochondria of the treated neurons

Injury to mitochondria may initiate the mitochondrial apoptosis cascade by release of pro-apoptotic factors such as cytochrome c and Smac/Diablo from the mitochondrial inter-membrane space into the cytoplasm, which eventually triggers apoptosis via a caspase-3-dependent pathway (Liu *et al*., 1996; Du *et al*., 2000; van Loo *et al*., 2002; Kuwana and Newmeyer, 2003; Saelens *et al*., 2004). Because caspase-3 activation was observed (Fig. 3.7), I wished to know whether treatment of the neurons by progesterone and U18666A would cause the release of these toxic mitochondrial proteins. Western blot analysis of cytosolic extracts showed that both progesterone (50 μM) and U18666A (2 μg/ml) induced the release of cytochrome c and Smac/Diablo at 12 h post-treatment (Fig. 3.8). These results suggest that injury to mitochondria caused by treatment with progesterone and U18666A might induce release of cytochrome c and Smac/Diablo, which in turn led to the downstream activation of caspase-3, resulting in the neuronal apoptotic cell death.

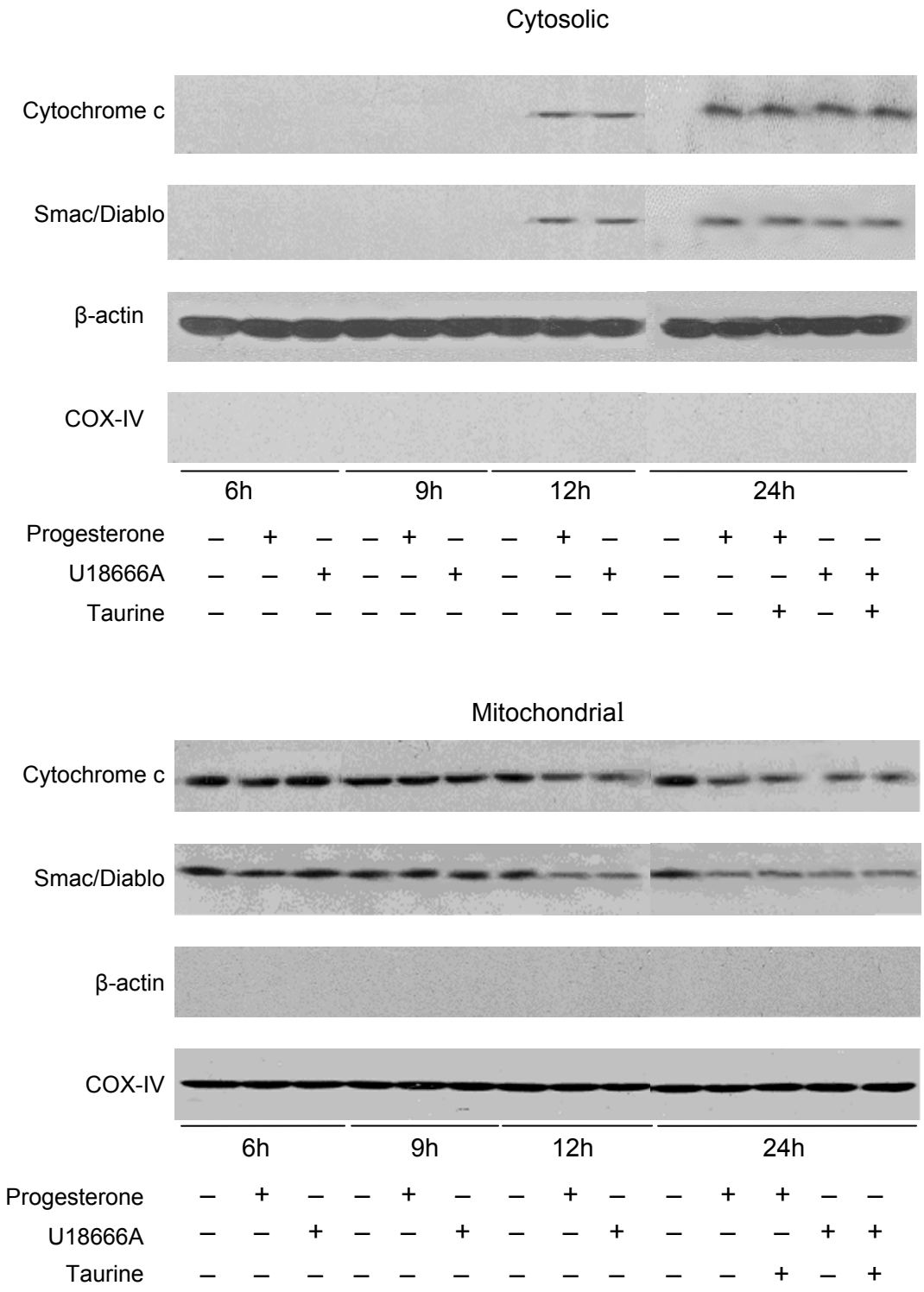

Figure 3.8 Mitochondrial release of pro-apoptotic proteins after treatment with progesterone or U18666A for 6 - 24 h in the absence or presence of taurine. COX-IV was used as a marker and loading control for the mitochondrial fraction and β-actin was used as a loading control for the cytosolic fraction. The blots are representative of at least three independent experiments.

3.2.8. Progesterone- and U18666A-induced neuronal cell death with no involvement of nuclear translocation of AIF

AIF is a mitochondrial intermembrane flavoprotein that is released into the cytosol and translocated to the nucleus in response to certain cell death stimuli (Susin *et a*l., 1999; Daugas *et al*., 2000; Kroemer and Reed, 2000). It is involved in induction of caspase-independent apoptosis in many types of cells, including neurons (Cregan *et al*., 2002). To determine whether AIF was released from the mitochondria during progesterone- and U18666A-induced neuronal death, confocal microscopy was used to examine the cellular localization of AIF after treatment of the neurons with the amphiphiles for 72 h. Representative confocal images shown in Figure 3.9 A revealed that there was no significant (<10%) translocation of AIF to the nuclei between 15 min – 72 h post treatment (Figure 3.9 B), demonstrating that AIF nuclear translocation did not contribute to the progesterone- and U18666A-induced neuronal cell death. This conclusion was further confirmed by Western blot analysis in which neither mitochondrial release nor nuclear translocation of AIF was found in neurons treated with the amphiphiles (Figure 3.9 C).

A.

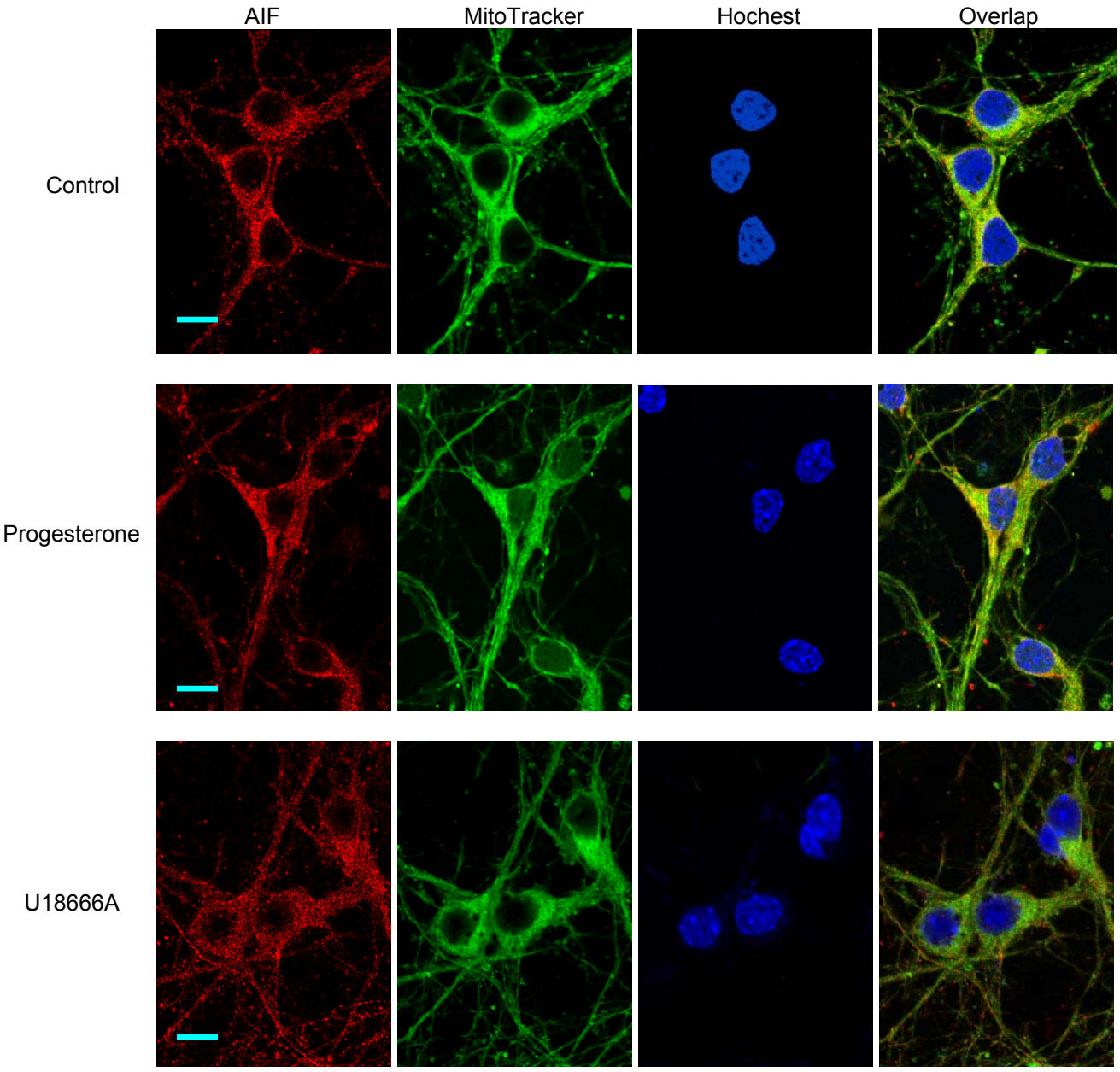
AIF
MitoTracker
Hochest
Overlap
Control
Progesterone
U18666A

B.

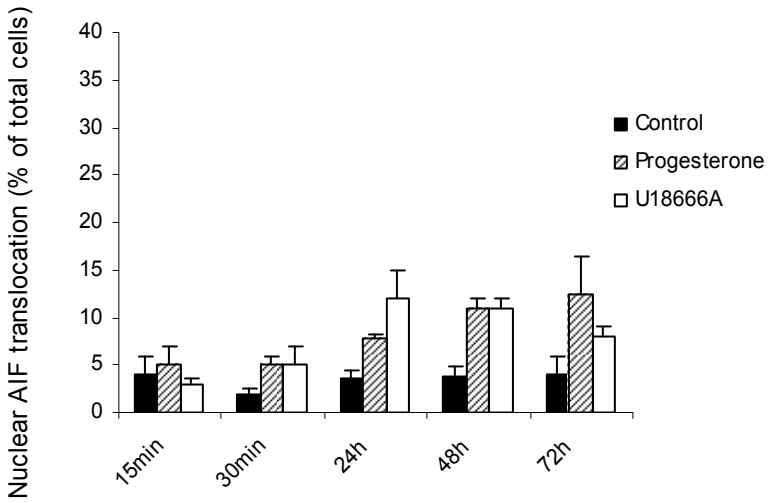

C.

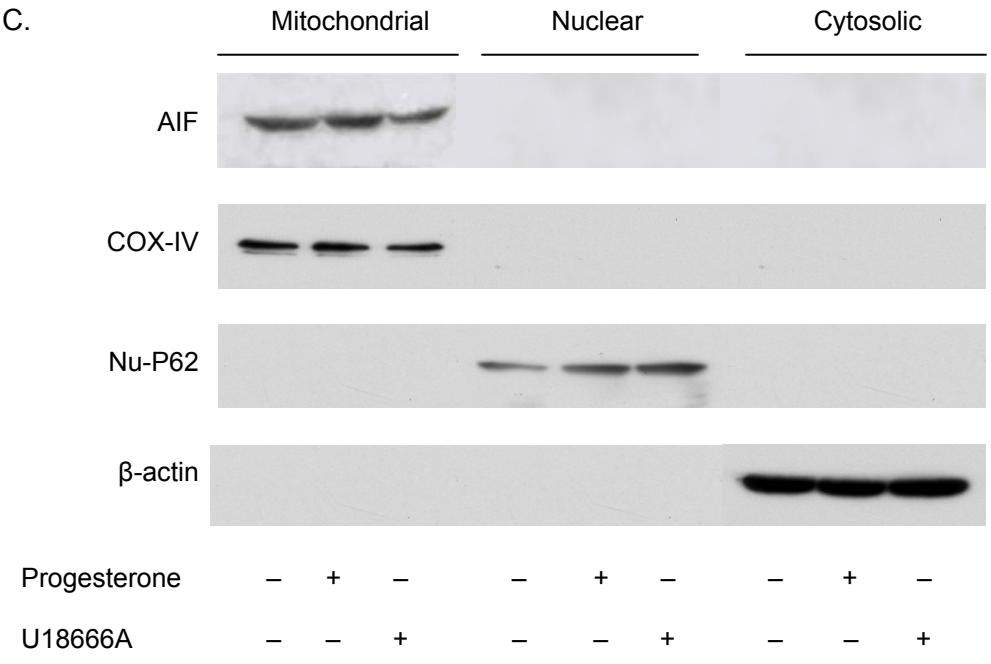

Figure 3.9 Effect of progesterone and U18666A on AIF translocation. A. the neurons were treated with 50 μM progesterone or 2 μg/ml U18666A for 24 h before fixed, permeabilized and stained with antibodies to AIF (red). Nuclei were visualized by Hochest (blue) and mitochondria by MitoTracker Green (green) staining. The overlap level of AIF and Hochest staining, which indicates AIF translocation from mitochondria to nuclei, is low. Bar = 10 μm. B. Quantitative analysis of AIF translocation from

mitochondria to nuclei after treatment with 50 μM progesterone or 2 μg/ml U18666A. The data were obtained from 10 randomly selected fields of neurons (~700 cells total) for each condition. C. The neurons were treated with or without 50 μM progesterone or 2 μg/ml U18666A for 24 h. Mitochondrial, cytosolic and nuclear fractions were obtained and the samples were analyzed by Western blot with anti-AIF antibody. COX-IV was used as the marker for mitochondrial fraction, nucleoporin P62 (Nu-P62) the marker for the nuclear fraction, while β-actin the loading control for the cytosolic fraction. The blots are representative of 3 independent experiments.

3.2.9. Taurine inhibited caspases activation

When cytochrome c enters the cytoplasm, it binds, in the presence of dATP, to the apoptotic protease activating factor-1 (Apaf-1) to form a large apoptosome complex. The initiator caspase, caspase-9, is recruited and processed by the apoptosome, which then in turn activates the downstream effector caspases such as caspase-3 (Li *et al*., 1997; Zou *et al*., 1997; Cain *et al.,* 2002; Adams and Cory, 2002). In order to establish the importance of caspase-9 activation in amphiphile-induced neuronal apoptosis, the neurons were co-treated with taurine, which is known to interfere directly the assembly of apoptosome and thus blocking activation of caspase-9 (Takatani *et al*., 2004). Figure 3.10 showed that exposure of the neurons to 20 μM taurine completely inhibited progesterone-induced cleavage of caspase-9 and caspase-3, whose activity should have reached its maximum 24 h post-treatment with 50 μM progesterone in the absence of taurine (Figure 3.7 A). Similar inhibitory effect of taurine on caspase activation was observed in U18666A-treated neurons (data not shown). As a result, the neurons were rescued from apoptotic death by exposure to taurine (Figure 3.10 B). It is interesting to note that taurine treatment had no effect on amphiphile-induced mitochondrial release of cytochrome c

and Smac/Diablo (Figure 3.8). Taken together, these results demonstrated that caspase-9 was the caspase activated by cytosolic cytochrome c and was responsible for activation of effector caspase-3 and the ultimate neuronal apoptosis observed in this study.

A.

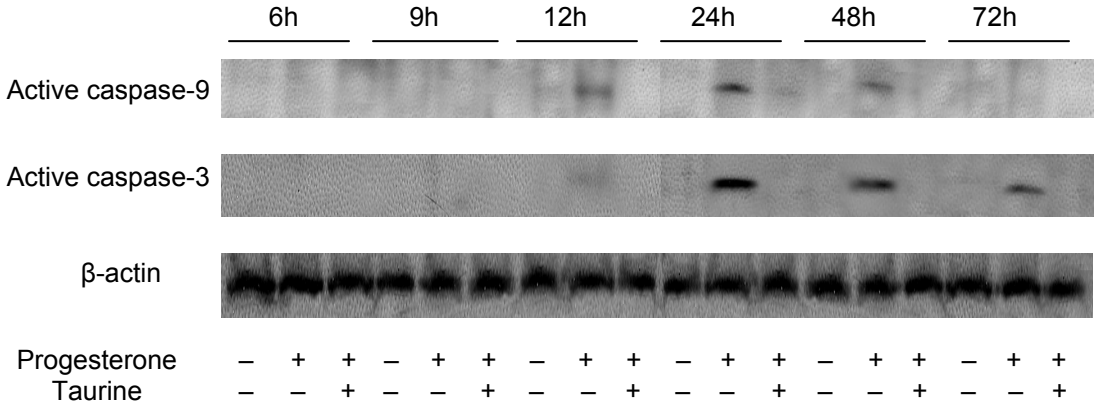

B.

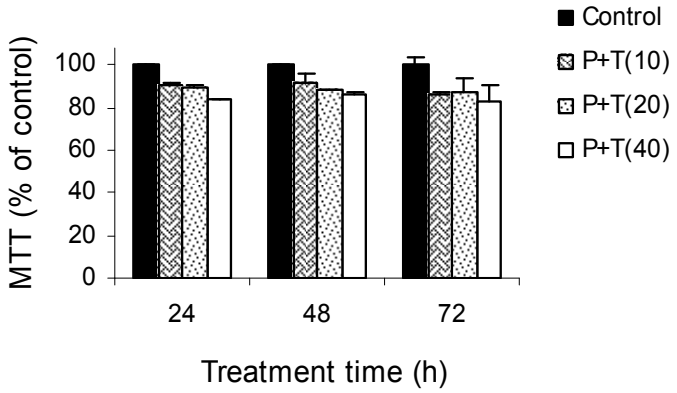

Figure 3.10 Inhibition of caspase-9 and caspase-3 activation by taurine protected the neurons from apoptotic cell death induced by progesterone. A. The neurons were exposed to 50 μM progesterone in the presence or absence of 20 μM taurine for 6 – 72 h. β-Actin was used as a loading control. The blots are representative of three independent experiments. B. MTT assay of neurons treated without (control) or with 50 μM progesterone (P) and 10 μM (P + T(10)), 20 μM (P + T(20)) or 40 μM (P + T(40)) taurine (T) for 24 – 72 h. Data represent the mean ± SE of three independent experiments.

3.3. Discussions

Using NPC1 mouse model, it has been demonstrated that defective intracellular cholesterol trafficking may disrupt cholesterol homeostasis of neuronal mitochondria and results in severe mitochondrial dysfunction that may be responsible for neurodegeneration in NPC1 disease (Yu *et al*., 2005). I have recently found that treatment of cultured murine cortical neurons by U18666A, which is known to cause NPC1-like characteristics in cultured cells, induces apoptotic neuronal cell death (Cheung *et al*., 2004). I confirmed here the apoptotic nature of such neuronal death by exposure of the cells to either progesterone or U18666A (Figure 3.3). Since the Fas pathway of apoptosis is known to be responsible for death of neurons exposed to certain stimuli (Morishima *et al*., 2001; Jayanthi *et al*., 2005), I examined this possibility in the preliminary experiments and found that presence of anti-Fas ligand antibody (25 μg/ml) failed to block the death of neurons treated with progesterone (50 μM) or U18666A (2 μg/ml) for 72 h (data not shown), suggesting that the Fas pathway was unlikely to be involved in the progesterone- and U18666A-induced neuronal cell death. In the present study, I have demonstrated that the mitochondria-dependent death cascade played a central role in the neuronal apoptosis observed. Taken together, the results are consistent with a cascade of events, in which impairment of mitochondrial function resulted in release of both cytochrome c and Smac/Diablo from the mitochondrial compartment into the cytoplasm, where cytochrome c helped to form apoptosome complex that in turn activated the initiator caspase, caspase-9. The effector caspase, caspase-3, was subsequently activated through proteolytic cleavage by the initiator caspase, resulting in apoptosis of the neurons.

The mitochondrial damage caused by progesterone and U18666A treatment was apparently not sufficient to induce translocation of AIF from mitochondria to nuclei, suggesting that the neuronal apoptosis was caspase-dependent.

It is tempting to speculate that inhibition of cholesterol intracellular trafficking by the amphiphiles directly resulted in impaired ATP synthesis (Figure 3.6), which would mimic the situation in NPC1 mouse brains (Yu *et al*., 2005), and activation of the mitochondrial apoptosis pathway. Proof of this idea may be obtained, at least partly, from the sequence of events including progesterone- and U18666A-induced accumulation of cholesterol, decrease in ATP/ADP ratio, cytochrome c and Smac/Diablo release and caspase activation. Accumulation and sequestration of cholesterol, as determined by filipin staining, became evident 6 h after exposure of the neurons to the amphiphiles (Figure 3.4). This was apparently followed by a decrease in ATP biosynthesis and release of cytochrome c and Smac/Diablo (all significantly evident at 12 h; Figure 3.6 and Figure 3.8). Both the initiator caspase-9 and the effector caspase-3 were then activated thereafter (significantly evident at 24 h, Figure 3.7 and Figure 3.10), while initial neuronal cell death as measured by MTT assay was observed at 24 h post-treatment (Figure 3.3). If impairment of mitochondrial function and the subsequent events leading to the neuronal cell death described above were triggered by the amphiphile-induced interruption to cholesterol intracellular trafficking, removal of the triggering factors should help to prevent the neurons from death. This was indeed the case as shown by progesterone washout (Figure 3.5). In order to avoid triggering neuronal cell death, however, removal of progesterone had to be performed in time before the injury to the mitochondria became

irreversible. These results are consistent with past observations in which no significant cell injury was found in cortical neurons exposed to U18666A for 8 h (Runz *et al*., 2002), while prolonged treatment with the same amphiphile resulted in apoptosis of the neurons (Cheung *et al*., 2004).

The release of pro-apoptotic factors such as cytochrome c, Smac/Diablo and AIF from the injured mitochondria triggers the mitochondrial apoptosis cascade. Cytochrome c released into the cytosol promotes caspase-3 activation through the formation of cytochrome c/Apaf-1 apoptosome complex that activates procaspase-9, whereas Smac/Diablo acts as a sensitizer for caspase activity following cytochrome c-induced activation of caspase-9 by binding to inhibitor of apoptosis proteins (IAPs), thereby antagonizing the inhibitory effect of IAPs on the activation of effector caspases. Both cytochrome c and Smac/Diablo are involved in caspase-dependent apoptosis, while AIF plays a central role in mediating the caspase-independent apoptosis pathway (van Loo *et al*., 2002; Saelens *et al*., 2004; Cregan *et al.*, 2004). Apparently, progesterone- and U18666A-induced injury to mitochondria was not sufficient to cause AIF release (Figure 3.9). In this regard, it has recently been reported that permeabilization of the mitochondrial outer membrane readily causes translocation of cytochrome c and Smac/Diablo, whereas AIF remains bound to mitochondria, probably because mature AIF is a type-1 inner mitochondrial protein and proteolytic cleavage is necessary for AIF release (Arnoult *et al*., 2002; Uren *et a*l., 2005; Otera *et al.,* 2005; Polster *et al.,* 2005; Yuste *et al.,* 2005). The different kinetics of cytochrome c and AIF release were also reported in cortical neurons undergoing p53-mediated cell death (Cregan *et al*., 2002).

Another important mechanistic issue is related to the observation that AIF was not released at the activation of caspase-9 and caspase-3, suggesting that caspase activation, in addition to outer membrane permeabilization, was insufficient to cause AIF release, in contrast to some previous reports (Arnoult *et al*., 2002; 2003a; 2003b) but in agreement with the observations by others (Uren *et al*., 2005). Taken together, one may hypothesize that the precise molecular mechanism of mitochondrial apoptosis cascade may depend upon the extent of mitochondrial damage, which in turn is determined by the nature of the cell death stimuli.

In progesterone- and U18666A-treated cortical neurons, both caspase-9 and caspase-3 were activated. When either of these two caspases was blocked by specific inhibitors, neuronal cell death was inhibited (Figure 3.7 and Figure 3.10). Furthermore, inhibition of caspase-9 by taurine led to lack of activation of caspase-3 (Figure 3.10A), indicating that the latter was the downstream effector caspase of the former. All these observations are widely believed as the features for apoptosis in the nervous system (Yuan and Yankner, 2000). In addition, both *in vitro* treatment of the neurons with the amphiphiles and *in vivo* analysis of the NPC1 mouse neurons revealed the deterioration of neuronal mitochondrial function (Figure 3.6; Yu *et al*., 2005), which was believed being induced by disruption of the intracellular cholesterol homeostasis and to be responsible for neurodegeneration in NPC1 disease. Taken together, the model system used in this study should have represented the essential features of neuronal cell death in NPC1 disease. The mitochondrial apoptosis cascade described here is therefore likely to represent at least one of the neuronal cell death pathways in this disorder. It should be pointed out that

the molecular mechanism leading to apoptosis in the brain of NPC disease may be distinct in terms of the types of neurons. In $NPC^{-/-}$ mice, although apoptotic cells could be detected in the cerebellum and cerebral cortex, loss of Purkinje cells are much more severe and faster than other neurons (Wu *et al*., 2005; Li *et al*., 2005), implying that neuronal apoptosis in different regions of the brain may be regulated differently.

Elucidation of the molecular events that control the neuronal death is essential for development of therapeutic strategies for treatment of these neuronal disorders including NPC1 disease. I have shown that caspase-dependent neuronal apoptosis might be caused by impaired mitochondrial function due to disrupted intracellular cholesterol trafficking, whereas caspase-independent neuronal cell death was not involved. Therefore, effective therapeutics should target the caspase-dependent pathway. It is interesting to note that taurine, which is known to perform neuroprotective roles in mammalian brains (Khan *et al*., 2000; Shuaib, 2003), rescued the amphiphile-insulted neurons from apoptotic death (Figure 3.10B), apparently by inhibiting activation of caspase-9 (Figure 3.10). It also prevented the neurotoxicity of β-amyloid in Alzheimer's disease (Louzada *et al.*, 2004), a neurological disorder, like NPC disease, in which intracellular cholesterol trafficking is considered as a risk factor (Runz *et al*., 2002; Burns *et al.,* 2003). Taking these findings together, it should be worth exploring taurine as a promising treatment for NPC1 disease and other neurological disorders correlated with abnormal cholesterol metabolism.

In summary, I have demonstrated that inhibition of intracellular cholesterol trafficking induces neuronal cell death through the mitochondrial apoptosis pathway in a caspase-

dependent manner. Moreover, it was also shown that targeting caspase-9 activation and activity of apoptosome by taurine provides neuroprotection that may represent a new approach to treat NPC1 disease.

Chapter 4. Protection effect of cAMP and forskolin on neurons and NPC1 fibroblasts

4.1. Introduction

Cell-permeable analogues of cAMP have been shown to improve the survival of cells (Nakao N, 1998; Vaudry D, et al., 1998; Michel PP, et al., 1996; Schildberg FA, et al., 2005). The NPC-1 gene is upregulated by cAMP, which plays a role in normal cholesterol homeostasis and is essential for normal adrenal development and function (Gévry NY and Murphy BD, 2002). cAMP, also coordinately enhances the expression of Rab5a and Rab7, which promote Tg endocytosis and transfer to lysosomes, respectively, resulting in accelerated thyroid hormone production (Croizet-Berger K, et al., 2002).

Extracellular signal-regulated protein kinase 1 and 2 (ERK1/2), which are members of the mitogen-activated protein kinase superfamily, have been well characterized and are known to be involved in cell survival. The cAMP-->ERK-->CREB cascade may thus constitute a molecular integrator for converging signals. However, the effect of cAMP on ERK phosphylation still remains controversial. A study has shown that cAMP treatment reduced phosphorylation of ERK in human endothelial cells (Schildberg et al., 2005). Moreover, recent evidence suggests that activation of ERK1/2 also contribute to cell death in some cell types and organs under certain conditions (Jin KL, et al., 2002). Sawamura N, et al. showed that the activation of Erk1/2 has shown to promote tau phosphorylation by MAP kinase Erk1/2 is accompanied by reduced cholesterol level in

detergent-insoluble membrane fraction in Niemann-Pick C1-deficient cells (Sawamura et al., 2003); the hyperphosphorylated tau was the major component for the formation of neurofibrillary tangles, indicating a pathological hallmark of Alzheimer's disease. In our first part of study, I showed that inhibition of intracellular cholesterol trafficking induces neuronal cell death through the mitochondrial apoptosis pathway in a caspase-dependent manner. The U18666A treatment on cortical neuron mimic the NPC1 phenotype. I further carry out studies on the effect of cAMP to both neuron and NPC1 deficient fibroblast.

4.2. Results

4.2.1. cAMP and forskolin promote neuronal cell survivals.

I have showed U18666A induced neuronal cell death (Huang Z, et al., 2006). In the present study, I further examined whether the cell death could be rescued by cAMP or forskolin (Branton et al., 1998; Schildberg et al., 2005).

The cultured neuron was pre-incubated with 0.3 mM cAMP or 20 μM forskolin for 30 min, thereafter, U18666A was added to culture medium with a final concentration of 2 μg/ml, neuron was further incubate for 12-72 h. In the absence of cAMP or forskolin, U18666A induced cell death occurred at 24 h, 48 h and 72 h, consistent with our previous result. Interestingly, in the presence of cAMP or forskolin, neuronal cell death was

reduced. As compared to U18666A treatment alone, co-treatment of U18666A with cAMP or forskolin, significantly promotes cell survivals.

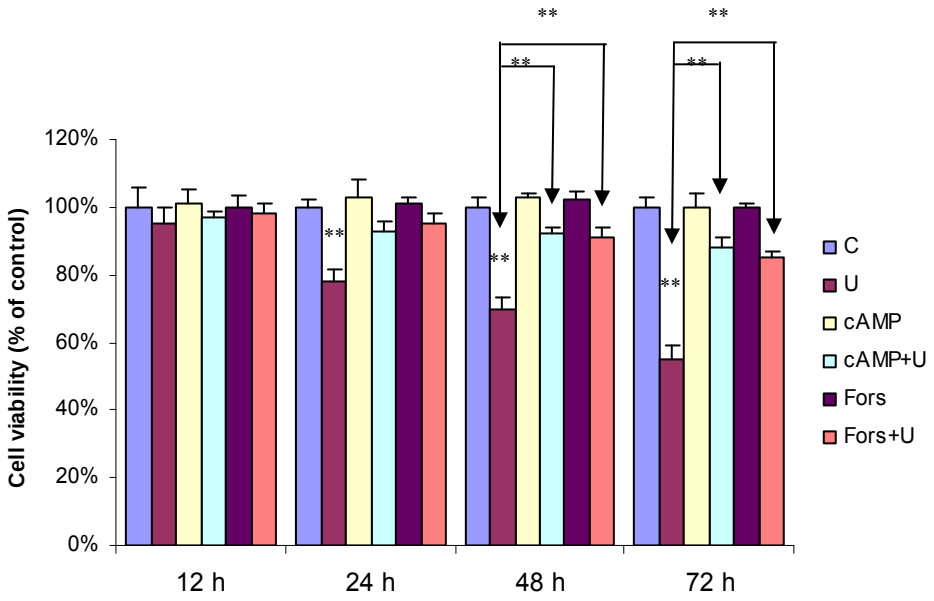

Figure 4.1 Effect of cAMP and forskolin on neuronal cell survivals.
Neuron was preincubated with cAMP 0.3 mM and Forskolin 20 μM or 0.5h, followed by addition of U18886A to medium with a final concentration of 2 μg/ml. Neuron was treated for 12-72 h. All data reporesent the mean ± SE of three independent experiments. *p <0.05, and **p < 0.01 versus the control for each time point or between various treatments.

4.2.2. Effect of cAMP and forskolin treatment on neuronal intracellular free cholesterol

To examine whether cholesterol accumulation in the cortical neurons has reduction upon addition of cAMP or forskolin. Our previous result show impairment of mitochondrial function, the unesterified cholesterol was stained with filipin and cholesterol accumulation was observed as early as 6 h after exposure of the neurons to 2 μg/ml U18666A (Figure 4.2). In the presence of cAMP or forskolin, U18886A induced free cholesterol accumulation was significantly reduced, although it was not completely diminished.

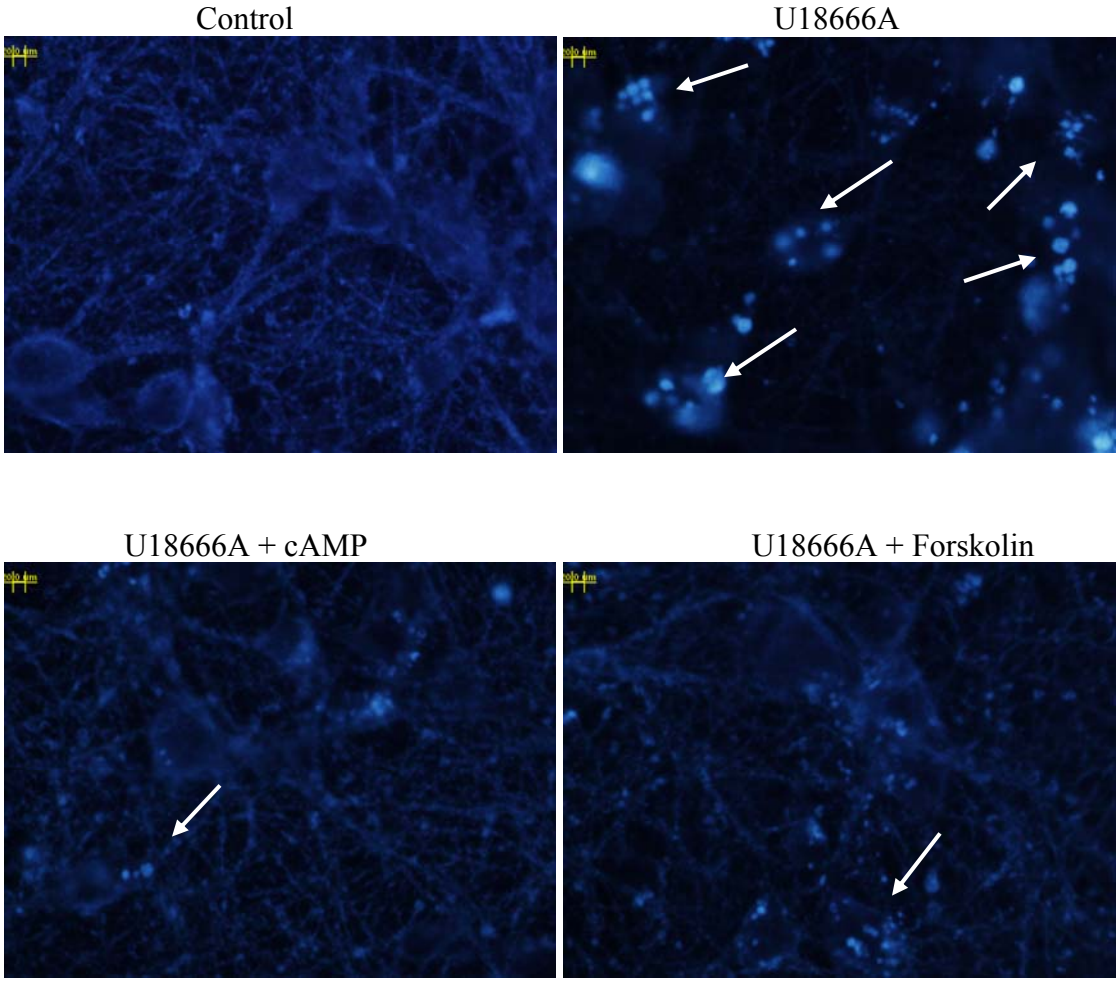

Figure 4.2 Effect of cAMP or forskolin on intracellular cholesterol accumulation. Accumulation of intracellular cholesterol was observed in cortical neurons 6 h after treatment with U18666A (2μg/ml), less accumulation in case of co-treatment of cAMP with U18666A or forskolin with U18666A. Bar = 10 μm; Arrows: accumulated cholesterol as stained by filipin.

4.2.3. Rgulation of cAMP and forskolin on the expression of rab7, rab9, rab5 and rab11 in neuron

The reduction of free cholesterol accumulation led me to further investigate the Rab proteins in the intracellular cholesterol trafficking path, a few candidates of Rab proteins were selected, such as Rab7, Rab9, Rab 5 and Rab 11. I treated neurons with U18666A 2ug/ml, or co-treatment with either cAMP 0.3 mM or forskolin 20 μM for 6h, 24h, 48h and 72h. Rab7, which mediate intracellular transportation from endosome to lysosome, was up-regulated with treatment of cAMP or forskolin. This upregulation effect is more apparent in the 48 h or 72 h time point (Figure 3.4 A). However, with the treatment of cAMP and forskolin, Rab9 expression level had mild changes only (Figure 3.4 A), and Rab5 and Rab11 were not significant changes (Figure 3.4 B).

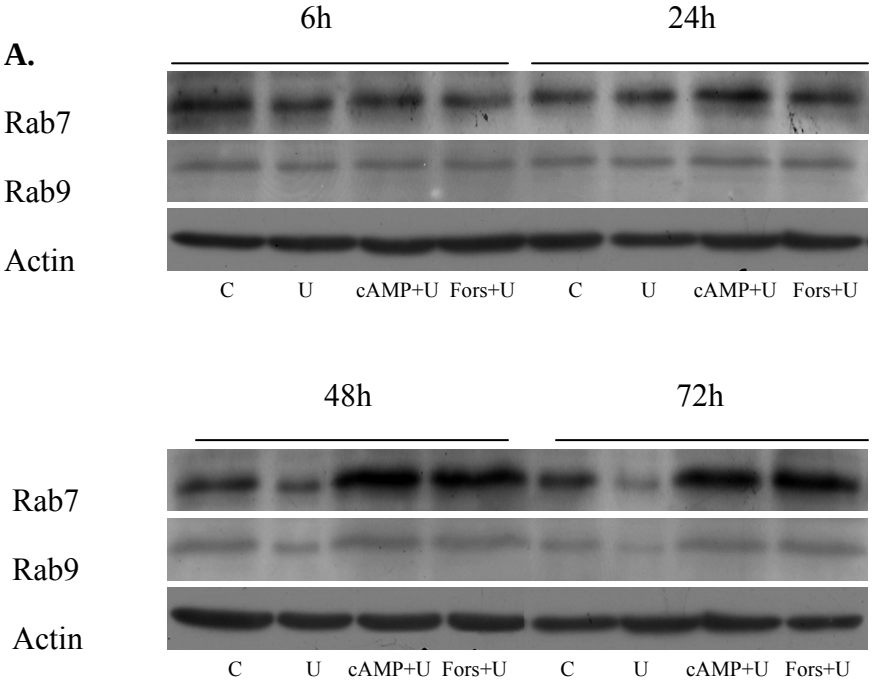

B.

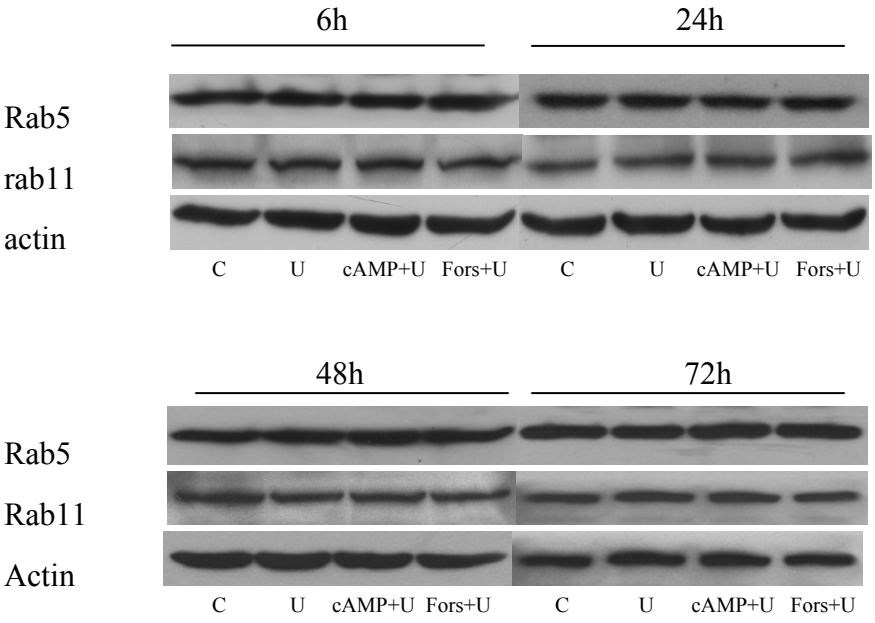

Figure 4.3 Effect of cAMP or forsolin on the expression of rab7, rab9, rab5 and rab11 in neuron by western blotting. Neuron was treated for 6h, 24h, 48h and 72h, with U18666A 2ug/ml, or co-treatment with either cAMP 0.3 mM or forskolin 20 μM. U: U18666A; Fors: forskolin.

4.2.4. Effect of cAMP and forskolin treatment on [H^3] cholesteryl oleate formation in neuron

The neurons were treated with various reagents for 32h and co-incubated with [^{3}H]oleic acid (1 μCi/ml) at 37 °C for further 16 h. Lipid extracted by Chloroform/methanol was separated by thin-layer chromatography. The radioactivity of cholesteryl oleate was measured by liquid scintillation counting (Kitatani K, et al. 2002). Figure 4.4 A showed that cholestryl oleate increase with cAMP or forskolin alone increased by 4-5 folds. With co-incubation of cAMP with forskolin, the increase of cholesteryl oleate was 3-4 folds, as compared to U18666A treatment. This explained the reduction of free cholesterol

accumulation in figure 4.2. To examine whether Rab7 has an important role in transportation of free cholesterol, I have knocked down Rab7 by siRNA (Figure 4.4B). The efficiency of siRNA was examined by western blotting. Upon knock down of Rab7, the induction of cAMP or forskolin has much less effect on choleteryl oleate formation as compared to no-treatment control (no-drug, no-siRNA), while with knock down with not specific target gene, has no effect on Rab7 and cholesteryl oleate formation remain 2-3 fold increase as compared to non-treatment control (Figure 4.4C).

A.

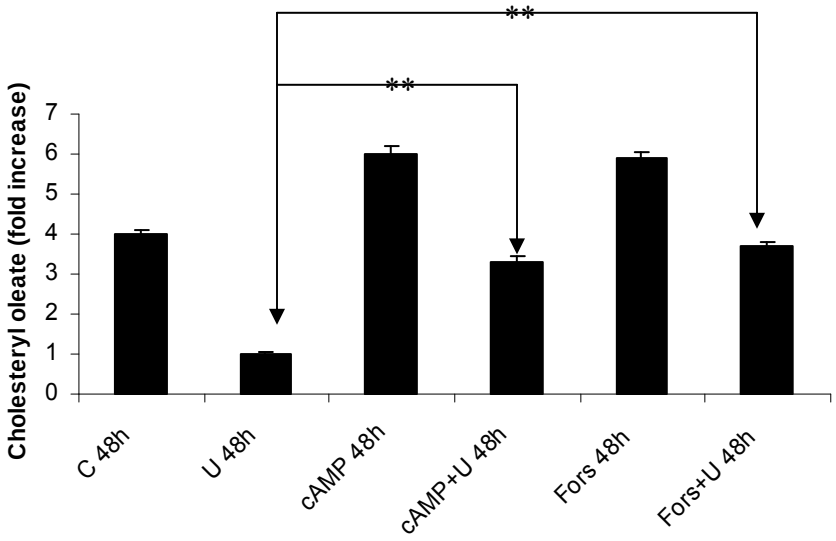

B.

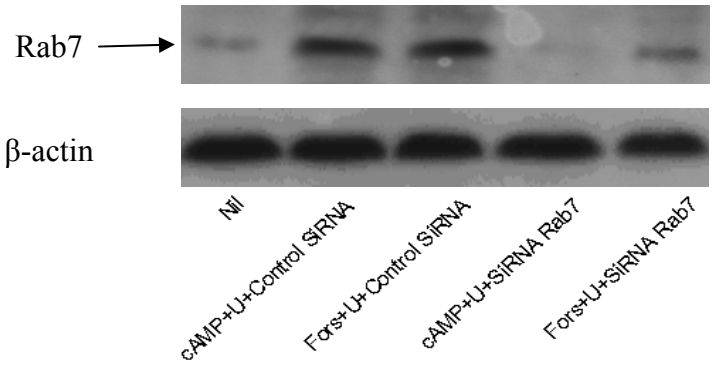

C

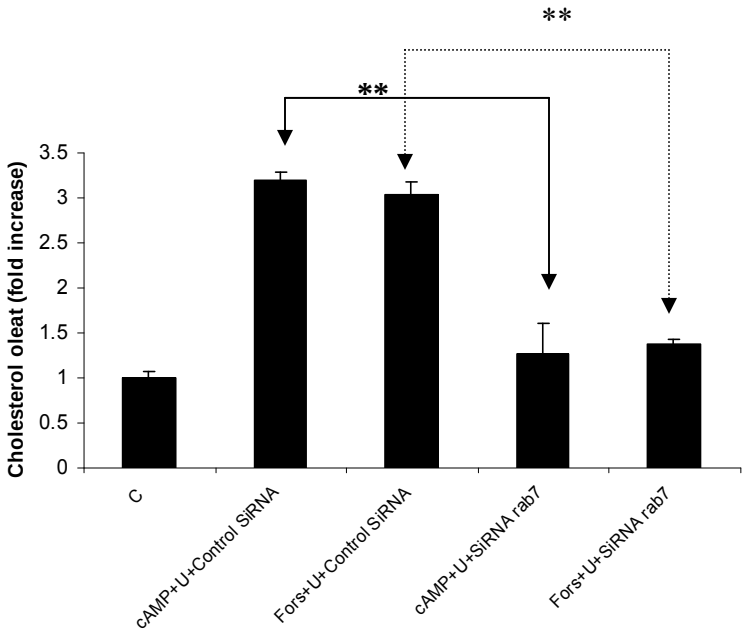

Figure 4.4 Effect of cAMP and forskolin treatment on [H^3] cholesteryl oleate formation in neuron. ** $p < 0.01$.

4.2.5. Effect of cAMP and forskolin on ERK phosphorylation

I further examine ERK phosphorylation by cAMP (0.3 mM) and forskolin (20 μM) stimulation. Western blotting showed co-treatment of cAMP or forskolin with U18666A activated ERK. The activation of ERK occurred at 10 min treatment, and it sustained to 60min (Figure 4.5), even to a longer period of 24 h (data not shown).

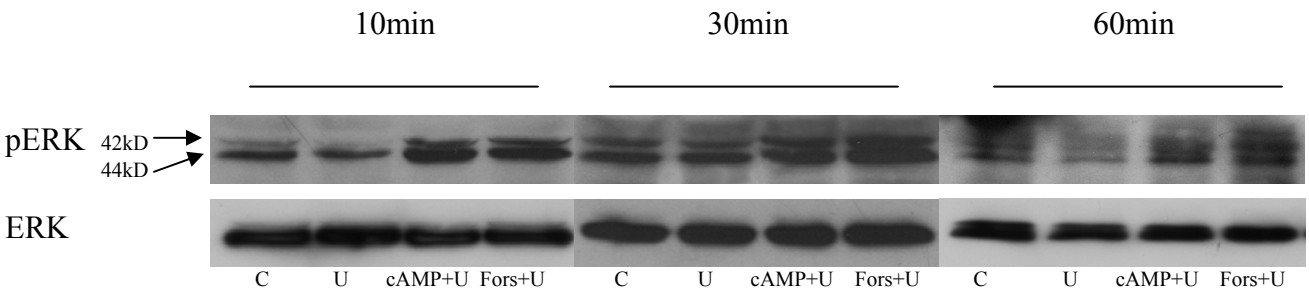

Figure 4.5 Activation ERK with stimulation of cAMP or forskolin. C: no-treated control; U: U18666A 2 μg/ml; cAMP: 0.3 mM; Fors: forskolin 20 μM.

4.2.6. Effect of inactivation of ERK on cholesteryl oleate formation

PD98059 is the inhibitor of MEK 1/2, which in turn would inhibit ERK activation.

I further examined whether ERK activation has effect on cholesteryl oleate formation. Figure 4.6 showed neurons with cAMP or forskolin alone, will have about 2-3 fold of cholesteryl oleate formation as compared to the no-treated control. However, with the addition of inhibitor PD98059 (20 μM) to cAMP or forskolin, the cholesteryl oleate formation return to baseline as no-treated control, indicating phosphorylation of ERK could be a up-stream activator, which would play a role in the intracellular cholesterol transportation.

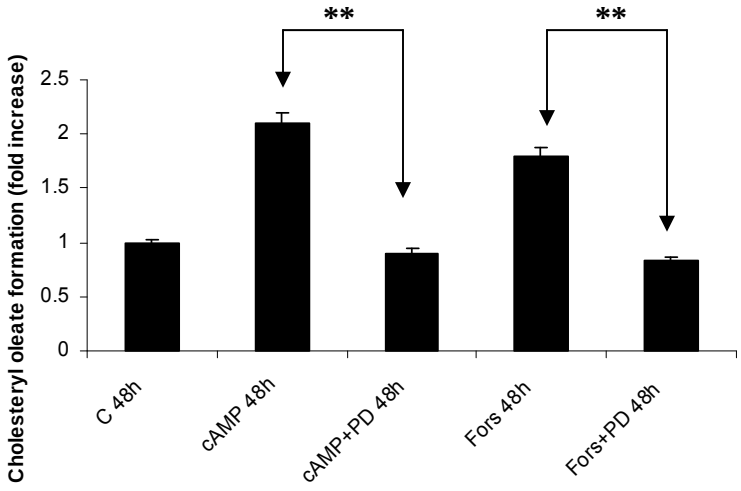

Figure 4.6 Effect of inactivation of ERK on cholesteryl oleate formation

C: no-treated control; U: U18666A 2 μg/ml; cAMP: 0.3 mM; Fors: forskolin 20 μM.

4.2.7. Up-regulation of cAMP and forskolin on Rab7 expression and cholesteryl oleate formation in NPC1 fibroblast

NPC1 deficient cell line GM3123 was chosen to study the effect of cAMP and forskolin on Rab7 expression. NPC1 fibroblast was treated with cAMP or forskolin in the presence or absence of LDL, Expression of Rab7 was detected by Western blotting at 48 hour treatment. Similar effect of Rab7 up-regulation was observed by Western blotting (Figure 4.7)

A.

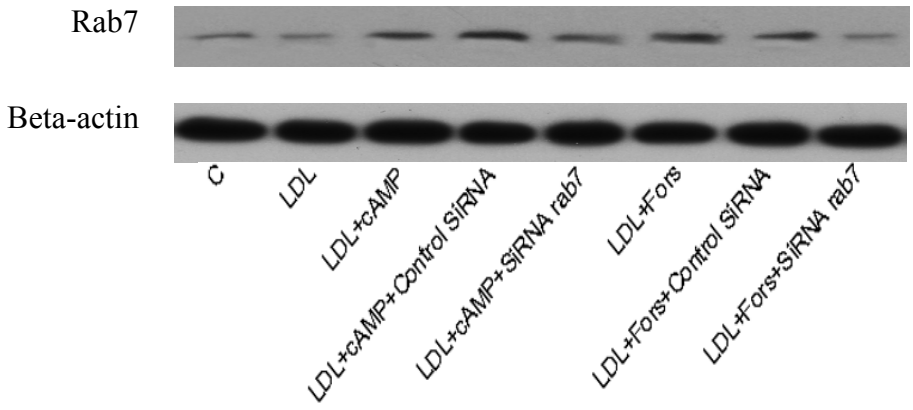

B.

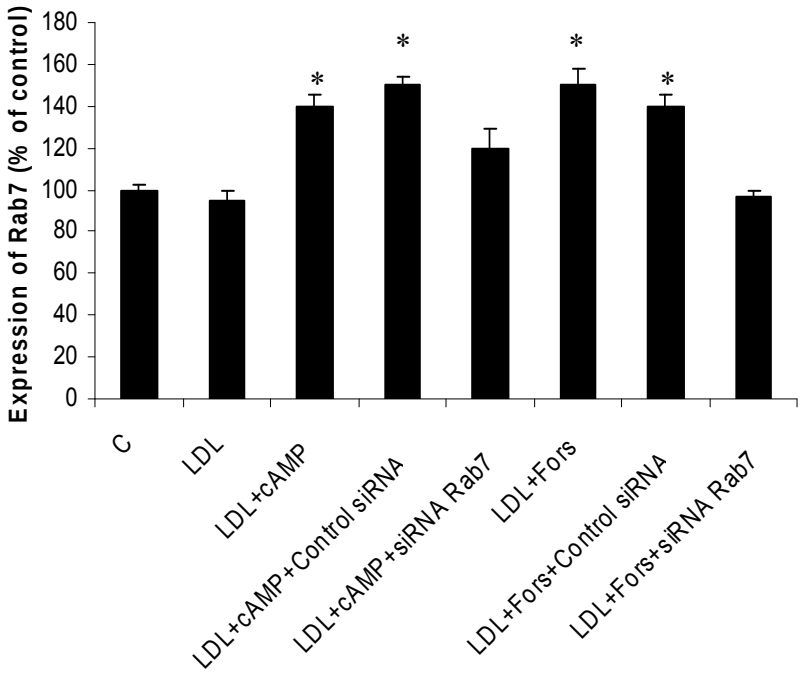

Figure 4.7 Effect of cAMP and forskolin on Rab7 expression and cholesteryl oleate formation in NPC1 fibroblast with 48 hour treatment. (A) Western blot analysis of Rab7 expression; (B) Quantitative analysis of Rab7 expression level, the mean expression level of Rab7 in untreated cells was set as 100%. Values are mean±SE. C: non-treated, incubated with LPDS medium; LDL: low density lipoprotein 50 μg/ml; cAMP: cyclic AMP 0.3 mM; Fors: forskolin 20 μM. Western blotting with anti-Rab7, β-actin used as a loading control. **P*<0.05.

4.2.8. Effect of cAMP and forskolin on intracellular free cholesterol and cholesteryl oleate formation in NPC1 fibroblasts

Up-regulation of Rab7 could help cholesterol intracellular transportation, filipin staining on firbroblast treated with cAMP 0.3 mM or forskolin 20 μM for 48 hour, in the presence of low density lipoprotein (LDL) 50 μg/ml. LDL incubation could induce mass amount of free cholesterol accumulation in NPC1 (-/-) fibroblast. With co-incubation of cAMP or

forskolin, free cholesterol accumulation was significantly reduced (Figure 4.8A), which was consistent with increase of cholesteryl oleate formation (Figure 4.8B). However, with the siRNA knock-down of Rab7 (efficiency of siRNA showed in Figure 4.7), the cholesteryl oleate formation returned to baseline close to non-treated NPC1 (-/-) fibroblasts (Figure 4.8B).

A.

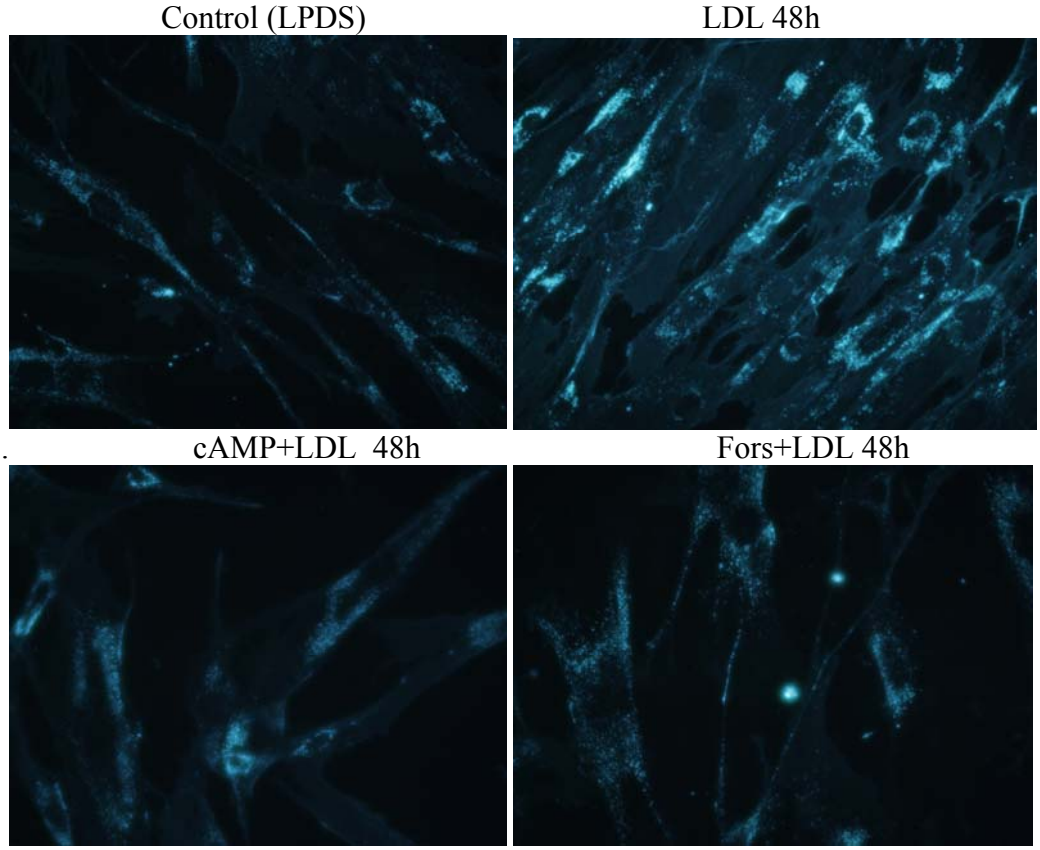

B.

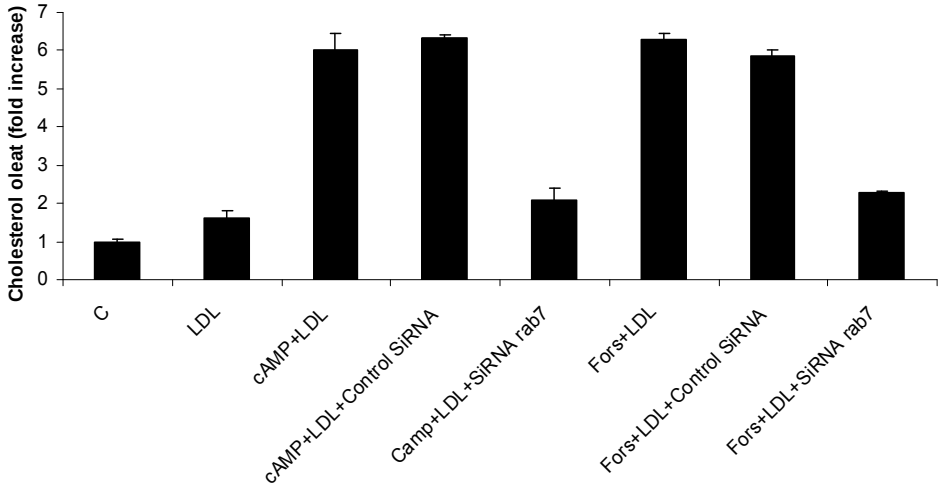

Figure 4.8 Effect of cAMP and forskolin on intracellular free cholesterol and cholesteryl oleate formation in NPC1 fibroblast with 48 hour treatment. C: non-treated, with LPDS medium; LDL: low density lipoprotein 50 μg/ml; cAMP: cyclic AMP 0.3 mM; Fors: forskolin 20 μM.

4.2.9. Effect of cAMP and forskolin on ERK phosphorylation and cholesteryl oleate formation in NPC1 fibroblasts

In case of NPC1(-/-) fibroblasts, cAMP or forskolin stimulate ERK phosphorylation at 30 min as shown in Figure 4.9A. In the presence of LDL, cAMP (0.3 mM) or forskolin (20 μM) increase cholesteryl formation for about 5 folds (Figure 4.9) at the time-point of 48 hour treatment. PD98059 was known to inhibit MEK 1/2 kinase, which in turn inactivate ERK. With the addition of PD98059 (20 μM), cholesteryl oleate formation was significantly reduced by about 2-3 fold to a much lower level, which was observed at time-point of 48 hour treatment (Figure 4.9B).

A.

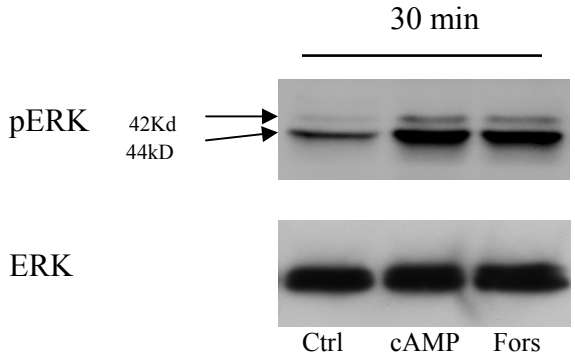

B.

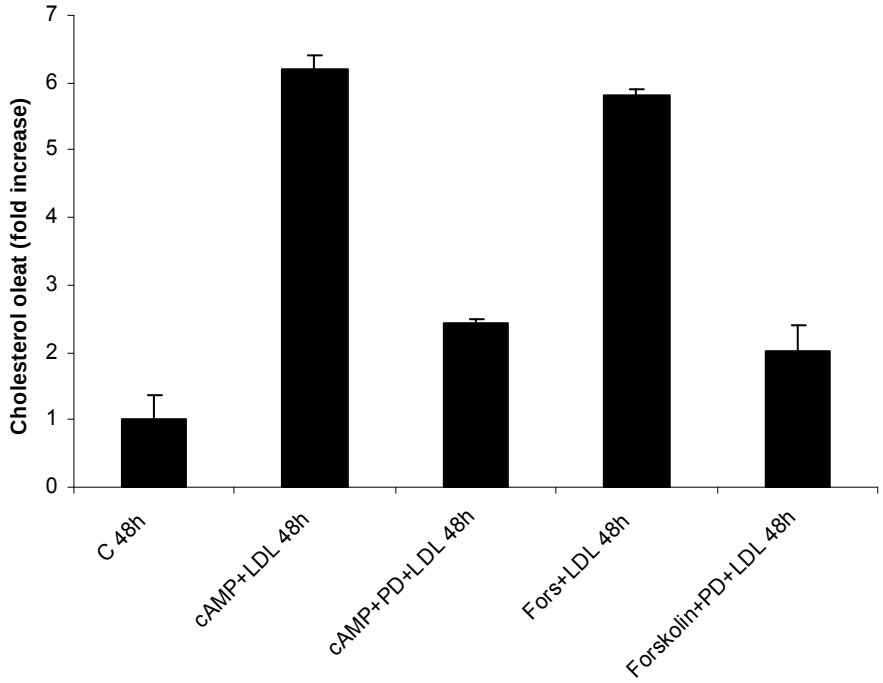

Figure 4.9 Effect of cAMP and forskolin on ERK phosphorylation and cholesterol oleate formation in NPC1 fibroblast. C: no-treated control, incubated with LPDS medium; LDL: low density lipoprotein 50 μg/ml; cAMP: cyclic AMP 0.3 mM; forskolin: 20 μM; PD: PD98059 20 μM

4.3. Discussions

I have explored the biochemical events occurring after induction of neuronal apoptosis in primary cortical neurons after treatment with U18666A. This drug leads to an inhibition of cholesterol trafficking, results in the accumulation of cholesterol in normal cells, and is commonly used to mimic the cellular effects of NPC (Liscum et al, 1989; Lange et al., 2000; Mohammadi 2001).

Cell-permeable analogues of cAMP have been shown to improve the survival of cells (Nakao 1998; Vaudry et al., 1998; Michel et al., 1996; Schildberg et al., 2005). The NPC-1 gene is up regulated by cAMP, which plays a role in normal cholesterol homeostasis and is essential for normal adrenal development and function (Gévry and Murphy 2002).

In the present study, I had further examined whether the cell death could be rescued by cAMP or forskolin. The cultured neuron was pre-incubated with 0.3 mM cAMP or 20 uM forskolin and/or U18666A 2μg/ml for 12-72 h. In the absence of cAMP or forskolin, U18666A induced cell death occurred at 24 h, 48 h and 72 h, consistent with our previous result. Interestingly, in the presence of cAMP 0.3 mM or forskolin 20 μM, neuronal cell death was reduced by approximate 10% at 24 h, 20% at 48h, and 30% at 72h, as compared to U18666A treatment alone (Figure 4.1). Co-treatment of U18666A with cAMP or forskolin, has significantly promote cell survivals.

Promotion of cell survival by cAMP or forskolin could be via ERK1/2 signaling. ERK are members of the mitogen-activated protein kinase superfamily, have been well characterized and are known to be involved in cell survival (Jin et al., 2002; Jiang et al., 2005; Park and Cho 2006; Zhang and Abdel-Rahman 2008). Especially, ERKs are involved in a wide range of neuronal functions including differentiation, synaptic plasticity, survival, migration (Thelen et al, 2002), and long-term changes in gene expression (Hevroni et al., 1998) that may underlie aspects of learning and memory (Impey et al., 1999). For example, studies showed cAMP activation of ERKs mediates some of the neuroprotective actions of selected hormones and neurotransmitters (Elliott-Hunt, et al., 2002; Troadec et al., 2002). Forskolin, an adenylate cyclase activator, was an agent that increases intracellular levels of cAMP, protects keratinocytes from UVB-induced apoptosis independently from the amount of melanin in the skin (Passeron et al., 2008). Forskolin could induce late long-term potentiation in hippocampal neurons via ERK, and PI3K in hippocampal pyramidal cells (Gobert 2008**)**. However, the effects of cAMP on ERK phosphorylation still remain controversial. Study has shown that cAMP treatment reduced phosphorylation of ERK in human endothelial cells (Schildberg et al., 2005). Moreover, recent evidence suggests that activation of ERK1/2 also contribute to cell death in some cell types and organs under certain conditions. Garg and Chang showed that oxidative stress causes ERK phosphorylation and cell death in cultured retinal pigment epithelium (Garg and Chang, 2003). Sawamura et al. showed that the activation of Erk1/2 has shown to promote tau phosphorylation by MAP kinase Erk1/2 is accompanied by reduced cholesterol level in detergent-insoluble membrane fraction in Niemann-Pick C1-deficient cells (Sawamura et al., 2003), the hyperphosphorylated tau

was the major component for the formation of neurofibrillary tangles, indicating a pathological hallmark of Alzheimer's disease. In our first part of study, I showed that inhibition of intracellular cholesterol trafficking induced neuronal cell death through the mitochondrial apoptosis pathway in a caspase-dependent manner. Arany I et al. demonstrated that cisplatin-induced cell death is EGFR/*src*/ERK signaling dependent in mouse proximal tubule cells, and suggested that the prodeath effect of ERK is injury type dependent (Arany et al., 2004).

I am interested to further examine the effect of ERK phosphorylation by cAMP (0.3 mM) and forskolin (20 μM) stimulation in our case. Western blotting showed co-treatment of cAMP or forskolin with U18666A activated ERK. The activation of ERK occurred at 10 min treatment, and it sustained to 60min (Figure 4.5), even to a longer period of 24 h (data not shown). Our result was consistent with the studies done by others. It has been report that N-acetyl-O-methyldopamine (NAMDA) enhances forskolin-induced ERK-CREB activation and potentiated forskolin-induced resistance to apoptosis. The study indicated that enhancing endogenous survival pathways by NAMDA combined with other neuroprotective measure(s) might be a useful strategy to reduce apoptosis (Park and Cho, 2006). Activation of the ERK signaling cascade indicates that visceral primary afferents may sensitize after gastric noxious stimulation involving N-methyl-D-aspartate receptors. The ERK pathway therefore may not only be of importance for somatic but also for visceral nociception (Schicho et al., 2005). Spatiotemporal distribution of cerebellar pERK-IR suggesting that the ERK-pathway plays a dynamic role in regulating neuronal and glial migration, proliferation and differentiation in the developing

cerebellum. In the mature cerebellum, ERK signaling may also mediate postsynaptic information processing (Zsarnovszky and Belcher 2004). There is a study showed that cAMP promotes neurite outgrowth and extension through protein kinase A but independently of ERK activation in cultured rat motoneurons (Aglah et al., 2008). The ability of cAMP/PKA to activate ERKs in neuronal cells appears to depend on the development stage (Vogt Weisenhorn, et al., 2001), which might explain some controversial on the effect of ERK on cell survivals.

My previous study has shown intracellular cholesterol accumulation is related to neuronal apoptosis. The death mechanism through mitochondrial dysfunction has been illustrated. Addition of cAMP or forskolin protects neuronal cell death, likely via ERK signaling pathway. I further examine whether cAMP and forskolin have effect on attenuation of intracellular cholesterol accumulation. Accumulation of intracellular cholesterol was observed in cortical neurons after treatment with U18666A (2μg/ml), much less accumulation in case of co-treatment of cAMP with U18666A or forskolin with U18666A (figure 4.2), the intracellular cholesterol homeostasis could be restored.

Rab family is involved in multiple trafficking events in both endocytotic and biosynthetic pathways, and is located in specific intracellular compartments. Rab5 is involved in early endosome function, Rab4, Rab11 are involved in the sorting/recycling endosome, and Rab7 is involved in the lysosome/vacuole as the target organelle for degradation. Cholesterol contributes to regulate the Rab7 cycle, and that Rab7 in turn controls the net

movement of late endocytic elements. Motor functions can be regulated by the membrane lipid composition via the Rab7 cycle (Lebrand et al., 2002).

Studies showed Thyroid-stimulating hormone via cAMP, or forskolin increased Rab5a and Rab7 expression. (Croizet-Berger et al., 2002); overexpression of wild-type Rab7 or Rab9, but not Rab11, in Niemann-Pick type C lipid storage disease fibroblasts resulted in correction of lipid trafficking defects, including restoration of Golgi targeting of fluorescent lactosylceramide and endogenous GM1 ganglioside, and a dramatic reduction in intracellular cholesterol stores (Choudhury et al., 2002; Narita et al., 2005). The correction of membrane traffic in NPC cells by Rab protein overexpression may lead to new therapeutic approaches for treatment of this disease.

A few candidates of Rab proteins were selected in our study, such as Rab7, Rab9, Rab 5 and Rab 11. I treated neuron with U18666A 2ug/ml, or co-treatment with either cAMP 0.3 mM or forskolin 20 μM for 6h, 24h, 48h and 72h. Western blot showed that Rab5 and Rab11 were not significant changes with the induction of cAMP or forskolin, whereas Rab 9 expression level had mild changes. Rab7, which mediate intracellular transportation from endosome to lysosome, was up-regulated with co-treatment of cAMP or forskolin. This up-regulation effect is more apparent in the 48 h or 72 h time point (Figure 4.5). This is the first study I showed cAMP and forskolin has effect on Rab7 expression in the cultured cortical neurons.

Both activation of ERK and Rab7 has increased intracellular cholesterol esterification. This was confirmed with the inhibition of ERK activation by PD98059, choleteryl oleate formation in neuron was reduced; while knock-down of Rab7 by siRNA similar results shown. Both ERK activation and Rab7 may play roles in cholesterol transportation and esterification, through direct or indirect effects. Further studies should be carried out on the association between Rab7 upregulation and ERK phosphorylation, the mechanism of Rab7 upregulation, and also exam the mitochondria function as mitochondrial dysfunction shown in progesterone or U18666A induced neuronal apoptosis. Thus, therapies targeting basic mitochondrial processes, such as energy metabolism or free-radical generation, or specific interactions of disease-related proteins with mitochondria, may hold promise.

The system that I used for U18666A treatment on cortical neuron is a model that mimics the NPC1 phenotype, therefore, NPC1 (-/-) fibroblasts were chosen to be an *in vitro* system to study the effect of cAMP and forskolin. In the present study, Western blot showed cAMP or forskolin increase Rab7 about 2 folds at 48 hours treatment (Figure 4.7). Free cholesterol accumulation in the NPC1 fibroblast also apparently reduced (Figure 4.2); while cholesterol esterification was increased by about 3-4 fold. Knock-down of Rab7 by siRNA, showed the impact on cholesterol esterification too (Figure 4.8B), indicating Rab7 was required to transport free cholesterol for esterification. cAMP or forskolin also activation ERK in NPC1 fibroblast, inhibition of ERK activation by PD98059 is concurrently occurred with reduction of cholesteryl oleate formation, indicating that phosphorylation of ERK could be a up-stream factor of cholesterol

esterification. Further studies should be carried out on the association between Rab7 upregulation and ERK phosphorylation. A comparison of candidate Rab proteins between normal fibroblast and NPC1 (-/-) fibroblast may be worth to carry out. If possible, study can be extended to a translational level, from bench to bedside, one may get more valuable information on the regulation of cholesterol transportation, and apply such information on therapeutic strategies.

Thus, therapies targeting basic mitochondrial processes, such as energy metabolism or free-radical generation, or specific interactions of disease-related proteins with mitochondria, hold great promise.

Charpter 5. Conclusions

Elevated level of cholesterol in mitochondrial membranes of Niemann-Pick disease type C1 (NPC1) mouse brains and neural cells has been found to cause mitochondrial dysfunction. In the first part of the present study, I demonstrated in this study that inhibition of intracellular cholesterol trafficking in primary neurons by class 2 amphiphiles, which mimics the major biochemical and cellular feature of NPC1, led to not only impaired mitochondrial function but also activation of the mitochondrial apoptosis pathway. In activation of this pathway both cytochrome c and Smac/Diablo were released but apoptosis-inducing factor (AIF) was not involved. Treatment of the neurons with taurine, a caspase-9 specific inhibitor, could prevent the amphiphile-induced apoptotic cell death, suggesting that formation of apoptosome, followed by caspase-9 and caspase-3 activation, might play a critical role in the neuronal death pathway. Taken together, the mitochondria-dependent death cascade induced by blocking intracellular cholesterol trafficking was caspase-dependent.

Cell-permeable analogues of cAMP have been shown to improve the survival of cells, via ERKs mediates some of the neuroprotective actions of selected hormones and neurotransmitters. cAMP also coordinately enhances the expression of Rab5a and Rab7, which promote Tg endocytosis and transfer to lysosomes, respectively, resulting in accelerated thyroid hormone production. In our second part of study, I found cAMP and forskolin were effective in rescue neuronal injury induced by U18666A, concurrently with reduction of free cholesterol accumulation and increase of cholesterol esterification in both U18666A induced mimic model (cortical neuron) and npc1 (-/-) fibroblast, via

activation of ERK and up-regulation of Rab7 expression. These findings in the present study provide clues for both understanding the molecular basis of neurodegeneration in NPC1 disease and developing therapeutic strategies for treatment of this disorder.

Further studies should be carried out on the association between Rab7 up-regulation and ERK phosphorylation, the mechanism of Rab7 up-regulation, as well as the effect of cAMP and forskolin on the mitochondria function. Therapies targeting basic mitochondrial processes, such as energy metabolism or free-radical generation, or specific interactions of disease-related proteins with mitochondria, may hold promise.

References

Adams JM and Cory S. 2002. Apoptosomes: engines for caspase activation. Curr Opin Cell Biol 14, 715-720.

Aglah C, Gordon T, Posse de Charves EI. 2008. cAMP promotes neurite outgrowth and extension through protein kinase A but independently of Erk activation in cultured rat motoneurons. Neuropharmacology, 2008 Apr 15.

Alberts B, Johnson A, Lewis J, Raff M, Roberts K, Walter P. 2002. Molecular Biology of the Cell. New York: Garland Science.

Arany I, Megyesi JK, Kaneto H, Price PM, and Safirstein RL. 2004. Cisplatin-induced cell death is EGFR/src/ERK signaling dependent in mouse proximal tubule cells. Am J Physiol Renal Physiol 287: F543–F549.

Arnoult D, Gaume B, Karbowski M, Sharpe JC, Cecconi F, and Youle RJ. 2003a. Mitochondrial release of AIF and EndoG requires caspase activation downstream of Bax/Bak-mediated permeabilization. EMBO J. 22, 4385-4399.

Arnoult D, Karbowski M and Youle RJ. 2003b. Caspase inhibition prevents the mitochondrial release of apoptosis-inducing factor. Cell Death Differ. 10, 845-849.

Arnoult D, Parone P, Martinou JC, Antonsson B, Estaquier J, and Ameisen JC. 2002. Mitochondrial release of apoptosis-inducing factor occurs downstream of cytochrome c release in response to several proapoptotic stimuli. J Cell Biol 159, 923-929.

Bae SH, Lee JN, Fitzky BU, Seong J and Paik YK. 1999. Cholesterol biosynthesis from lanosterol: molecular cloning, tissue distribution, expression, chromosomal localization, and regulation of rat 7-dehydrocholesterol reductase, a Smith-Lemli-Opitz syndrome-related protein. J Biol Chem 274: 14624–14631.

Berger AC, Salazar G, Styers ML, Newell-Litwa KA, Werner E, Maue RA, Corbett AH, and Faundez V. 2007.The subcellular localization of the Niemann-Pick Type C proteins depends on the adaptor complex AP-3. J Cell Sci 120(pt20): 3640-3652.

Blanchette-Mackie EJ. 2000. Intracellular cholesterol trafficking: role of the NPC1 protein. Biochim Biophys Acta 1486:171–183.

Boatright KM, Renatus M, Scott FL, Sperandio S, Shin H, Pedersen IM, Ricci JE, Edris WA, Sutherlin DP, Green DR and Salvesen GS. 2003. A unified model for apical caspase activation. Mol Cell 11(2): 529-541.

Brady RO, Kanfer JN, Mock MB, and Fredrickson DS. 1966. The metabolism of sphingomyelin. II. Evidence of an enzymatic deficiency in Niemann-Pick diseae. Proc Natl Acad Sci USA. 55(2): 366-369.

Branton RL, Love RM, and Clarke DJ. 1998. cAMP included during cell suspension preparation improves survival of dopaminergic neurons in vitro. 1998. Neruroreport. 9(14):3223-3227.

Brown MS and Goldstein JL. 1980. Multivalent feedback regulation of HMG CoA reductase, a control mechanism coordinating isoprenoid synthesis and cell growth. J Lipid Res. 21(5):505-517.

Brown MS and Goldstein JL. 1986. A receptor-mediated pathway for cholesterol homeostasis. Science 232: 34–47.

Brown MS and Goldstein JL. 1999. A proteolytic pathway that controls the cholesterol content of membranes, cells, and blood. Proc. Natl. Acad. Sci. USA 96: 11041–11048.

Burns M, Gaynor K, Olm V, Mercken M, LaFrancois J, Wang L, Mathews PM, Noble W, Matsuoka Y, and Duff K. 2003. Presenilin redistribution associated with aberrant cholesterol transport enhances beta-amyloid production in vivo. J Neurosci. 23, 5645-5649.

Butler JD, Blanchette-Mackie J, Goldin E, O'Neill RR, Carstea G, Roff CF, Patterson MC, Patel S, Comly ME, and Cooney A. 1992. Progesterone blocks cholesterol translocation from lysosomes. J. Biol. Chem. 267, 23797-23805.

Cain K, Bratton SB and Cohen GM. 2002. The Apaf-1 apoptosome: a large caspase-activating complex. Biochimie 84, 203-214.

Carstea ED, Morris JA, Coleman KG, Loftus SK, Zhang D, Cummings C, Gu J, Chen Y, Cann MJ, Litvin TN, Iourgenko V, Sinclair ML, Levin LR, and Buck J. 2000. Soluble adenylyl cyclase as an evolutionarily conserved bicarbonate sensor. Science 289:625–628.

Cheung EC, Melanson-Drapeau L, Cregan SP, Vanderluit JL, Ferguson KL, McIntosh WC, Park DS, Bennett SA, and Slack RS. 2005. Apoptosis-inducing factor is a key factor in neuronal cell death propagated by BAX-dependent and BAX-independent mechanisms. J Neurosci25, 1324-1334.

Cheung NS, Koh CH, Bay BH, Qi RZ, Choy MS, Li Q-T, Wong KP, and Whiteman M. 2004. Chronic exposure to U18666A induces apoptosis in cultured murine cortical neurons. Biochem Biophys Res Commun 315, 408-417.

Cheung NS, Pascoe CJ, Giardina SF, John CA, and Beart PM. 1998. Micromolar L-glutamate induces extensive apoptosis in an apoptotic-necrotic continuum of insult-

dependent, excitotoxic injury in cultured cortical neurones. Neuropharmacology 37, 1419-1429.

Choudhury A, Dominguez M, Puri V, Sharma DK, Narita K, Wheatley CL, Marks DL, Pagano RE. 2002. Rab proteins mediate Golgi transport of caveola-internalized glycosphingolipids and correct lipid trafficking in Niemann-Pick C cells. J Clin Invest 109:1541–1550.

Cooper DM. 2003. Regulation and organization of adenylyl cyclases and cAMP. Biochem J 375:517–529.

Corbeel L and Freson K. 2008. Rab proteins and Rab-associated proteins: major actors in the mechanism of protein-trafficking disorders. Eur J Pediatr 167(7):723-729.

Cotman CW and Anderson AJ, 1995. A potential role for apoptosis in neurodegeneration and Alzheimer's disease. Mol Neurobiol 10(1), 19-45.

Cregan SP, Dawson VL, and Slack RS. 2004. Role of AIF in caspase-dependent and caspase-independent cell death. Oncogene 23, 2785-2796.

Cregan SP, Fortin A, MacLaurin JG., Callaghan SM, Cecconi F, Yu SW, Dawson T M, Dawson VL, Park DS, Kroemer G, and Slack RS. 2002. Apoptosis-inducing factor is involved in the regulation of caspase-independent neuronal cell death. J Cell Biol.158, 507-517.

Croizet-Berger K, Daumerie C, Couvreur M, Courtoy PJ, and van den Hove MF. 2002. The endocytic catalysts, Rab5a and Rab7, are tandem regulators of thyroid hormone production. Proc Natl Acad Sci U S A 99(12):8277-82.

Cui Q, Yip HK, Zhao RC, So KF, and Harvey AR, 2003. Intraocular elevation of cyclic AMP potentiates ciliary neurotrophic factor-induced regeneration of adult rat retinal ganglion cell axons, Mol Cell Neurosci 22, 49–61.

Daugas E, Susin SA, Zamzami N, Ferri KF, Irinopoulou T, Larochette N, Prevost M C, Leber B, Andrews D, Penninger J, and Kroemer G. 2000. Mitochondrio-nuclear translocation of AIF in apoptosis and necrosis. FASEB J. 14, 729-739.

Davies JP and Ioannou YA. 2003. Topological analysis of Niemann-Pick C1 protein reveals that the membrane orientation of the putative sterol-sensing domain is identical to those of 3-hydroxy-3-methylglutaryl-CoA reductase and sterol regulatory element binding protein cleavage-activating protein. J Biol Chem 275: 24,367– 24,374.

Dawson TM and Dawson VL. 2004. Apoptosis-inducing factor substitutes for caspase executioners in NMDA-triggered excitotoxic neuronal death. J Neurosci 24, 10963-10973.

DeGrella RF and Simoni RD. 1982. Intracellular transport of cholesterol to the plasma membrane. J Biol Chem 257:14256–14262.

Dietschy JM and Turley SD. 2001. Cholesterol metabolism in the brain. Curr Opin Lipidol 12: 105–112.

Dive C, Gregory CD, Phipps DJ, Evans DL, Milner AE, Wyllie AH, 1992. Analysis and discrimination of necrosis and apoptosis (programmed cell death) by multiparameter flow cytometry Biochim. Biophys Acta 1133(3):275-285.

Du C, Fang M, Li Y, Li L and Wang X. 2000. Smac, a mitochondrial protein that promotes cytochrome c–dependent caspase activation by eliminating IAP inhibition. Cell 102, 33-42.

Earnshaw WC, Martins LM, and Kaufmann SH. 1999. Mammalian caspases: structure, activation, substrates, and functions during apoptosis. Annu Rev Biochem68:383-424.

Eckert A, Marques CA, Keil U, Schüssel K, Müller WE. 2003. Increased apoptotic cell death in sporadic and genetic Alzheimer's disease. Ann N Y Acad Sci 1010: 604-609.

Edinger AL, Cinalli RM and Thompson CB. 2003. Rab7 prevents growth factor-independent survival by inhibiting cell-autonomous nutrient transporter expression. Dev Cell 5, 571-582.

Edmond J, Korsak RA, Morrow JW, Torok-Both G, and Catlin DH. 1991. Dietary cholesterol and the origin of cholesterol in the brain of developing rats. J Nutr 121: 1323– 1330.

Elliott-Hunt CR, Kazlauskaite J, Wilde GJ, Grammatopoulos D. K. and Hillhouse EW. 2002. Potential signalling pathways underlying corticotrophin-releasing hormone-mediated neuroprotection from excitotoxicity in rat hippocampus. J Neurochem 80, 416–425.

Fadok VA, Voelker DR, Campbell PA, Cohen JJ, Bratton DL, and Henson PM. 1992. Exposure of phosphatidylserine on the surface of apoptotic lymphocytes triggers specific recognition and removal by macrophages. J Immunol, 148, 2207-2216.

Falk T, Garver WS, Erickson RP, Wilson JM, and Yool AJ. 1999. Expression of Niemann-Pick type C transcript in rodent cerebellum in vivo and in vitro. Brain Res. 839: 49–57.

Feng B, Yao PM, Li Y, Devlin CM, Zhang D, Harding HP, Sweeney M, Rong JX, Kuriakose G, Fisher EA, Marks AR, Ron D, Tabas I. 2003. The endoplasmic reticulum is the site of cholesterol-induced cytotoxicity in macrophages. Nat Cell Biol 5:781–792.

Feng Y, Press B and Wandinger-Ness A. 1995. Rab7: an important regulator of late endocytic membrane traffic. J Cell Biol. 131, 1435-1452.

Fielding CJ and Fielding PE. 1997. Intracellular cholesterol transport. J Lipid Res. 38(8):1503-1521.

Friedland N, Liou HL, Lobel P, and Stock AM. 2003. Structure of a cholesterol-binding protein deficient in Niemann-Pick type C2 disease. Proc Natl Acad Sci 100:2512–2517.

Friedlander RM. 2003. Apoptosis and caspases in neurodegenerative diseases. N Engl J Med. 348:1365-1332

Frolov A, Zielinski SE and Crowley JR. 2000. NPC1 and NPC2 regulate cellular cholesterol homeostasis through generation of LDL-derived oxysterols. J Biol Chem 278:25,517–25,525.

Garcia-Ruiz C, and Fernandez-Checa JC. 2006. Mitochondrial glutathione: hepatocellular survival-death switch. J Gastroenterol Hepatol 21 (Suppl) 3:S3-6.

Garg TK and Chang Y. 2003.Oxidative stress causes ERK phosphorylation and cell death in cultured retinal pigment epithelium: Prevention of cell death by AG126 and 15-deoxy-delta 12, 14-PGJ2. BMC Ophthalmol 3:5-20.

Geppert M, Goda Y, Stevens CF and Sudhof TC. 1997. The small GTP-binding protein Rab3A regulates a late step in synaptic vesicle fusion. Nature 387, 810-814.

Gévry NY and Murphy BD. 2002. The role and regulation of the Niemann-Pick C1 gene in adrenal steroidogenesis. Endocr Res 28(4):403-412.

Gobert D, Topolnik L, Azzi M, Huang L, Badeaux F, Desgroseillers L, Sossin WS, and Lacaille JC. 2008. Forskolin induction of late-LTP and up-regulation of 5' TOP mRNAs translation via mTOR, ERK, and PI3K in hippocampal pyramidal cells. J Neurochem May 29 (Epub ahead of print).

Griffin LD, Gong W, Verot L, and Mellon SH. 2004. Niemann–Pick type C disease involves disrupted neurosteroidogenesis and responds to allopregnanolone. Nat Med 10, 704–711.

Grosshans BL, Ortiz D and Novick P. 2006. Rabs and their effectors: achieving specificity in membrane traffic. Proc. Natl. Acad. Sci. USA 103, 11821–11827.

Hampton RY. 2002. Proteolysis and sterol regulation. Annu. Rev. Cell Dev. Biol. 18: 345–378.

Guo YJ, Li WH, Wu R, Xie Q, Zhang ZH, and Cui LQ. 2008. Niemann-Pick type C1 protein influences the delivery of cholesterol to the SREBP:SCAP complex. Braz J Med Biol Res 41(1):26-33.

Hansen M. B., Nielsen S. E. and Berg K. 1989. Re-examination and further development of a precise and rapid dye method for measuring cell growth/cell kill. J Immunol Methods 119, 203-210.

Hao M, Lin SX, Karylowski OJ, Wustner D, McGraw TE, Maxfield FR. 2002. Vesicular and non-vesicular sterol transport in living cells. The endocytic recycling compartment is a major sterol storage organelle. J Biol Chem 277:609–617.

Herz J and Bock HH. 2002. Lipoprotein receptors in the nervous system. Annu Rev Biochem. 71, 405-434.

Hevroni D, Rattner A, and Bundman M. 1998. Hippocampal plasticity involves extensive gene induction and multiple cellular mechanisms. J Mol Neurosci 10: 75–98.

Hickey MA and Chesselet MF. 2003. Apoptosis in Huntington's disease. Prog. Neuropsychopharmacol. Biol Psychiatry 27: 255-265.

Higgins ME, Davies JP, Chen FW, and Ioannou YA. 1999. Niemann-Pick C1 is a late endosome-resident protein that transiently associates with lysosomes and the trans-Golgi network. Mol Genet Metab 68(1):1-13.

Holtta-Vuori M, Tanhuanpaa K, Mobius W, Somerharju P, Ikonen E. 2002. Modulation of cellular cholesterol transport and homeostasis by Rab11. Mol Biol Cell 13:3107–3122.

Hopker VH, Shewan D, Tessier-Lavigne M, Poo M, and Holt C. 1999. Growthcone attraction to netrin-1 is converted to repulsion by laminin-1. Nature 401:69 –73.

Hsiung SC, Tin A, Tamir H, Franke TF, and Liu KP. 2008. Inhibition of 5-HT(1A) receptor-dependent cell survival by cAMP/protein kinase A: Role of protein phosphatase 2A and Bax. J Neurosci Res 86(10):2326-2338.

Infante RE, Abi-Mosleh L, Radhakrishnan A, Dale JD, Brown MS, and Goldstein JL. 2007. Purified NPC1 protein: I Bing of cholesterol and oxysterols to a 1278-amino acid membrane protein. J Biol Chem 283(2):1052-1063.

Impey S, Obrietan K and Storm DR. 1999. Making new connections: role of ERK/MAP kinase signaling in neuronal plasticity. Neuron 23: 11–14.

Ioannou YA, Higgins ME, Comly M, Cooney A, Brown A, Kaneski CR, Blanchette-Mackie EJ, Dwyer NK, Neufeld EB, Chang TY, Liscum L, Strauss JF 3rd, Ohno K, Zeigler M, Carmi R, Sokol J, Markie D, O'Neill RR, van Diggelen OP, Elleder M, Patterson MC, Brady RO, Vanier MT, Pentchev PG, and Tagle DA.1997. Niemann-Pick

C1 disease gene: homology to mediators of cholesterol homeostasis. Science 277(5323): 228-231.

Jayanthi S, Deng X, Ladenheim B, McCoy MT, Cluster A, Cai NS, and Cadet JL. 2005. Calcineurin/NFAT-induced up-regulation of the Fas ligand/Fas death pathway is involved in methamphetamine-induced neuronal apoptosis. Proc Natl Acad Sci USA 102: 868-873.

Jiang H, Zhang L, Koubi D, Kuo J, Groe L, Rodriguez AI, Hunter TJ, Tang S, Lazarovici P, Gautam SC, and Levine RA. 2005. Role of Ras-Erk in apoptosis of PC12 cells induced by trophic factor withdrawal or oxidative stress. J Mol Neurosci 25(2):133-140.

Jin K, Mao XO, Zhu Y and Greenberg DA. 2002. MEK and ERK protect hypoxic cortical neurons via phosphorylation of Bad. J of Neurochem 80:119-125.

Jurevics H and Morell P. 1995. Cholesterol for synthesis of myelin is made locally, not imported into brain. J. Neurochem 64: 895–901.

Karten B, Vance DE, Campenot RB, and Vance JE. 2002. Cholesterol accumulates in cell bodies, but is decreased in distal axons, of Niemann-Pick C1-deficient neurons. J. Neurochem 83: 1154-1163.

Karten B, Vance DE, Campenot RB, and Vance JE. 2003. Trafficking of cholesterol from cell bodies to distal axons in Niemann Pick C1-deficient neurons. J Biol Chem 278: 4168-4175.

Kashimoto R, Kurimoto T, Miyoshi T, Okamoto N, Tagami Y, Oono S, Ito Y, and Mimura O. 2008. Cilostazol promotes survival of axotomized retinal ganglion cells in adult rats. Neuroscience Letters 436 (2): 116-119.

Khan SH, Banigesh A, Baziani A, Todd KG, Miyashita H, Eweida M and Shuaib A. 2000. The role of taurine in neuronal protection following transient global forebrain ischemia. Neurochem Res 25:217-223.

Ko DC, Binkley J, Sidow A, Scott MP. 2003. The integrity of a cholesterolbinding pocket in Niemann-Pick C2 protein is necessary to control lysosome cholesterol levels. Proc Natl Acad Sci USA. 100: 2518–2525.

Ko DC, Gordon MD, Jin JY, and Scott MP. 2001. Dynamic movements of organelles containing Niemann-Pick C1 protein: NPC1 involvement in late endocytic events. Mol Biol Cell 12: 601-614.

Ko DC, Gordon MD, Jin JY, Scott MP. 2003. Dynamic movements of organelles containing Niemann-Pick C1 protein: NPC1 involvement in late endocytic events. Mol Biol Cell 12:601– 614.

Kobayashi T, Beuchat MH, Lindsay M, Frias S, Palmiter RD, Sakuraba H, Parton RG, and Gruenberg J. 1999. Late endosomal membranes rich in lysobisphosphatidic acid regulate cholesterol transport. Nat Cell Biol 1: 113-118.

Koudinov AR and Koudinova NV. 2001. Essential role for cholesterol in synaptic plasticity and neuronal degeneration. FASEB J 15(10): 1858-1860.

Kroemer G. and Reed JC. 2000. Mitochondrial control of cell death. Nat Med 6: 513-519.

Kuwana T. and Newmeyer DD. 2003. Bcl-2-family proteins and the role of mitochondria in apoptosis. Curr Opin Cell Biol 15: 691-699.

Lange Y, Ye J, Rigney M, and Steck T. 2000. Cholesterol movement in Niemann-Pick type C cells and in cells treated with amphiphiles. J Biol Chem 275: 17468-17475.

Lange Y, Ye J, Rigney M, and Steck TL. 1993. Role of the plasma membrane in cholesterol esterification in rat hepatoma cells. J Biol Chem 268: 13838-13843.

Lange Y. and Steck TL. 1994. Cholesterol homeostasis. Modulation by amphiphiles. J Biol Chem. 269: 29371-29374.

Langmade SJ, Gale SE, Frolov A, Mohri I, Suzuki K, Mellon SH, Walkley SU, Covey DF, Schaffer JE, and Ory DS. 2006. Pregnane X receptor (PXR) activation: a mechanism for neuroprotection in a mouse model of Niemann-Pick C disease. Proc Natl Acad Sci U S A. 103(37):13807-13812.

Lebrand C, Corti M, Goodson H, Cosson P, Cavalli V, Mayran N, Fauré J, and Gruenberg J. 2002. Late endosome motility depends on lipids via the small GTPase Rab7. EMBO J 21(6):1289-1300.

Li H, Repa JJ, Valasek MA, Beltroy EP, Turley SD, German DC, and Dietschy JM. 2005. Molecular, anatomical, and biochemical events associated with neurodegeneration in mice with Niemann-Pick type C disease. J. Neuropathol. Exp Neurol 64: 323-333.

Li P, Nijhawan D, Budihardjo I, Srinivasula SM, Ahmad M, Alnemri ES, and Wang X. 1997. Cytochrome c and dATP-dependent formation of Apaf-1/caspase-9 complex initiates an apoptotic protease cascade. Cell 91: 479-489.

Liscum L and Munn NJ. 1999. Intracellular cholesterol transport. Biochim Biophys Acta 1438(1):19-37.

Liscum L, Ruggiero RM, and Faust JR. 1989. The intracellular transport of low density lipoprotein-derived cholesterol is defective in Niemann-Pick type C fibroblasts. J Cell Biol 108: 1625-1636.

Liscum L. and Faust JR. 1989. The intracellular transport of low density lipoprotein-derived cholesterol is inhibited in Chinese hamster ovary cells cultured with 3-beta-[2-(diethylamino)ethoxy]androst-5-en-17-one. J Biol Chem. 264: 11796-11806.

Liu X, Kim CN, Yang J, Jemmerson R, and Wang X. 1996. Induction of apoptotic program in cell-free extracts: requirement for dATP and cytochrome c. Cell 86: 147-157.

Llewellyn JC, Ulrich H, Nadya GG Konstantin AL, and Samie RJ. 2008.
Intra-axonal translation and retrograde trafficking of CREB promotes neuronal survival.
Nat Cell Biol. 10 (2): 149-167.

Loftus SK, Erickson RP, Walkley SU, Bryant MA, Incao A, Heidenreich RA, Pavan WJ. 2002. Rescue of neurodegeneration in Niemann-Pick C mice by a prion-promoter-driven Npc1 cDNA transgene. Hum Mol Genet. 11(24):3107-3114.

Louzada PR, Lima AC, Mendonca-Silva DL, Noel F, De Mello FG, and Ferreira ST. 2004. Taurine prevents the neurotoxicity of beta-amyloid and glutamate receptor agonists: activation of GABA receptors and possible implications for Alzheimer's disease and other neurological disorders. FASEB J 18: 511-518.

Lowry OH, Rosebrough NJ, Farr AL, and Randall RJ. 1951. Protein measurement with the Folin phenol reagent. J Biol Chem 193: 265-275.

Mansour-Robaey S, Clarke DB, Wang YC, Bray GM and Aguayo AJ. 1994. Effects of ocular injury and administration of brain-derived neurotrophic factor on survival and regrowth of axotomized retinal ganglion cells. Proc Natl Acad Sci USA 91: 1632–1636.

Mattson MP. 2000. Apoptosis in neurodegenerative disorders. Nat Rev Mol Cell Biol 1(2):120-129.

Mauch DH, Nagler K, Schumacher S, Goritz C, Muller EC, Otto A, and Pfrieger FW. 2001. CNS synaptogenesis promoted by glia-derived cholesterol. Science 294 (5545), 1354-1357.

Mellon S, Gong W, and Griffin LD. 2004. Niemann pick type C disease as a model for defects in neurosteroidogenesis. Endocr Res 30(4):727-35.

Michel PP and Agid Y. 1996. Chronic activation of the cyclic AMP signaling pathway promotes development and long-term survival of mesencephalic dopaminergic neurons.
J Neurochem 67: 1633–1642.

Ming GL, Song HJ, Berninger B, Holt CE, Tessier-Lavigne M, and Poo MM. 1997. cAMP-dependent growth cone guidance by netrin-1. Neuron 19:1225–1235.

Mohammadi A, Perry RJ, Storey MK, Cook HW, Byers DM, Ridgway ND. 2001. Golgi localization and phosphorylation of oxysterol binding protein in Niemann-Pick C and U18666A-treated cells. J Lipid Res. 42: 1062-1071.

Moore SW and Kennedy TE. 2006. Protein kinase A regulates the sensitivity of spinal commissural axon turning to netrin-1 but does not switch between chemoattraction and chemorepulsion. J Neurosci 26: 2419 –2423.

Morishima Y, Gotoh Y, Zieg J, Barrett T, Takano H, Flavell R, Davis RJ, Shirasaki Y, and Greenberg ME. 2001. Beta-amyloid induces neuronal apoptosis via a mechanism that involves the c-Jun N-terminal kinase pathway and the induction of Fas ligand. J. Neurosci 21: 7551-7560.

Mukherjee S and Maxfield FR. 2004. Lipid and cholesterol trafficking in NPC. Biochim Biophys Acta 1685: 28-37.

Nakao N. An increase in intracellular levels of cyclic AMP produces trophic effects on striatal neurons developing in culture. 1998. Neuroscience 82: 1009–1020.

Narita K, Choudhury A, Dobrenis K, Sharma DK, Holicky EL, Marks DL, Walkley SU, Pagano RE. 2005. Protein transduction of Rab9 in Niemann-Pick C cells reduces cholesterol storage. FASEB J 19(11):1558-1560.

Naureckiene S, Sleat DE, Lackland H, Fensom A, Vanier MT, Wattiaux R, Jadot M, Lobel P. 2000. Identification of HE1 as the second gene of Niemann-Pick C disease. Science. 290:2298–2301.

Neufeld EB, Wastney M, Patel S, Suresh S, Cooney AM, Dwyer NK, Roff CF, Ohno K, Morris JA, Carstea ED, Incardona JP, Strauss JF 3rd, Vanier MT, Patterson MC, Brady RO, Pentchev PG, Blanchette-Mackie EJ. 1999. The Niemann-Pick C1 protein resides in a vesicular compartment linked to retrograde transport of multiple lysosomal cargo. J Biol Chem. 274(14):9627-9635.

Newmeyer DD and Ferguson-Miller S. 2003. Mitochondria: releasing power for life and unleashing the machineries of death. Cell 112: 481-490.

Nijhawan D, Honarpour N, and Wang X. 2000. Apoptosis in neural development and disease. Annu Rev Neurosci. 23:73-87.

Norman AW, Demel RA, de Kruyff B and van Deenen LL, 1972. Studies on the biological properties of polyene antibiotics. Evidence for the direct interaction of filipin with cholesterol. J Biol Chem. 247(6):1918-1929.

Otera H, Ohsakaya S, Nagaura Z, Ishihara N and Mihara K. 2005. Export of mitochondrial AIF in response to proapoptotic stimuli depends on processing at the intermembrane space. EMBO J 24: 1375-1386.

Paciorkowski AR, Westwell M, Ounpuu S, Bell K, Kagan J, Mazzarella C, Greenstein RM. 2008. Motion analysis of a child with Niemann-Pick disease type C treated with miglustat. Mov Disord. 23(1):124-128.

Park EM and Cho S. 2006. Enhanced ERK dependent CREB activation reduces apoptosis in staurosporine-treated human neuroblastoma SK-N-BE(2)C cells. Neurosci Lett. 402(1-2):190-194.

Passeron T, Namiki T, Passeron HJ, Le Pape E, Hearing VJ. 2008. Forskolin Protects Keratinocytes from UVB-Induced Apoptosis and Increases DNA Repair Independent of its Effects on Melanogenesis. J Invest Dermatol. Jun 26 (Epub adhead of print).

Patlerson MC, Vanier MT, Suzuki K, Morris JA, Carstea E, Neufeld EB, Branchetle-Mackie JE, and Pentchev PG. 2001. Niemann-Pick disease type C: a lipid trafficking disorder, in The metabolic and molecular basses of inherited disease, Scriver C, Beaudet R, Sly AL, W.S. and Valle D, eds, pp. 3611-3633. McGraw-Hill Inc., New York.

Pentchev PG, Kruth HS, Comly ME, Butler JD, Vanier MT, Wenger DA, and Patel S. 1986. Type C Niemann-Pick disease. A parallel loss of regulatory responses in both the uptake and esterification of low density lipoprotein-derived cholesterol in cultured fibroblasts. J Biol Chem 261: 16775-16780.

Pfeffer S and Aivazian D. 2004. Targeting Rab GTPases to distinct membrane compartments. Nat Rev Mol Cell Biol 5: 886–896.

Pfeffer S. 2003. Membrane domains in the secretory and endocytic pathways. Cell 112, 507–517.

Polster BM and Fiskum G. 2004. Mitochondrial mechanisms of neuronal cell apoptosis. J Neurochem 90: 1281-1289.

Polster BM, Basanez G, Etxebarria A, Hardwick JM, and Nicholls DG. 2005. Calpain I induces cleavage and release of apoptosis-inducing factor from isolated mitochondria. J Biol Chem 280: 6447-6454.

Prasad A, Fischer WA, Maue RA, and Henderson LP. 2000. Regional and developmental expression of the Npc1 mRNA in the mouse brain. J Neurochem. 75: 1250–1257.

Prattes S. 2000. Intracellular distribution and mobilization of unesterified cholesterol in adipocytes: triglyceride droplets are surrounded by cholesterol-rich ER-like surface layer structures. J Cell Sci. 113 (Pt 17): 2977-2989.

Prinz W. 2002. Cholesterol trafficking in the secretory and endocytic systems. Semin Cell Dev Bio. 2002;13:197–203.

Putcha GV, Harris CA, Moulder KL, Easton RM, Thompson CB, and Johnson EM Jr. 2002. Intrinsic and extrinsic pathway signaling during neuronal apoptosis: lessons from the analysis of mutant mice. J Cell Biol 157: 441-453.

Reid PC, Sakashita N, Sugii S, Ohno-Iwashita Y, Shimada Y, Hickey WF, Chang TY. 2004. A novel cholesterol stain reveals early neuronal cholesterol accumulation in the Niemann-Pick type C1 mouse brain. J Lipid Res 45:582–591.

Ribeiro L, Azevedo I, Martel F. 2002. Comparison of the effect of cyclic AMP on the content and release of dopamine and 1-methyl-4-phenylpyridinium (Mpp+) in PC12 cells. Auton Autacoid Pharmacol 22(5-6):277-289

Roff CF, Goldin E, Comly ME, Cooney A, Brown A, Vanier MT, Miller SP, Brady RO and Pentchev PG. 1991. Type C Niemann-Pick disease: use of hydrophobic amines to study defective cholesterol transport. Dev Neurosci 13, 315-319.

Rooney GE, Howard L, O'Brien T, Windebank AJ, and Barry FP. 2008. Elevation of cAMP in Mesenchymal Stem Cells Transiently Upregulates Neural Markers rather than Inducing Neural Differentiation. Stem Cells Dev 2008 Jun 13.

Rosenfeld MA, Pavan WJ, Krizman DB, Nagle J, Polymeropoulos MH, Sturley SL, Reid PC, Lin S, Vanier MT, Ohno-Iwashita Y, Hartwood HJ Jr, Hickey WF, Chang CC, Chang TY. 2008. Partial blockage of sterol biosynthesis with a squalene synthase inhibitor in early postnatal Niemann-Pick type C npcnih null mice brains reduces neuronal cholesterol accumulation, abrogates astrogliosis, but may inhibit myelin maturation. J Neurosci Methods 168(1):15-25.

Runquist M, Parmryd I, Thelin A, Chojnacki T and Dallner G. 1995. Distribution of branch point prenyltransferases in regions of bovine brain. J Neurochem 65: 2299–2306

Runz H, Rietdorf J, Tomic I, de Bernard M, Beyreuther K, Pepperkok R, and Hartmann T. 2002. Inhibition of intracellular cholesterol transport alters presenilin localization and amyloid precursor protein processing in neuronal cells. J Neurosci 22: 1679-1689.

Saelens X, Festjens N, Vande Walle L, van Gurp M, van Loo G, and Vandenabeele P. 2004. Toxic proteins released from mitochondria in cell death. Oncogene 23: 2861-2874.

Sakai J and Rawson RB. 2001. The sterol regulatory element-binding protein pathway: control of lipid homeostasis through regulated intracellular transport. Curr Opin Lipidol 12: 261–266.

Salvesen GS and Dixit VM. 1997. Caspases: intracellular signaling by proteolysis. Cell 91: 443-446.

Sastry PS. 1985. Lipids of nervous tissue: composition and metabolism. Prog Lipid Res 24: 69–176.

Sawamura N, Gong JS, Chang TY, Yanagisawa K, and Michikawa M. 2003. Promotion of tau phosphorylation by MAP kinase Erk1/2 is accompanied by reduced cholesterol level in detergent-insoluble membrane fraction in Niemann-Pick C1-deficient cells. J Neurochem 84 (5):1086-1096.

Schicho R, Liebmann I and Lippe IT. 2005. Extracellular signal-regulated kinase-1 and -2 are activated by gastric luminal injury in dorsal root ganglion neurons via N-methyl-D-aspartate receptors. Neuroscience 134(2):505-514.

Schildberg FA, Schulz S, Dombrowski F, Minor T. 2005. Cyclic AMP alleviates endoplasmic stress and programmed cell death induced by lipopolysaccharides in human endothelial cells. Cell Tissue Res 320(1):91-8.

Schmitz G and Orso E. 2001. Intracellular cholesterol and phospholipid trafficking: comparable mechanisms in macrophages and neuronal cells. Neurochem. Res 26:1045–1068.

Seabra MC, Mules EH and Hume AN. 2002. Rab GTPases, intracellular traffic and disease. Trends Mol Med 8: 23-30.

Searle J, Kerr JFR, Bishop CJ, 1982. Necrosis and apoptosis: distinct modes of cell death with fundamentally different significance. Pathol Annu 17: 229-259.

Shuaib A. 2003. The role of taurine in cerebral ischemia: studies in transient forebrain ischemia and embolic focal ischemia in rodents. Adv Exp Med Bio. 526: 421-431.

Simons K and Ikonen E. 2000. How cells handle cholesterol. Science 290: 1721–1726

Su JH, Anderson AJ, Cummings BJ, and Cotman CW. 1994. Immunohistochemical evidence for apoptosis in Alzheimer's disease. Neuroreport 5: 2529-2533.

Susin SA, Lorenzo HK, Zamzami N. 1999. Molecular characterization of mitochondrial apoptosis-inducing factor. Nature 397: 441-446.

Tabas I. 2002. Consequences of cellular cholesterol accumulation: basic concepts and physiological implications. J Clin Invest. 110: 905–911.

Tabas I. 2007. A two-carbon switch to sterol-induced autophagic death. Autophagy. 3(1):38-41.

Takatani T, Takahashi K, Uozumi Y, Shikata E, Yamamoto Y, Ito T, Matsuda T., Schaffer SW, Fujio Y, and Azuma J. 2004. Taurine inhibits apoptosis by preventing

formation of the Apaf-1/caspase-9 apoptosome. Am. J. Physiol. Cell Physiol. 287: C949-C953.

Tasken K and Aandahl EM. 2004. Localized effects of cAMP mediated by distinct routes of protein kinase A. Physiol Rev 84:137–167.

Tatton WG, Chalmers-Redman R, Brown D, and Tatton N. 2003. Apoptosis in Parkinson's disease: signals for neuronal degradation. Ann. Neurol. 53 (Suppl 3): S61-S70.

Teixeira CA, Lin S, Mangas M, Quinta R, Bessa CJ, Ferreira C, Sá Miranda MC, Boustany RM, Ribeiro MG. 2006. Gene expression profiling in vLINCL CLN6-deficient fibroblasts: Insights into pathobiology. Biochim Biophys Acta 1762(7):637-646.

te Vruchte D, Lloyd-Evans E, Veldman RJ, Neville DC, Dwek RA, Platt FM, van Blitterswijk WJ, Sillence DJ. 2004. Accumulation of glycosphingolipids in Niemann-Pick C disease disrupts endosomal transport. J Biol Chem 279(25):26167-26175

Thelen K, Kedar V, Panicker A K, Schmid RS, Midkiff BR, and Maness PF. 2002. The neural cell adhesion molecule L1 potentiates integrin-dependent cell migration to extracellular matrix proteins. J Neurosci 22: 4918–4931.

Thornberry NA and Lazebnik Y. 1998. Caspases: enemies within. Science 281: 1312-1316.

Turley SD, Burns DK, and Dietschy JM. 1998. Preferential utilization of newly synthesized cholesterol for brain growth in neonatal lambs. Am J Physiol 274: E1099–E1105.

Underwood KW, Andemariam B, McWilliams GL, and Liscum L. 1996. Quantitative analysis of hydrophobic amine inhibition of intracellular cholesterol transport. J Lipid Res 37:1556–1568.

Urbani L and Simoni RD. 1990. Cholesterol and vesicular stomatitis virus G protein take separate routes from the endoplasmic reticulum to the plasma membrane. J Biol Chem 265(4):1919-1923.

Uren RT, Dewson G, Bonzon C, Lithgow T, Newmeyer DD, and Kluck RM. 2005. Mitochondrial release of pro-apoptotic proteins: electrostatic interactions can hold cytochrome c but not Smac/DIABLO to mitochondrial membranes. J Biol Chem 280: 2266-2274.

van Loo G, Saelens X, van Gurp M, MacFarlane M, Martin SJ, and Vandenabeele P. 2002. The role of mitochondrial factors in apoptosis: a Russian roulette with more than one bullet. Cell Death Differ. 9: 1031-1042.

Vanier MT, Duthel S, and Rodriguez-Lafrasse C. 1996. Genetic heterogeneity in Niemann-Pick C disease: a study using somatic cell hybridization and linkage analysis. Am J Hum Genet 58:118– 125.

Vaudry D, Gonzalez BJ, and Basille M. 1998. Pituitary adenylate cyclase-activating polypeptide stimulates both c-fos gene expression and cell survival in rat cerebellar granule neurons through activation of the protein kinase A pathway. Neuroscience 84: 801–812.

Verhagen AM, Ekert PG, Pakusch M, Silke J, Connolly LM, Reid GE, Moritz RL, Simpson RJ, and Vaux DL. 2000. Identification of DIABLO, a mammalian protein that promotes apoptosis by binding to and antagonizing IAP proteins. Cell 102: 43-53.

VogtWeisenhorn DM, Roback LJ, Kwon JH, andWainer BH. 2001. Coupling of cAMP/PKA and MAPK signaling in neuronal cells is dependent on developmental stage. Exp Neurol 169: 44–55.

Wang H, Yu SW, Koh DW, Lew J, Coombs C, Bowers W, Federoff HJ, Poirier GG, Watanabe M, Tokita Y, Kato M, and Fukuda Y. 2003. Intravitreal injections of neurotrophic factors and forskolin enhance survival and axonal regeneration of axotomized beta ganglion cells in cat retina. Neuroscience 116: 733–742.

Watari H, Blanchette-Mackie EJ, and Dwyer NK. 1999. Niemann-Pick C1 protein: obligatory roles for N-terminal domains and lysosomal targeting in cholesterol mobilization. Proc Natl Acad Sci 96: 805– 810.

Watari H, Blanchette-Mackie EJ, and Dwyer NK. 2000. Determinants of NPC1 expression and action: key promoter regions, posttranscriptional control, and the importance of a ‘‘cysteine-rich’’ loop. Exp Cell Res 259: 247–256.

Wu YP, Mizukami H, Matsuda J, Saito Y, Proia RL, and Suzuki K. 2005. Apoptosis accompanied by up-regulation of TNF-alpha death pathway genes in the brain of Niemann-Pick type C disease. Mol Genet Metab 84: 9-17.

Yaar M, Zhai S, Pilch PF, Doyle SM, Eisenhauer PB, Fine RE, and Gilchrest BA. 1997. Binding of beta-amyloid to the p75 neurotrophin receptor induces apoptosis. A possible mechanism for Alzheimer's disease. J Clin Invest 100: 2333-2340.

Yu W, Gong JS, Ko M, Garver WS, Yanagisawa K, and Michikawa M. 2005. Altered cholesterol metabolism in Niemann-Pick type C1 mouse brains affects mitochondrial function. J Biol Chem 280: 11731-11739.

Yuan J and Yankner BA. 2000. Apoptosis in the nervous system. Nature 407, 802-809.

Yuan J, Shaham S, Ledoux S, Ellis HM, and Horvitz HR. 1993. Cell 75: 641-652.

Yuste VJ, Moubarak RS, Delettre C, Bras M, Sancho P, Robert N, d'Alayer J, and Susin SA. 2005. Cysteine protease inhibition prevents mitochondrial apoptosis-inducing dactor (AIF) release. Cell Death Differ. 12: 1445-1448.

Zerial M and McBride H. 2001. Rab proteins as membrane organizers. Nat Rev Mol. Cell Biol 2: 107–117.

Zhang J and Abdel-Rahman AA. 2008. Inhibition of nischarin expression attenuates rilmenidine-evoked hypotension and phosphorylated extracellular signal-regulated kinase 1/2 production in the rostral ventrolateral medulla of rats. J Pharmacol Exp Ther.324(1):72-78.

Zhang M, Dwyer N, and Neufeld EB. 2001a. Sterol-modulated glycolipid sorting occurs in Niemann-Pick C1 late endosomes. J Biol Chem 276:3417– 3425.

Zhang Y, Appelkvist EL, Kristensson K, and Dallner G. 1996. The lipid compositions of different regions of rat brain during development and aging. Neurobiol. Aging 17: 869–875

Zhao H, Laitala-Leinonen T, Parikka V, Väänänen HK. 2001. Downregulation of small GTPase Rab7 impairs osteoclast polarization and bone resorption. J Biol Chem 276(42):39295-39302.

Zhu WJ, Wang JF, Krueger KE, and Vicini S. 1996. Delta subunit inhibits neurosteroid modulation of GABAA receptors. J Neurosci 16: 6648–6656.

Zhu WJ and Vicini S. 1997. Neurosteroid prolongs GABAA channel deactivation by altering kinetics of desensitized states. J Neurosci 17: 4022–4031.

Zou H, Henzel WJ, Liu X, Lutschg A, and Wang X. 1997. Apaf-1, a human protein homologous to C. elegans CED-4, participates in cytochrome c-dependent activation of caspase-3. Cell 90: 405-413.

Zsarnovszky A and Belcher SM. 2004. Spatial, temporal, and cellular distribution of the activated extracellular signal regulated kinases 1 and 2 in the developing and mature rat cerebellum. Brain Res Dev Brain Res 150(2):199-209.